8629759

Tischler, Frances

THE HYDROCHLORINATION OF TRANS-1,4-POLYISOPRENE CRYSTALLIZED FROM SOLUTION

City University of New York Ph.D. 1986

University
Microfilms
International 300 N. Zeeb Road, Ann Arbor, MI 48106

PLEASE NOTE:

In all cases this material has been filmed in the best possible way from the available copy. Problems encountered with this document have been identified here with a check mark ✓.

1. Glossy photographs or pages ✓
2. Colored illustrations, paper or print ______
3. Photographs with dark background ______
4. Illustrations are poor copy ______
5. Pages with black marks, not original copy ______
6. Print shows through as there is text on both sides of page ______
7. Indistinct, broken or small print on several pages ✓
8. Print exceeds margin requirements ______
9. Tightly bound copy with print lost in spine ______
10. Computer printout pages with indistinct print ______
11. Page(s) ______ lacking when material received, and not available from school or author.
12. Page(s) ______ seem to be missing in numbering only as text follows.
13. Two pages numbered ______. Text follows.
14. Curling and wrinkled pages ______
15. Dissertation contains pages with print at a slant, filmed as received ______
16. Other ______

THE HYDROCHLORINATION OF TRANS-1,4-POLYISOPRENE CRYSTALLIZED FROM SOLUTION

by

FRANCES TISCHLER

A dissertation submitted to the Graduate Faculty in Chemistry in partial fulfillment of the requirements for the degree of Doctor of Philosophy, The City University of New York.

1986

This manuscript has been read and accepted for the Graduate Faculty in Chemistry in satisfaction of the dissertation requirements for the degree of Doctor of Philosophy.

9/9/86
Date

Arthur E. Woodward
Chairman of Examining Committee

9/9/86
Date

Executive Officer

Leonard H. Schwartz

Supervisory Committee

The City University of New York

Abstract

THE HYDROCHLORINATION OF TRANS-1,4-POLYISOPRENE CRYSTALLIZED FROM SOLUTION

by

Frances Tischler

Adviser: Professor Arthur E. Woodward

Solution grown lamellas and hedrites of trans-1,4-polyisoprene (TPI) in the α form, prepared by precipitation from amyl acetate, were reacted in suspension using an excess of HCl at -7 to -10^{o}C. The product was followed with time. The resulting regular block copolymers were quantitatively analysed by 50.33 MHz carbon-13 NMR spectroscopy using assignments made with the aid of solution hydrochlorinated TPI. The average number of monomer units in the reacted (<B>) and unreacted (<A>) blocks were thus obtained. When acetone was used as the reacting medium <B> remained constant after 1-2 days of hydrochlorination at an average value of 4.8 +/- 0.3; the average value of <A> increases with the crystallization temperature, T_c. The hydrochlorination fraction is approximately one-half the noncrystalline fraction calculated from density measurements. The block copolymers were dissolved in $CDCl_3$, in 4-methyl-2-pentanone or in heptane and precipitated by solvent evaporation or by cooling. DSC and x-ray diffraction suggest that the product is noncrystalline. When hydrochlorination was carried out in amyl acetate suspension a 'peeling-off' effect occurred with HCl penetration into the crystalline core, particularly at T_c's of 10 and 20°C. Wide angle x-ray diffraction studies show the presence of some completely hydrochlorinated material in the product. 100% reacted TPI is shown by x-ray diffraction and by DSC to be crystalline.

In memory of my dear father, Benjamin Tischler,

who died on July 15, 1985.

Acknowledgements

I would like to extend sincere thanks to:

* my mentor, Dr.Arthur E. Woodward,in appreciation for his belief in me, his excellent leadership and friendship in the laboratory and the classroom, and without whom this research would not have been possible;
* my supervising committee member and friend, Dr. Leonard Schwartz, for many years of counseling and caring;
* Dr. William Grossman, also in my supervisory committee, for his patience and help with my thesis;
* my M.S. advisor, Dr. Derek Lindsay, for the extensive exposure he gave me to mechanics, electronics, and state-of-the-art spectroscopy;
* all the professors at CUNY, and especially at CCNY, who have supported me throughout;
* all the technicians without whom this work would not have been possible;
* my friends at the university who shared my good times as well as my hard times;
* finally, my parents, Benjamin Tischler and Eva Tischler, and my brother, Henrique, for their continuous encouragement and pride in my work;
* and last but not least, my dear husband and friend, Izzy Sobkowski, for his undying support and understanding throughout these years.

Thank you for the chance you have given me to learn and grow towards a more rewarding and fulfilling future.

Table of contents

List of tables

List of figures

I. INTRODUCTION

The preparation of macromolecular crystals from solution has been reported for a variety of polymers, and has been well summarized by Wunderlich [1] for work up to 1970.

Flexible chain polymers may be crystallized from dilute solution to form thin platelets or lamellas 5-25 nm thick depending on the solvent, the polymer, and the crystallization temperature. These crystals have been termed self-seeding or precooled [2] since crystal nucleation is brought about by preformed nuclei. Some spiral staircase growths due to the presence of screw dislocations are evident on these crystals. When crystallization is carried out from more concentrated solutions using the same crystallization technique, more overgrown lamellas are formed. Crystallization carried out directly by cooling the polymer solution from an elevated temperature to its crystallization temperature leads to the formation of multilamellar objects, where the amount of branching and the lamellar thickness depends on the crystallization temperature. These objects range from simpler multilamellas, called hedrites , to the very highly branched, or spherulites.[3] According to Keith's theory,[4] the transitional multilayered hedrite structures which develop during the early stages in the growth of spherulites, and the spherulitic structures into which they ultimately evolve, represent, respectively, successive stages in the evolution of an initially formed lamellar chain-folded single crystal. The above work has been extensively studied and reported by Kuo et al.[5]

In 1957 Keller [6] showed that polyethylene molecules could form single crystals from dilute solution. Based on his studies of the properties of such crystals, he concluded that the polymer molecules in the crystals were folded back upon themselves. Keller's conclusions were supported by similar, independent observations by Fischer [7] and Till.[8] Later this fold theory was reported [9] for many other polymers. From the work on the crystal structure of polyethylene by Bunn [10], electron diffraction experiments proved that the polymer chain axes in the body of the crystals were essentially perpendicular to the large, flat faces of the crystal. The lamellar thickness (5-20nm) is much smaller than the other dimensions of the crystal (10^3 to $2x10^4$nm) and the chain length (10^2 to 10^4nm). The chains must, therefore, fold back and forth on themselves creating chain folds on the upper and lower surfaces of the crystal. Further studies indicated that the lamellas contain a noncrystalline component, as determined by such methods as density, X-ray diffraction and broad-line proton magnetic resonance. All these facts support the postulate that in addition to the chain traverses through the crystal core of the lamella, chain folds exist which connect one chain traverse to another. Whether the traverses connected to one another are predominantly adjacent (tight or loose) or nonadjacent (switch board) is still a matter of considerable controversy.[11-14] In either case, however, the polymer chain in a lamella is made up of alternating sections,one of which is part of a crystalline array and the other is part of the amorphous material at the crystal surfaces. Figure 1 shows a schematic of the different types of reentry- folding.

Figure 1 : Models [7] of chain folding in single crystal lamellas. a) switchboard (random adjacent reentry) b) regular adjacent reentry (tight fold) c) irregular adjacent reentry (loose fold).

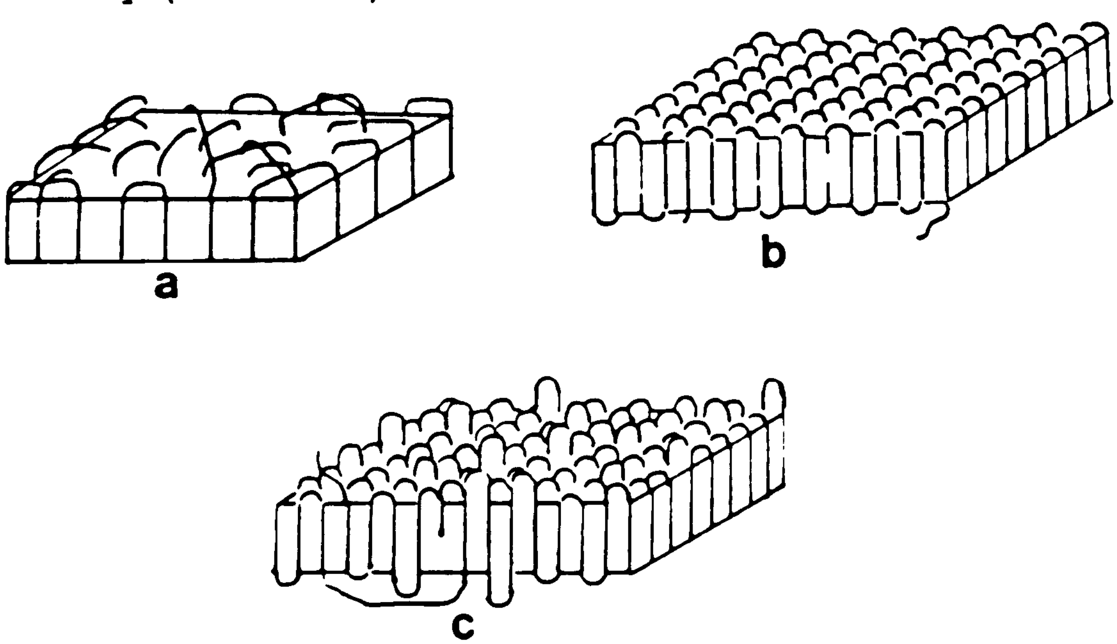

The idealized schematic representation of successive stages in the evolution of a hedrite and eventually a spherulite are summarized in figure 2. Rows (a) and (b) represent respectively edge-on and flat-on views of the evolution of the crystals. Column i shows a chain-folded, monolayered single crystal precursor. The progressive evolution of the spherulite, as shown in columns ii-v, consists of a radiating array of ribbon like, chain folded lamellas. They occur within a radial span beyond which growth progresses in a spherically symmetric fashion. Figure 3 shows the defect structures between the chain folded lamellas that form the hedrite or spherulite. These defects include interlamellar links, chain ends, chain folds and entanglements. In recent years a more detailed appreciation of the variety of morphological forms exhibited by lamellar crystals has developed, largely as a result of studies by Bassett and Hodge.[15-20] For melt grown spherulites the lamellas that first grow radially outward during primary crystallization will usually show curved cross-sectional profiles, commonly in the form of S-bends.[21] The sense of the S-bend is not only the same for adjacent lamellas in a given region but is related to the sense (handedness) in that region of the twisting of molecular orientation about the radius. In a related study of lath-shaped crystals of polyethylene grown from solution in poor solvents, Khoury[22] has observed variations in molecular orientation similar to the S-bending, though less pronounced. Permitted degrees of disorder in chain folding are limited more stringently in already-grown regions of a lamellar crystal than at, or very close to, an edge where it is still growing. The reason is that, whereas chains emerging from the middle of a fold surface are surrounded on all sides by other emergent chains competing with them for space, chains emerging from stems in a growing edge are subject to competition for space only on the crystal side of the edge. With rapid growth, initial attachment of chains at the edge is likely to involve substantial disorder in terms of contour lengths and disposition of folds. When a number of identical crystals grow parallel to one another, an S-bent tip may, at some point, touch an adjacent lamella and lock together as the crystal continues to grow.

Figure 2 : Schematic representation of successive stages in the development of a spherulite from a chain folded precursor crystal: a. edge-on b. flat-on views.[23]

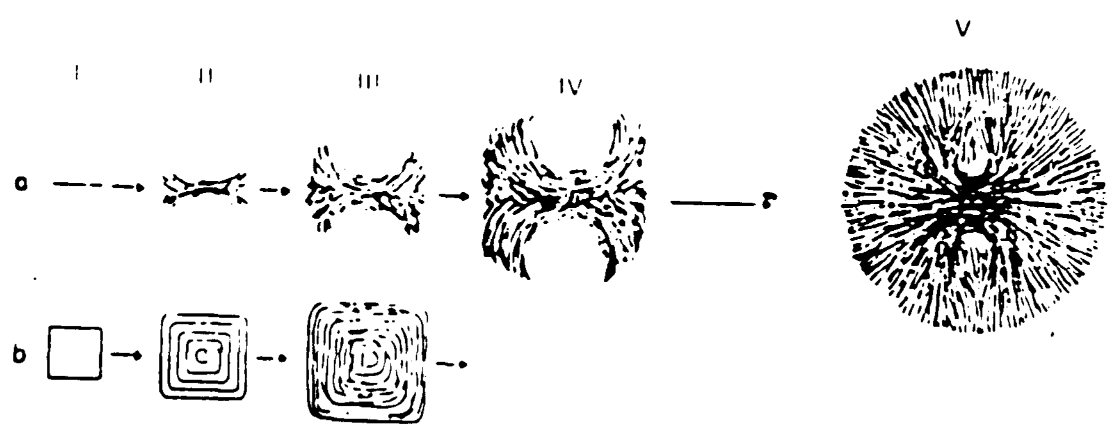

Figure 3 : Model of a spherulite with chain folded lamellas showing interlamellar defect structures.[23]

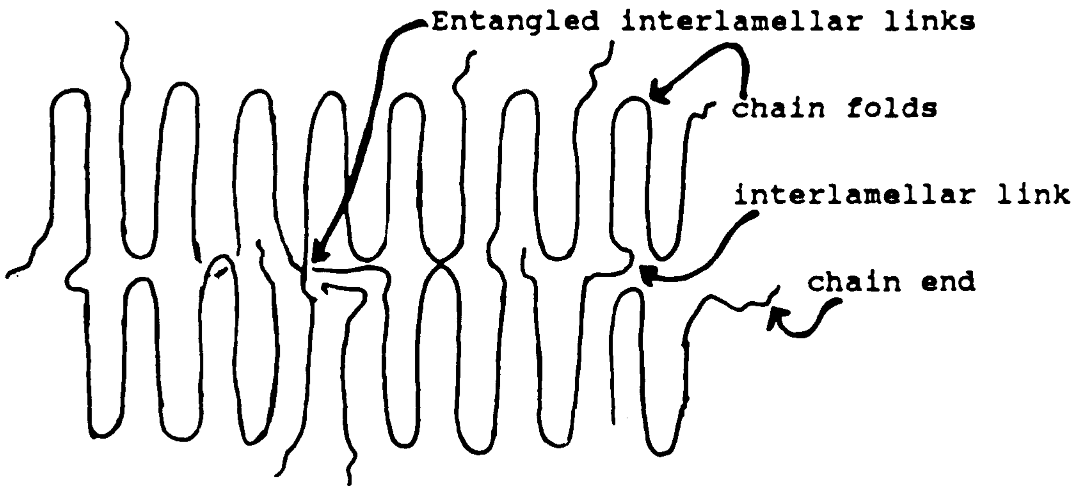

Investigation of the crystalline and amorphous content of lamellas, and the type of folding of the latter, has been carried out using a variety of non-destructive methods, such as wide angle X-ray diffraction, density, calorimetry, IR spectroscopy, and broadline NMR. A large number of these investigations have been on linear polyethylene. This literature has been reviewed by Mandelkern.[24]

A disordered fraction of 15-20% and of 11% has been reported from heat of fusion experiments on polyethylene crystals grown from xylene solutions and dried, and crystals measured in silicon oil suspension,[25] respectively. Subsequent similar experiments [26] agreed within experimental error. Further, the crystallinity derived from heat of fusion measurements, density, or wide angle X-ray diffraction were found to be in excellent agreement. Analyzing the characteristic crystal field splittings in the IR spectrum of polyethylene single crystals formed from mixtures of deuterated and the normal hydrogen-bearing chains, Krimm [11,27,28] has been able to show that the predominant type of folding involves reentry of the emergent stem into an adjacent position on the crystal face (adjacent reentry). Using this polyethylene mixture on high resolution NMR Sillescu and Voegel [14] concluded that adjacent reentry folding with molecular clustering is predominant. Using long spacing X-ray results Udagawa and Keller [29] observed a disordered amorphous layer in the fold region which expands upon swelling polyethylene single crystals with a liquid. This increase in the long space is dependent mainly on the molecular weight of the polymer. Mandelkern [30] explained the dependence of the amount of swelling with molecular weight as a variation in size and distribution of amorphous loops connecting the crystalline sequence. Investigations [31-33] of the surface of dilute solution grown polyethylene lamellae available to penetration by low molecular weight liquids using broad line NMR were carried out. Values for this available material were considerably smaller than values for the disordered content (5-20) of polyethylene lamellae. Fisher[34] and Flory[35] measured the density of single crystal mats of polyethylene and found it to correspond to 15-20% of disordered chains. Since 5% of disorder is necessary for a regular fold structure it was concluded that a random irregular polymer chain entry is preferred. To explain the higher amorphous content on a regular folded model with adjacent reentry folding Hoffman et al.[36] have proposed that the noncrystalline chains are physically adsorbed at the lamellar surface and remain noncrystalline following drying and temperature change.

Attempts have been made to study the fold region of polyethylene crystals directly by chemical essay, but the degradative chemical reactions employed have resulted in destruction of the crystals themselves, and the results are difficult to interpret. Digestion with strong oxidizing agents such as HNO_3 and destructive reaction with ozone coupled with gel permeation chromatography has been used by Keller and coworkers[37-40] to obtain information about the distribution of the fold lengths in polyethylene lamellas. The results were interpreted as confirming the model of adjacently reentrant folds of various lengths, which includes some chain ends (cilia). Therefore, the lamellar thickness, L, includes the surface amorphous region, consisting of chain folds and chain ends, and the crystalline region with a crystalline thickness, L_c, which is smaller than L.

Substitution of bromine atoms onto polyethylene lamellas using ultraviolet or visible light activation of Br_2 in solution at room temperature and above has been studied by various authors.[41-44] Harrison and Baer[42] report an initial fast reaction with a changing rate corresponding to about 2-3% bromine by weight, following which, the rate of bromine addition remains constant up to at least a 7% bromine content by weight. Assuming tight reentry folding, it was estimated that 4.5% bromine by weight corresponds to 1 Br atom per fold. In work using hydrogenated polyethylene Eguiluz, Ishida and Hiltner[43] found that a constant value of 3.5% by weight bromine was reached at 40C using Br_2 in bromobenzene under ultraviolet activation. This corresponds to about one bromine atom for every 50-60 ethylene units in the polymer. In a recent study[44] a polyethylene lamella sample with a bromine content of 14.3% was used to perform a Friedel-Crafts substitution of toluene onto the chain. Substitution of chlorine atoms onto polyethylene lamellas using ultraviolet light activation of Cl_2 in solution at $7^{o}C$ without apparent damage to the crystalline parts, as monitored by X-ray diffraction, was carried out for lamellas with 4 to 38% chlorine added.[45] A chlorine content of 26% by weight corresponds to one chlorine atom per each polyethylene unit in the folds. For the crystals used the ethylene blocks would contain about 60 units and the chlorinated ethylene blocks about 14 units. It has recently been reported [46] by Hiltner et al that in the reaction of Cl_2 with polyethylene lamellas only about 2-3 wt% chlorine is present at the fold surfaces; IR spectroscopy and electron microscopy suggested that the remainder reacts with the chains in the crystal core with attack taking place from the sides.

Substitution, elimination, and addition reactions have been carried out on various other polymer lamellas to date. These polymers include not only polyethylene [41-44] but others such as poly(4 methylpentene-1),[47] polyvinyl alcohol,[48] poly(vinylidine chloride),[49] trans-1,4-polyisoprene,[50-53] and trans-1,4-polybutadiene.[54-60] When such chemical modification occurs only at the fold surfaces of polymer lamellas it gives rise to block copolymer formation of the $(AB)_x$ type. Examples of the latter follow, below.

Three general requirements for the formation of such block copolymers are necessary: the polymer must crystallize as folded chains; each repeat unit of the polymer must be quantitatively reactive towards a small molecule with a minimum of side reactions, particularly scission and depolymerization; and if a liquid is necessary to disperse the nonpolymeric reactant it should not penetrate the crystalline parts of the polymer lamellas.

The copolymer prepared consists of blocks of unreacted polymer units alternating with blocks of reacted units. The number of repeat units in the former depends on the crystal thickness along the chain direction, as determined by the crystallization temperature and solvent. The average size of the reacted blocks is dictated by the average number of monomer units per fold. The average size will be smallest and the width of the size distribution sharpest for the reacted blocks if only adjacent reentry using the minimum number of chain units occurs. If fold looseness is present then a distribution of fold lengths, ranging from tight to loose, is expected. The largest values for the average fold length and the broadest size distributions are expected if a significant amount of nonadjacent reentry takes place. The number of blocks per molecule decreases as the lamellar thickness increases,and increases with increasing molecular weight. As a class of hybrid polymers, these block copolymers also offer unique opportunities for gaining new insight into such areas as morphology, phase separation, polymer-polymer interfaces, and mechanical properties. Furthermore, they provide industry with new products that often combine the best properties of individually useful homopolymers.

While many substitution reactions were carried out on polyethylene crystals, as mentioned above, other substitution reactions with different polymers were studied.[47] Reacting mats of poly(4-methylpentene-1) lamellas using chlorine gas at 60°C gave up to a 15% weight gain. The resulting structure however, was not identified. Acylation of poly(vinylalcohol) lamellas has been carried out with formaldehyde, propionaldehyde, and benzaldehyde using aqueous sulfuric acid (and methanol in the benzaldehyde reaction) at 60-70^{o}C.[48] The reaction rate decreases markedly after one hour. The mole % acylation for benzaldehyde and for proprionaldehyde were 13-14 and 23-26, respectively, while a slow increase of acylation continues after the first hour. The curve found for formaldehyde reaches values of 30 mole % acylation after 5 hours, suggesting penetration of the crystalline lamellar core.

Elimination reactions such as the dehydrohalogenation of poly(vinylidene chloride) lamellas were carried out using pyridine at 45^{o}C in benzyl and isopropyl alcohols.[49] After an initial fast reaction the % HCl removed continued to increase linearly to 6-7% over the time period the reaction was studied.

Addition reactions were studied for the epoxidation and bromination of trans-1,4-polybutadiene and trans-1,4-polyisoprene lamellas in suspension, which aided in the elucidation of the chain fold length.[50-60] Wichacheewa and Woodward [59] carried out an epoxidation reaction of trans-1,4-polybutadiene in suspension . The fraction of double bonds reacted with the epoxidizing agent meta-chloroperbenzoic acid (MCPBA) was obtained by observing the IR intensity ratio of the carbonyl absorption for MCPBA and meta-chlorobenzoic acid (MCBA). The number of monomer units per fold was calculated for heptane and toluene grown crystals. By comparison with the theoretically estimated values for possible tightest reentrant fold it has been concluded that TPBD crystals grown from heptane principally contain regular reentrant folds and TPBD crystals grown from toluene contain irregular adjacent reentrant folds. There was a variation in the number of monomer units obtained for reacted and unreacted sections of TPI and TPBD crystals using proton NMR and lamellar thickness measurements.[50-52,54-56] The samples were epoxidized in the presence of metachloroperbenzoic acid, as the epoxidizing agent, at low temperatures ($0^{o}C$ for TPI and $6^{o}C$ for TPBD) to avoid crosslinking. Various molecular weight samples, crystallization concentrations, crystallization temperatures, and suspension liquids [61] were used, all of which were shown to affect the crystal block lengths. More recent ^{13}C NMR spectroscopy [51,54] results for TPBD and TPI, as discussed in detail below, show that block copolymers containing epoxidiene and diene units were formed with the exclusion of random units. Agreement between the amount brominated and the amount epoxidized for the TPBD lamellas suggest that block copolymers of the dibromodiene and the diene units are also formed. The bromination of trans-1,4-polyisoprene lamellas however, seem to result in both substitution as well as addition reactions.[53] This work is, however, inconclusive and needs further investigation.

Jelinski and coworkers [62] used the different ^{13}C NMR chemical shifts of poly(butylene terephthalate) hard segments in a series of Hytrel copolyesters to determine the mole fraction and the weight percent of the copolymers. Williams and coworkers,[63] in a careful and detailed analysis, showed, using a combination of ^{13}C and ^{29}Si NMR, the structure and the chemistry involved in the synthesis of bisphenol A polycarbonate-poly(dimethyl siloxane) block copolymers. Klesper and coworkers [64] used proton NMR spectroscopy to distinguish between random, blocky, and alternating sequences caused by partial hydrolysis of syndiotactic poly(methyl methacrylate). Using carbon-13 NMR spectroscopy, Komoroski and coworkers [65] studied the two phase reaction of dichlorocarbene (:CCl_2) with cis- and trans-1,4-polybutadiene to produce copolymers containing dichlorocyclopropane rings. Their carbon-13 NMR results showed that the blockiness of the product was dependent upon the method used to generate the dichlorocarbene. A random product obeying Bernoullian statistics was obtained when the carbene was produced from chloroform plus a concentrated aqueous sodium hydroxide solution. In contrast, solid sodium hydroxide plus chloroform produced a higher concentration of blocky units. The presence of blocky units was confirmed by thermal analysis.

Detailed characterization[66] of the products of lamellar block copolymer preparations can be carried out spectroscopically by such methods as the above mentioned carbon-13 solution NMR and proton NMR, as well as solid state carbon-13 NMR.[67] High pressure liquid chromatography have also been employed to characterize the degradation products of polyamide lamellar block copolymers.[68] Techniques such as density,[55] X-ray,[69] dynamical mechanical behavior,[69] IR,[57] Raman spectroscopy,[70] and differential scanning calorimetry[71,72,73] can also be used to measure the total noncrystalline content of a lamella without any chemical modification of the surface. Hendrix, Whiting and Woodward[57] followed the ratio of an amorphous and a crystalline IR band of TPBD crystals. The ratio changed upon annealing the crystal and upon changing the crystallization temperature. Ng, Stellman, and Woodward[71] studied TPBD crystals using DSC. The heat of transition for the conversion of low to high temperature modifications was found to be proportional to the crystallinity, and the results were in agreement with the IR measurements. Tseng et al.[55] extrapolated a straight line obtained by plotting the enthalpy of the crystal-crystal transition versus specific volume to 100% crystallinity and obtained a value for the heat of fusion of TPBD, in agreement with literature value.

Schilling et al.[67] have employed solid state NMR techniques to calculate the amorphous surface content of TPBD crystals both with and without a surface chemical modification. With the appropriate use of magic angle spinning and proton decoupling they were able to measure chemical shifts, relaxation times, and nuclear Overhauser enhancements (NOE) of carbon nuclei in the crystal stems and amorphous regions of the TPBD crystal. Using dipolar decoupling without magic angle spinning the chemical shift anisotropy of the olefinic carbons were examined. Using magic angle spinning with dipolar decoupling but without ^{1}H-^{13}C cross polarization, the fraction of crystallinity was determined to be 0.73. Spin-lattice relaxation of the fold-surface carbons is shown to be predominantly dipolar. The less than maximal NOE values, ca.2, are consistent with anisotropic chain motion. Both these findings and the chemical shifts of the fold-surface carbons agree with those reported by Jelinski et al. for bulk amorphous polybutadiene. The chemical shifts of the methylene carbons can be rationalized on the basis of the γ-gauche shielding effect and the accepted rotational isomeric state model for unperturbed TPBD, but the upfield shift of the olefinic carbons does not agree with calculations. The motions and conformations of the surface folds are similar to those of bulk polymer despite the constraints imposed on the folds by the requirement of adjacent reentry. Upon epoxidation with m-chloroperbenzoic acid, the folds give very broad carbon-13 resonances. They concluded that the introduction of oxirane rings immobilizes the chains sufficiently to prevent averaging of ^{1}H-^{13}C dipolar interactions and ^{13}C chemical shift anisotropies. Before epoxidation the spectrum contained two doublets, one for the CH and the other for the CH_2 carbon resonances, with the upfield component of each identified as due to the noncrystalline part. After the epoxidation four singlet resonances appear due to carbon atoms in the diene and epoxidized diene parts, suggesting that the noncrystalline fraction has completely reacted. Similar solid state NMR studies are currently been carried out on TPI at Bell Laboratories.

A combination of ^{1}H NMR, density measurements, electron microscopy, and X-ray techniques were employed by Woodward et al.[50-52,54,54,67] to determine the fold and crystalline stem lengths of TPBD and TPI crystals grown in solution and surface reacted in suspension:

Assuming that only the surface of the crystal contains the amorphous material, then the number of monomer units per fold, U, and the crystals thickness, L_c, can be expressed as:

$$U = (L_c/R)((M_n/M_o)(F_s)-C)/((M_n/M_o)(1-F_s)-(L_c/R)) \quad \text{eq. 1}$$

and,

$$L_c = ((1-F_s)\rho_A L)/((1-F_s)\rho_A+F_s\rho_c) \quad \text{eq. 2}$$

where M_n is the number average molecular weight; M_o is the monomer unit molecular weight; R is the crystallographic repeat distance per monomer unit along the chain direction in the crystal; L is the lamellar thickness obtained from electron microscopy measurements or small angle X-ray diffraction; ρ_a and ρ_c are the amorphous and crystalline densities, respectively; C is the number of monomer units per two chain ends or cilia. C is believed to be a linear function of L, and is represented as $C = a\ L/R$.[54] The surface fraction, F_s, is determined from proton NMR analysis.

In contrast to reactions on polymer crystals, a very large number of reactions in solution have also been reported. Such reactions include chlorination, hydrohalogenation, bromination with pyridinium perbromide, mercaptan addition, isocyanate addition, cycloolefin and maleic anhydride addition, aldehyde addition, cyanomethylation, oxoalkylation, attachment of organosilicone adducts, substituted cyclopropane ring formation, epoxide formation followed by ring expansion, oxidation and crosslinking on one or more 1,4-polydienes. Although many researches have studied the modification of polyisoprene, most have concentrated on the cis form, or natural rubber. Reactions with chlorine has been carried out with sheets of rubber,[74] rubber in solution,[75] or latex,[76] giving addition, substitution, and cyclization products. It has been found that for chlorination using phenyliodochloride and sulfuryl chloride in the presence of a peroxide catalyst [77,78] pure addition products may be obtained. Hydrogen chloride adds readily to solid natural rubber, rubber in solution, or latex [79] according to Markownicoff's rule. It is believed to occur via ionic addition of the hydrohalogen to the double bond. The product is found to be a crystalline, flexible, tough, film-forming material. The main use of rubber hydrochloride has been in packaging. Hydrochlorination of natural rubber in CCl_4 solution has been performed yielding a completely soluble rubber hydrochloride. Golub [80] has hydrochlorinated cis-1,4-polyisoprene and has proven, by high resolution NMR, that some cyclization occurs. Hypochlorous acid reacts with rubber in solution with some substitution products. Both Gemmer and Golub [81] and Hayashi, Takahashi, Kurihara, and Ueno [82] have reported their ^{13}C NMR findings on solution epoxidized TPBD and of TPI polymers.

Lately, carbon-13 NMR spectroscopy has become more extensively utilized in the study of the monomer sequence distribution of various polydienes.[83-91] Some reports have been published on the sequence distribution of 3,4- and 1,4- or of cis-1,4- and trans-1,4-isoprene units in polyisoprenes.[92-97] As for chemically modified polymers, however, few ^{13}C NMR investigations have been made both on the reaction site and the sequence distribution of modified and unmodified units.[98-100] Gemmer and Golub[81] reported the ^{13}C NMR spectra of partly epoxidized 1,4-polyisoprenes and 1,4 polybutadienes, and interpreted the prominent signals in terms of the dyad of 1,4 units and epoxidized units, though the signal assignments were not discussed in detail. The prominent resonances in the spectra of the epoxidized polymers were assigned by using lanthanide shift reagent and off-resonance decoupling experiments. The former was carried out by incremental additions of weighed amounts of [Eu(fod)$_3$] to the NMR sample. The rate of change in the chemical shift was determined as a function of added Eu(fod)$_3$; the faster the line changes position, the closer the associated carbon to the epoxide moiety.[101] The carbon-13 method of quantitative assessment of the epoxide content was developed following determination of relative spin-lattice relaxation time and nuclear Overhauser effect parameters of the various carbons in the epoxidized polymers. Hayashi et al.[82] have assigned the carbon-13 NMR signals of partly epoxidized trans-1,4-polyisoprene in terms of the triad of trans-1,4 and epoxidized units. Their results agreed very closely with that calculated on the basis of the random distribution of trans-1,4 and epoxidized isoprene units. These results suggest that the site of the epoxy group formed is not affected by such groups previously formed in polyisoprene. Tran and

Prud'homme[102] have studied 1,4-polyisoprene, randomly hydrochlorinated PI to 45%, and completely reacted PI using 22.63 MHz carbon-13 NMR spectroscopy. The polymer used contained 71% cis, 22% trans, and 7% 3,4 units. The spectrum of the partially reacted PI sample contained both the peaks found in polyisoprene and completely hydrochlorinated PI in addition to one extra methylene resonance. This latter resonance was assigned in terms of a BA dyad by the authors.

A very extensive ^{13}C NMR study of block copolymers has already been carried out by A. Woodward et al. at CCNY in collaboration with F. Bovey et al. at ATT Bell Labs. This work includes the epoxidation of 1,4-trans-polybutadiene[54,67] and of 1,4-trans-polyisoprene[51,52] crystals. The spectra were interpreted with the aid of both polymers epoxidized in solution, and with the aid of model compounds. The spectral assignments aided and are referenced in the interpretation of the present work.

The spectra of 3,7-decadiene, and its 50% and 100% epoxidation products were taken as model compounds for the study of TPBD. These in turn were interpreted by comparison with known diene spectra such as 2,6-cis,trans-octadiene, 2,6-trans,trans-octadiene,[103,104] trans-2-pentene, trans-2-pentene - 1,2 - epoxide,[105] (Z)-3-decene, (E)-3-decene.[106] The different isomers possible for 3,7-decadiene are designated in appendix 1.

When two trans oxirane rings are present in the same molecule (compound vi, appendix 1) four isomers are possible:

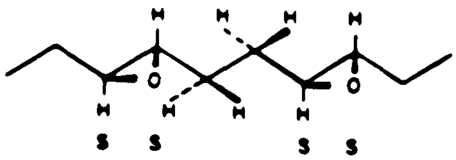

(vi-a)

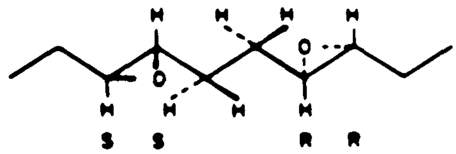

(vi-c)

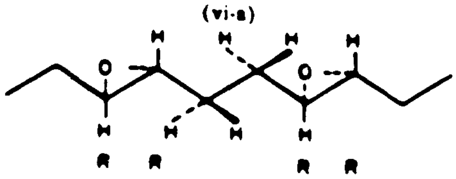

(vi-b)

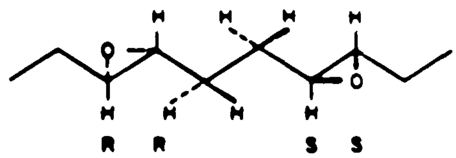

(vi-d)

Compounds a and b form a pair of enantiomers as do c and d. Such mirror image pairs cannot normally be distinguished by NMR (in the absence of a chiral environment), but each pair is spectroscopically distinct from the other because they are diastereomers. The ε methylene carbon resonance splits equally as do the ε carbon and the ζ carbon resonances of the cis,trans-dioxirane (compound vii,appendix 1) spectrum.

The ^{13}C NMR spectrum of the 50% epoxidized 3,7-decadiene has all the resonances of 100% reacted and unreacted 3,7-decadiene and new resonances of the monoepoxy diene, principally compound iii, OD-tE. These are of particular importance since they represent the junction of reacted and unreacted units in the polymer chain.

Carbon-13 NMR spectra of epoxidized 1,4-trans-polybutadiene in suspension and in solution show four spectral regions: CH_2 of oxirane units, CH_2 of butadiene units, oxirane ring CH, and double bond CH.

The crystals were suspended in toluene and epoxidized at 6^{o}C, and/or epoxidized in a homogeneous solution in chloroform to levels of 30% and 78% of completion.

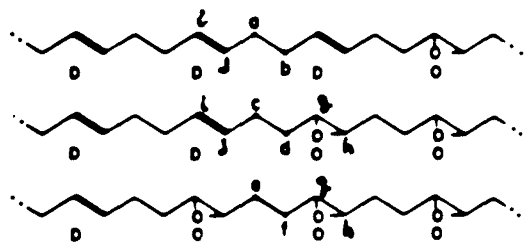

The resonance peaks of carbons c and d were used as a measure of junction units. The assignment is in agreement with that proposed by Gemmer and Golub,[81] which was based on the differential effect of a lanthanide shift reagent on a methylene carbon between a double bond and an oxirane ring. The oxirane ring carbon resonances show both positional splitting (in DOO) for carbons g and h and chirality splitting of each in OOO (where they are equivalent). It appears from the model compounds that each ring carbon is sensitive to the chirality only of the nearest neighboring ring. The olefinic carbon chemical shifts exhibit sensitivity to pentad sequences of O and D units.

Squalene was used as a model to help with the ^{13}C NMR spectra interpretation of epoxidized 1,4-trans-

Polyisoprene. The structure of squalene is that of six isoprene units with a tail-to-tail junction in the center. All of the double bonds are in the trans arrangement as in TPI. The NMR assignments are based upon chemical shift prediction rules,[107,108] and the results of DEPT [109,110] experiments carried out on squalene.

The olefinic carbons are converted into oxirane carbons upon epoxidation of squalene in solution. The reactions were carried out to levels of 5, 50, 88, and 100%. At the 5% level the oxirane units can be assumed to be isolated by the olefinic neighbors. The three possible structural environments are shown below:

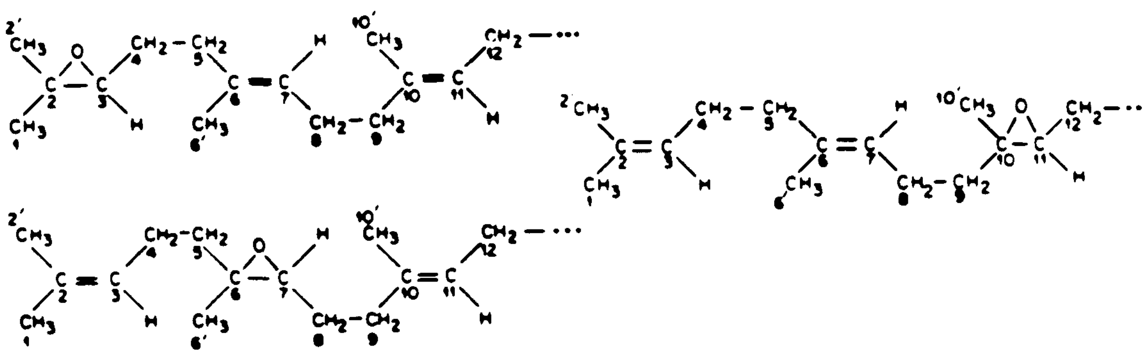

At 50% epoxidation there is an increase in the complexity of the oxirane carbon spectrum. Carbons C2 and C3 produce doublets due to their non-equivalence when a pair of oxirane units is present. Carbons 6, 7, 10, and 11 may each produce 9 individual resonances, considering triad sequences of oxirane and olefinic units and all possible stereosequences.

At 80% and 100% of epoxidation the intensities of the

C2 and C3 stereochemical isomer resonances increase. In addition, at 100% epoxidation non-equivalent carbons C7, C11, C6 and C10 can each generate four resonances reflecting the different stereoisomers. As the level of epoxidation increases there is an upfield shift for some of the resonances, particularly those of carbon C3, and alkyl carbons C5 and C9, and C4 and C8. Methyl carbons C6' and C10', on the other hand, move downfield. In addition, differences in magnitude of the chiral splitting of resonances can be observed. These small changes in chemical shift may result from longer range structural sensitivity or from changes in the solvent mixture at these high sample concentrations as one moves from an olefinic to an oxirane system. Carbons C5 and C9 split due to the sensitivity to the chirality of the neighboring oxirane units. The magnitude of the splitting for the C4 and C8 carbons is lower than C5 and C9 indicating that the methylene carbon attached to the protonated oxirane carbon is less sensitive to the difference between the diastereomers. Strong evidence for the preservation of the trans geometry of squalene after complete epoxidation is the absence of a cis-C5 or C9 resonance at about 32 ppm as would be expected based on the ^{13}C spectrum of solution epoxidized cis-polyisoprene.[81]

Appendices 2 - 4 show the carbon-13 spectra, assignments, and structural formulas for the olefinic, oxiranyl, and alkyl regions of the TPI epoxidized in homogeneous solution in chloroform to a level of 25% (spectrum a) and 90% (spectrum b) of completion and epoxidized as crystals suspended in amyl acetate at $0^{o}C$ (spectrum c). The designations shown are based on D for double bond and O for oxirane ring (epoxy unit).

The assignments in the olefinic region of resonances 1,3 and 4,6 (appendix 2) were determined by Gemmer and Golub [81] from experiments using lanthanide shift reagents. Some show fine splittings due to sensitivity to pentad sequences of O and D units, as was observed for TPBD. The oxirane region (appendix 3) shows a strong similarity between the spectrum of the 90% solution epoxidized (3b) and the crystal epoxidized TPI (3c). The C2 quarternary carbon shows a doublet, reflecting the chiral relationship with only the nearest neighbor unit. The C3 oxirane carbon is sensitive to the chirality of neighboring units in both directions along the chain and thus is split into a four line pattern produced by the four possible diastereomers. The assignments in spectrum (a) of the alkyl carbon region (appendix 4) are in agreement with those made previously on solution epoxidized TPI.[81,82] However, the original assignment of resonances 10 and 14 was made incorrectly [82] as a result of not considering sensitivity to the diastereomers. Resonances 19, 22, 24, and 25 represent junction units between olefinic and oxirane units.

The TPI crystals used in the above experiments were in the monoclinic or α form. TPI has been found to exist most commonly in two crystalline modifications, α and β. The β form can be described by an orthorhombic unit cell with angles $\alpha = \beta = \gamma = 90^{\circ}$ with a=7.78A, b=11.78A, and c=4.72A from X-ray diffraction [111] or with a=7.83A, b=11.87A, and c=4.75A from electron diffraction.[112] The structural parameters of the α form is a matter of dispute. Two different monoclinic unit cells have been proposed by Fisher [112] and by Takahashi, Sato, Tadokoro and Tanaka.[113] The unit cell due to Fisher has a=5.9A, b=7.9A, c=9.2A, $\alpha = \beta = 90^{\circ}$ and $\gamma = 94^{\circ}$. This cell corresponds to the γ-structure proposed by Bunn.[111] The unit cell proposed by Takahashi et al., has a=7.98A, b=6.29A, c=8.77A, $\alpha = \gamma = 90^{\circ}$ and $\beta = 102.0^{\circ}$. The three molecular models are shown in appendix 5.

The x-ray pattern of rubber hydrochloride has been studied by Bunn and Garner.[114] The crystal lattice was found to be monoclinic with a=5.83A, b=10.38A, c=8.95A, and $\beta = 90^{\circ}$.

In the investigation to follow TPI single lamellas in the α crystal form, were used. The α form is known to be more stable than the β form, and was therefore, chosen for this study. Further, a comparative study can be made with the above mentioned work on the epoxidation of α TPI crystals. TPI hedrites were also studied. These, however, were found to contain a mixture of α and β crystals.

The crystals were suspended in a nonsolvent and surface hydrochlorinated at low temperatures ranging from 30^{o} to -10^{o}C. The resulting block copolymers were dissolved and subjected to ^{13}C NMR analysis as the main investigative tool. Further, the original polymer was dissolved and hydrochlorinated to various degrees of completion, including 100% hydrochlorination. These, too, were subjected to carbon-13 NMR analysis. As per the discussion above, NMR spectroscopy has proven to be particularly well-suited for addressing structural problems concerning block copolymers, such as sequence distribution, extent of blockiness, and purity. The results, again, are compared with the NMR study on the epoxidation of TPI, squalene, and TPBD, as detailed above.

II. EXPERIMENTAL SECTION

II.1. Samples

Synthetic trans-1,4-polyisoprene (TPI) was obtained from Polyscience Inc., Warrington, PA; HCl gas from Matheson Co.; Amyl Acetate , carbon tetrachloride, methanol, toluene, deuterated chloroform from Fisher Co..

The trans-1,4 content has previously been determined [115] to be 99% for samples crystallized from amyl acetate solution at a polymer weight fraction of 5.7×10^{-4}. These determinations were made by F.A.Bovey and F.C.Schilling at Bell Laboratories by ^{13}C NMR using a Varian XL 200 instrument.[51,116]

The molecular weight distribution of unfractionated synthetic TPI has been determined by K. Anandakumaran [116] using a Waters 200 analytical Gel Permeation Chromatograph with toluene at $85^{o}C$ as the solvent. The M_n and M_w/M_n values are 3.5×10^4 and 4.8, respectively.

II.2. Fractionation

A few fractions of TPI were prepared by a fractional precipitation method with toluene as the solvent and methanol as the nonsolvent. A 1% (W/V) solution of TPI is treated with methanol and stirred well until a milky colour results at room temperature. 2,2-methylene-bis-(4-methyl-6-

tertiary butylphenol) antioxidant was used. It is then warmed to about 45^{o}C with constant stirring until the solution becomes clear again. It is then kept overnight in an isothermal bath at 29^{o}C. To the gelatinous phase the above procedure is repeated and to the supernatant phase a further increment of methanol is added and the process repeated. Such treatment to both phases yields two new phases each. These may be separated and used or they may be further fractionated for a sharper molecular weight distribution. All precipitates were dried under vacuum.

II.3. Crystallization

Two procedures for the growth of crystals were employed as described below :

II.3.1. Precooled crystallization from solution: Unfractionated and/or fractionated TPI solutions in amyl acetate of approximately 0.07% by weight are heated to 100^{o}C (dissolution temperature, T_D), to ensure the destruction of all nuclei present, and filtered. The solutions are cooled at 0^{o}C for one hour and then redissolved by increasing the temperature at a rate of approximately 0.2^{o}C/min to a redissolution temperature (T_R) of 34^{o}C, and finally isothermally crystallized at different crystallization temperatures (T_C) of 10^{o} - 30^{o}C for one day. They are then filtered and washed with amyl acetate and/or acetone at the same temperature. The crystal mats are then either dried at room temperature under vacuum for density measurements, DSC, X-ray diffraction, viscosity measurements, and NMR analysis, or resuspended in amyl acetate or acetone for hydrochlorination.

II.3.2. Direct crystallization from solution:
A 1% by weight TPI solution in amyl acetate is heated to a dissolution temperature (T_D) of 100°C. The solution is held at the same temperature for one hour, filtered, and removed to a constant temperature bath at 20°C for one to three days (T_C). The crystal mat is filtered, washed, and either dried or resuspended as mentioned above for the precooled crystals.

II.4. Crystal morphology

II.4.1. Optical microscopy: The crystals grown both from direct and precooled crystallizations were allowed to dry on glass slides and were studied under the optical microscope using both interference contrast optics and crossed nicols (to observe the birefringence). A photomicroscope (Zeiss) with magnification from 500 to 1000 was used. Photographs of the structures were taken with a 35 mm camera connected to the instrument on Kodak technical pan film 2415 with Estar AH base.

II.4.2. Electron microscopy: Crystals were deposited from suspension onto a copper grid (200 mesh/in^2) which has been coated with carbon. After the solvent is allowed to evaporate the grid is shadowed with Pt/Pd or Au/Pd vapor in a vacuum evaporator ($<10^{-4}$ mm Hg) to increase image contrast. The shadowing angle used is $\alpha = \tan^{-1} 1/3$. The crystals were observed in the transmission mode with a Phillips EM 300 electron microscope at 80 KV at magnifications of 5000 - 10000. Photographs of the crystals were taken with a plate camera connected to the instrument. The morphology of the crystal is thus easily observed and its thickness can be calculated from the shadow distance along the shadowing direction.

II.4.3. Wide angle X-ray diffraction: A Norelco X-ray generator (Philips Inc.) and a cylindrical camera of 57.3 mm diameter were used. The dried transpolyisoprene and hydrochlorinated transpolyisoprene crystals were flattened with a hydraulic press. Exposures were made with nickel-filtered (Cu-K_α) radiation using an accelerating potential of 35 KV and filament current of 15 mA for approximately 15 hours. For a random polycrystalline sample, diffraction from all crystals in the sample having (hkl) planes making the proper Bragg angle with the incident beam produces a cone of radiation with a semiapex angle of 2θ, which intersects the film of the camera. The most accurate measurements are made along the equator. The measured 2y (the diameter of the diffraction ring) equatorial values may be converted into 2Θ values by the equation:

$$2\Theta = 180^{o}(2y)/nD \qquad \text{equation 3}$$

where D is the diameter of the camera. The 2Θ values may be converted to d-spacings for the diffracting planes by the equation:

$$d = 1 / 2\sin(180y/nD) \qquad \text{equation 4}$$

Results were compared with literature values for α [5,112,113] and β [5,111,112] TPI crystals and for rubber hydrochloride.[114]

II.4.4. Differential scanning calorimetry (DSC): Measurements were made with a Dupont 1090 thermal analyzer with sample weights of approximately 2 mg. The temperature indicated by the analyzer were checked by comparing the melting point of pure Indium to its literature value. A scanning speed of $10^{o}C\ min^{-1}$ was used for the experiments. The melting points of the unreacted and the reacted TPI crystals were taken as the endotherm temperatures of these crystals and were compared with known values of TPI and rubber hydrochloride crystals.[5,102,115]

II.5. Molecular weight determination

Viscosity measurements: The average visccsity molecular weight was calculated using an Ubbelohde viscometer with toluene as the solvent at 30^{o}C. This method is a variation of the Ostwald pipet, especially adapted for work with solutions of polymeric materials.

The viscometer (figure 4) [117] allows the dissolved polymer to fall through its capillary tube. The time for the fixed volume of liquid to fall (from the upper to the lower mark on the capillary) is a function of the density and viscosity of the liquid and the dimensions of the viscometer. With polymer molecules the viscosity of the solution depends on the concentration of the solute, its molecular weight, and the shape of the solute molecule:

$$\eta_{SP} = \frac{\eta_c - \eta_o}{\eta_o} = \frac{\eta_c}{\eta_o} - 1 = \frac{t_c}{t_o} - 1 \qquad \text{equation 5}$$

η_{SP} = specific viscosity: the relative increase in viscosity due to the presence of the solute.

η_c = viscosity of the solution

η_o = viscosity of the pure solvent

t_c = flow time of the solution

t_o = flow time of the pure solvent

The intrinsic viscosity is related tc the molecular weight by the equation:

$$[\eta] = K\,M^{a} \qquad \text{equation 6}$$

$[\eta]$ = intrinsic viscosity: the viscosity value as infinite dilution is approached.

M = molecular weight (>10000)

K and a are constants characteristic of the solvent-solute system. The values used here were obtained by J. Xu [61] and are comparable with other literature values. They are 4.37×10^{-2} and 0.686 for K and a, respectively.

An 8% (W/V) solution was originally used. Additional portions of solvent were added to the reservoir and time flow measurements were taken. By substituting these values into a least squares analysis a value for $[\eta]$ may be obtained. By replacing the latter and the known values of K and a, into equation 6, M or M_v (the average viscosity molecular weight) are calculated. M_v is an average molecular weight, somewhere between the number average and the weight average values, but close enough to the latter to furnish a useful approximation.

A detailed example of the calculation is shown in appendix 6.

Figure 4: Ubbelohde dilution viscometer [117]

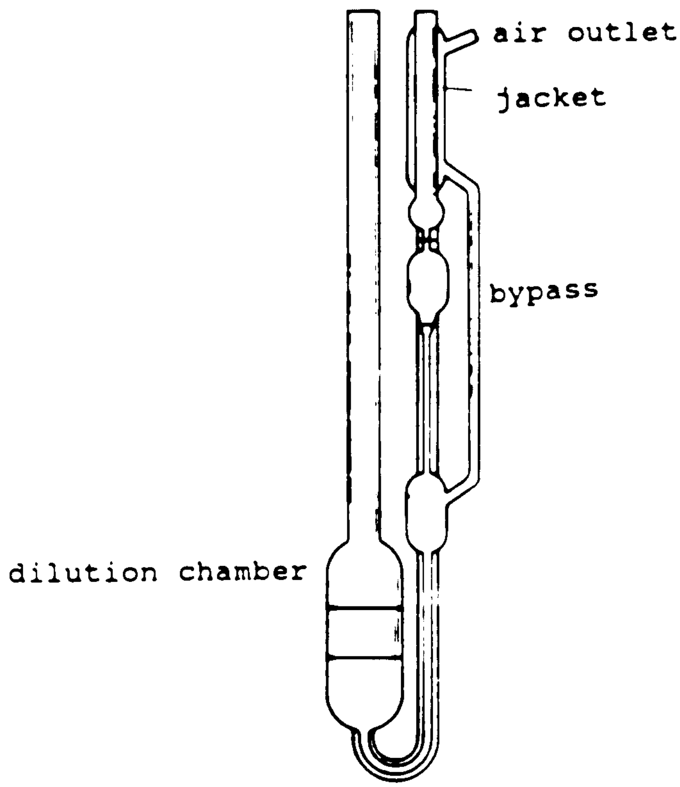

II.6. Hydrochlorination

Reaction of the double bonds at the surfaces of the crystals were carried out in amyl acetate and in acetone suspension at 20, 0, and -7 to -10^{o}C. Reaction of the double bonds of the polymer in solution were carried out at room temperature using chloroform as the solvent. The reaction set-up is shown in figure 5 . A glass manifold was designed which holds three reaction flasks, and has a gas inlet, a vacuum pump outlet and a manometer outlet. The number of reaction flasks per manifold were chosen so as to fit in the isothermal bath. These flasks, holding 0.25 - 0.30 grams of polymer lamellas in 30 ml of the suspension liquid, are evacuated with a mechanical pump. HCl gas is introduced and its pressure monitored with a manometer until approximately atmospheric pressure is obtained. The [HCl]/[double bond] ratio is estimated to be 30/1. The reaction in each flask is allowed to react for different time periods. The hydrochlorinated material was filtered and washed with methanol several times to remove any residual HCl that may be trapped in the polymer or in the solvent. Failure to do so resulted in crosslinking of the hydrochlorinated TPI. The polymer is then dried under vacuum and dissolved in a 10% (W/V) solution of deuterated chloroform for NMR analysis. From the NMR results percent hydrochlorination - time curves were plotted (usually in terms of <A> and <B>) to follow completion of reaction (figures 28 - 33).

Figure 5: Manifold set-up for the hydrochlorination of TPI.

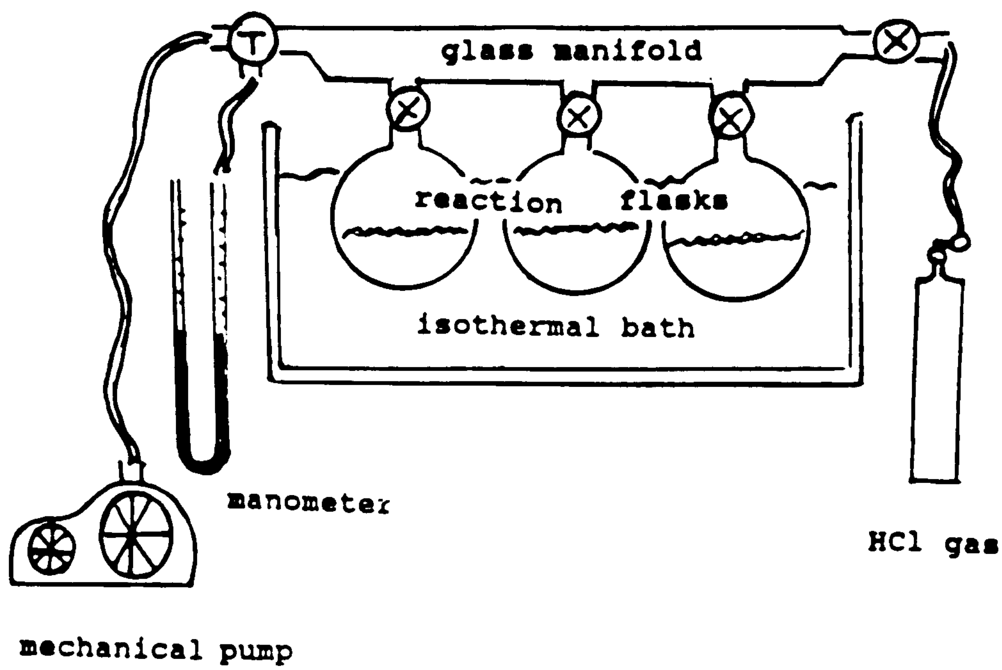

II.7 Recrystallization / microphase separation

Once hydrochlorinated, the hydrochlorinated TPI - TPI copolymer crystals were taken out of their suspension liquid (where the TPI crystals were reacted), washed and dissolved in different solvents by heating. Non-solvent methanol, at approximately -5^{o}C, was used as the first wash liquid to remove any excess HCl present in the suspension. The crystals were then washed with several portions of the same liquid used for the dissolution of the copolymer. The mixture was heated until dissolution occurred. The solution was then either (a) cooled isothermally at 0^{o} or 20^{o}C for 1 to 2 days, or (b) cooled at 0^{o}C for 1 hour, redissolved, and cooled isothermally at 0^{o} or 20^{o}C for 1 to 2 days.

The above procedure was performed in an attempt to study if recrystallization of the copolymer or any microphase separation between the hydrochlorinated and the unreacted domains of the polymer is possible. The products were characterized by optical and electron microscopy, differential scanning calorimetry, and wide angle x-ray diffraction. The copolymers were taken out of solution and dried under vacuum for the latter two experiments. For the microscope observations the copolymers were either dried under vacuum or cast as films. Some were stained with an osmium tetroxide solution while still in the liquid or after the film was cast. OsO_4 was dissolved in amyl acetate or in water to form a saturated solution and a couple of drops were applied on the polymer. Osmium tetroxide reacts with the double bonds of TPI, and stains them, without affecting the hydrochlorinated TPI sections of the polymer.This results in a contrast between the two domains.

II.8. Crystallinity

II.8.1. Density: The density of the TPI lamellas and hedrites grown at 10, 20 , and 30^{o}C were determined using a density gradient column, as shown in figure 6 . The apparatus consists of two Erlenmeyer flasks connected by glass tubing to a vertical glass column. A density gradient was set up by mixing various proportions of a high density liquid, water, and a less dense liquid, ethanol. Thus, the density in the glass column increases essentially linearly from top to bottom, and remains stable for two days until mutual diffusion of the liquids occurs. The gradient was determined with calibrated floats (hollow glass beads) accurate to four decimal places. The densities of the floats used were: 0.995, 0.9826, 0.9800, 0.9643, 0.9584 g/ml. All samples were pressed at $5x10^{7}$ P_a,to eliminate air, cut into small pieces, and dropped into the column. The densities were measured from the flotation levels. The weight fraction of crystallinity was calculated assuming a two phase system using an amorphous density, ρ_a, of 0.905 g/cm^3 and a crystalline density, ρ_c, of 1.05 g/cm^3.

Figure 6 : Density measurement apparatus

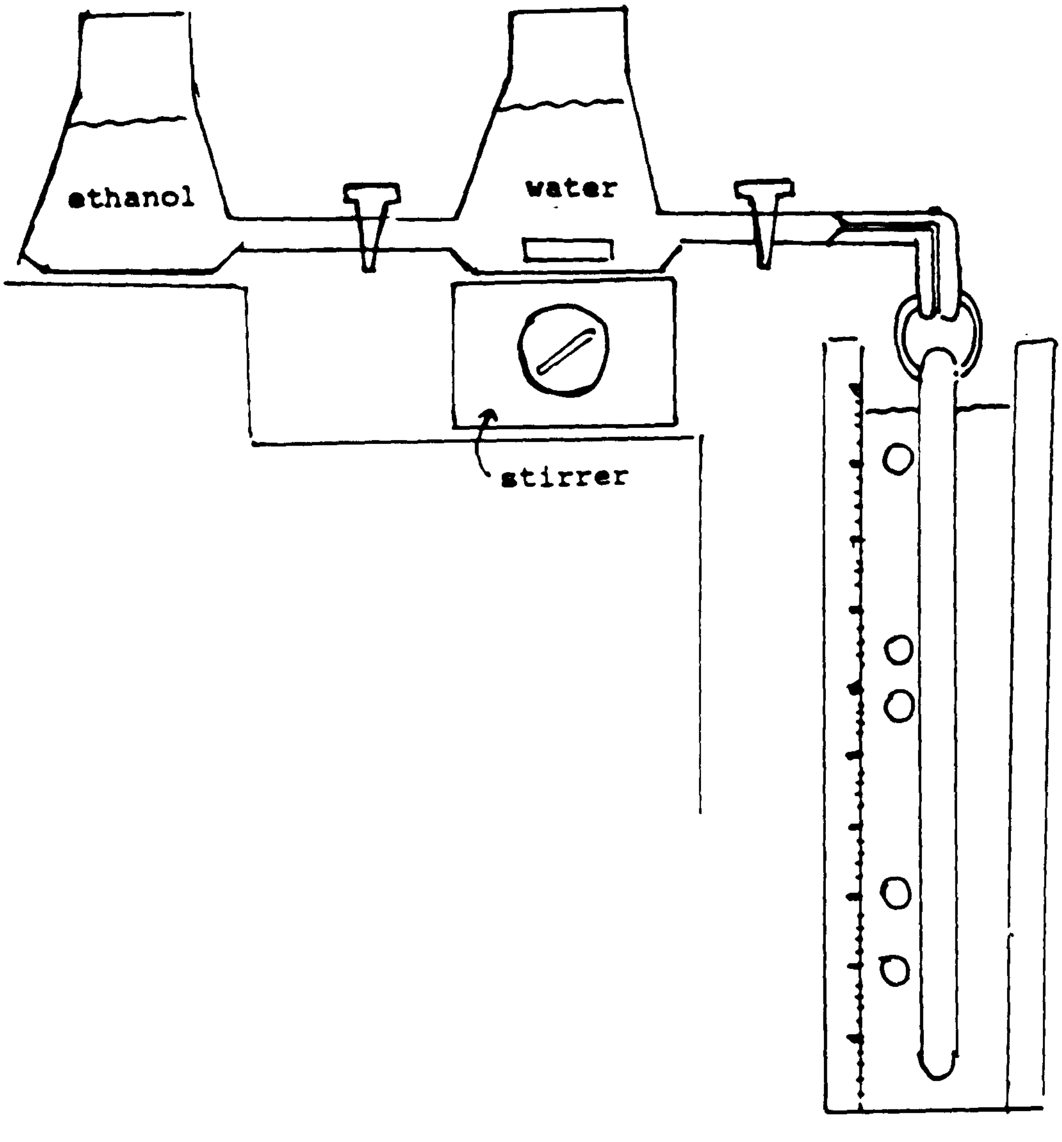

II.8.2. ^{1}H NMR: Hydrochlorinated and unreacted TPI and TPI crystals were vacuum dried and dissolved in deuterated chloroform and monitored using Varian NMR (60MHz), Jeolco NMR (100MHz), and Bruker IBM WP-200SY NMR (200MHz) spectrometers. The ratio of hydrogens in reacted and unreacted monomer units is obtained from the area under the resonance peaks by (1) weighing a photocopied paper cut of the spectral peaks (2) calculating the height versus half the width of each peak (3) using the computer's integration curves. The fraction hydrochlorinated and therefore the percent crystallinity may thus be obtained. In this work, ^{1}H NMR was used to qualitatively determine the hydrochlorination of TPI.

II.8.3. ^{13}C NMR: 50.31 MHz Carbon-13 NMR spectra of the samples, dissolved in 10%(W/V) deuterated chloroform, were recorded at 297K on a Bruker IBM WP-200SY NMR spectrometer. Tetramethylsilane (TMS) was used as an internal reference. A sweep width of 8333.333 Hz in 32 K of memory using a 90^o sampling pulse with a pulse width of 14 seconds was employed to collect 500-3000 scans. The relaxation delay used was 20 seconds and broad-band proton decoupling was applied. Quantitative measurements were made by computer graphical integration. ^{13}C spin-lattice relaxation, T_1, measurements were carried out by using a standard 180^o-τ-

90^{o} nonselective inversion - recovery sequence, with a total delay between 90^{o} sampling pulses being greater than $5T_1$. Both gated broad band as well as interrupted broad band proton decoupling techniques, with or without Nuclear Overhauser Enhancement (NOE), respectively, were applied. A 90^{o}-delay-180^{o}-delay spin echo ^{13}C NMR procedure was performed on a surface hydrochlorinated TPI crystal. The intensity and phase information allows multiplicities of carbons to be distinguished, thus helping in the NMR assignments.

NMR spectra were taken of trans-1,4-polyisoprene, 100% hydrochlorinated TPI, randomly hydrochlorinated TPI copolymers, and hydrochlorinated TPI - TPI block copolymers. The results were interpreted with the aid of α, β, γ effect values given in literature, and with comparison to work done on the epoxidation of TPI, transpolybutadiene, 3-7 decadiene, trans-2-pentene, and squalene.

III. RESULTS

III.1. TPI crystal morphology

High polymers are known to exhibit several different types of crystalline morphology. They range from single crystals, typically predominant at low undercooling from dilute solution, to multilayered hedrites or spherulites formed at higher undercooling from more concentrated solution. The morphology is dependent on the crystallization method and conditions such as molecular weight, crystallization temperature, solvent and polymer concentration.

The two crystallization methods, precooled and direct, used here resulted in lamellas and hedrites, respectively, both in the monoclinic, or α ,form. The latter was confirmed by microscopy (figs. 7, 8), X-ray (fig. 9), and DSC (fig. 12,13) analysis.

III.1.1. Method

Precooled method: This self-seeding technique is probably the most widely used method of growing single-layer crystals of polymers because the entire population is composed of similar crystals. The method involves first the complete dissolution of the polymer in solution, the dissolution temperature (T_D), and then quenching to a precipitation temperature (T_P) to crystallize. This process usually results in crystals which have a predominantly multilayer morphology. The suspension is then warmed up to a redissolution temperature (T_R). It has been found [118] that within a limited range above this clearing point, the solution retains a memory of the previous crystallization when crystallizing at T_C.

Following this method, TPI lamellas were grown from 0.07% (W/V) amyl acetate and investigated under the electron microscope as shown in figures 7a, 7b, and 7c, for crystallization temperatures of 30, 20, and 10^{o}C.

Single lamellas are easily obtained with such polymers as transpo`ybutadiene, while TPI crystals tend to result in slightly overgrown lamellas, where layers of single lamellas stack up against one another, probably through screw dislocations. These layers can be seen at the edges of the crystal. Figures 7a, b,and c also show an increase in the size of the crystals with an increase in the crystallization temperature. Crystal thickness has already been shown [5] to increase with increasing T_C. It is also clear from figure 7c that for low T_C's, where the crystal thickness is smaller, the otherwise oval, or lozenge, shape of the crystal becomes irregular.

Direct method: Multilayered crystals, in the form of sheaf-like lamellar aggregates, or hedrites, were prepared by directly cooling the polymer solution from an elevated temperature of 100°C to its crystallization temperature. The solution was first kept at 100°C for one hour, and then placed in an isothermal bath for crystallization. Figure 8a shows optical micrographs of "edge-on" and "flat-on" views of hedrites grown from amyl acetate at a crystallization temperature of 20°C. Figure 8b shows occasional overgrown hedrites, or spherulites, which are seen with the hedrites. Figure 8c represents the birefringence seen of such hedrites using crossed polaroids.

Figures 7a :Electron micrograph of TPI lamellas grown from 0.07% (W/V) amyl acetate with $T_D = 100^oC$ $T_P = 0^oC$, and $T_R = 34^oC$.

$T_c = 30^oC$

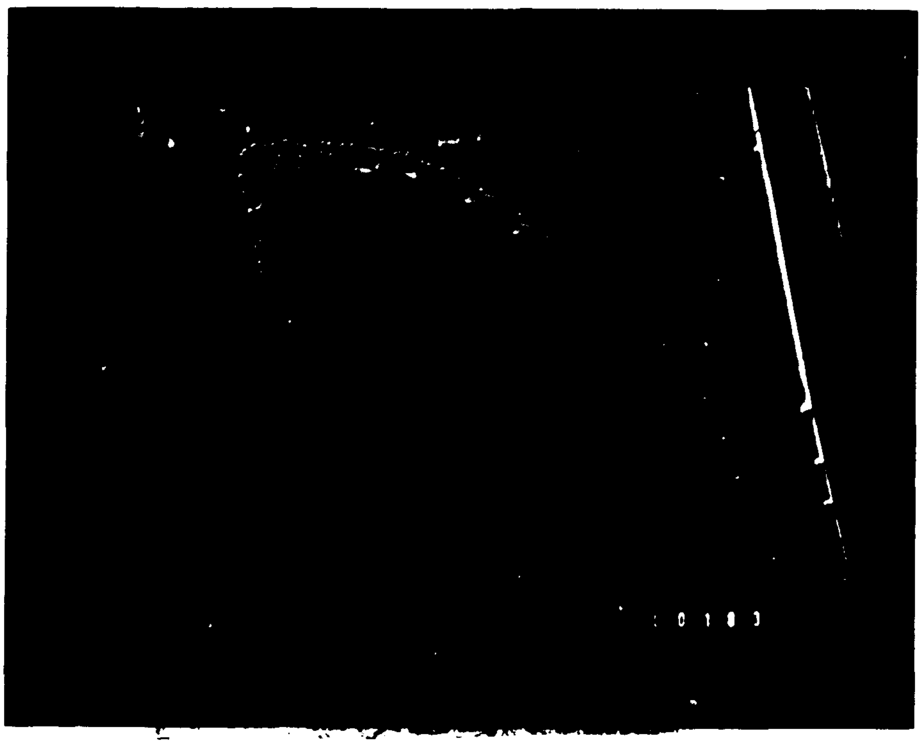

1μ

Figures 7b :Electron micrograph of TPI lamellas grown from 0.07% (W/V) amyl acetate with $T_D = 100^oC$ $T_P = 0^oC$, and $T_R = 34^oC$.

$T_c = 20^oC$

1μ

Figures 7c :Electron micrograph of TPI lamellas grown from 0.07% (W/V) amyl acetate with T_D = 100°C T_P = 0°C, and T_R = 34°C.

T_c = 10°C

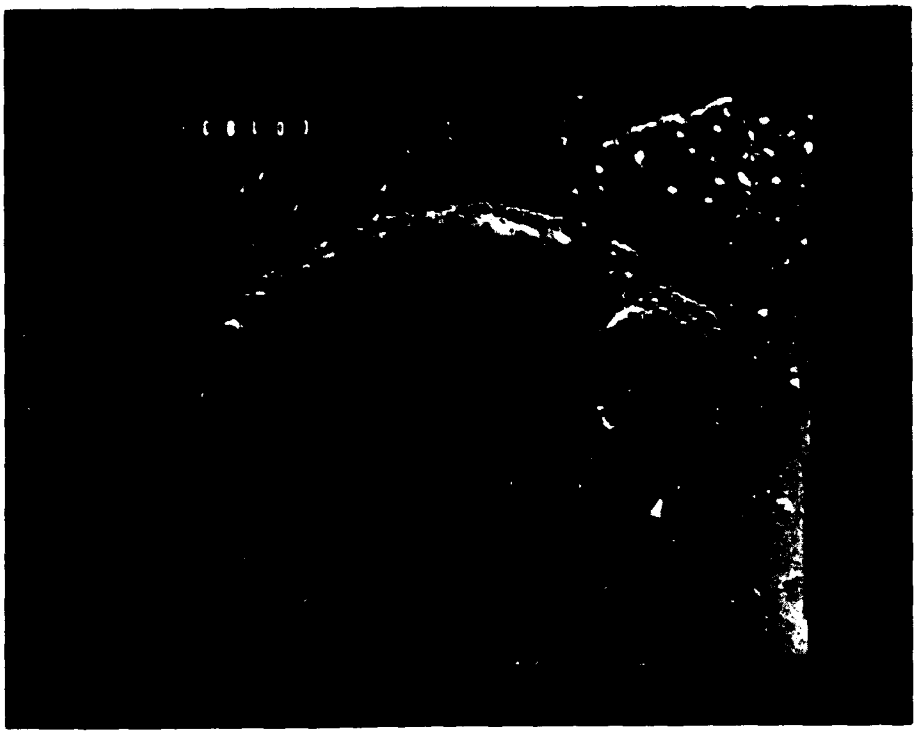

1μ

Figure 8a: Optical micrograph of TPI hedrites grown from 1% (W/V) amyl acetate with T_D = 100°C and T_C = 20°C *

* The figure shows flat-on and edge-on views of the hedrites.

Figure 8b: Optical micrograph of TPI hedrites and spherulites grown from 1% (W/V) amyl acetate with $T_D = 100^oC$ and $T_C = 20^oC$ *

* The figure shows flat-on and edge-on views of the hedrites.

Figure 8c: Optical micrograph of TPI hedrites grown from 1% (W/V) amyl acetate with $T_D = 100^oC$ and $T_C = 20^oC$ using crossed polaroids *

* The figure shows flat-on and edge-on views of the hedrites.

III.1.2. **Wide angle X-ray diffraction:**

Monoclinic and orthorombic crystal lattices are the most commonly found modifications for transpolyisoprene. Lamellas and hedrites grown here, at 10, 20, and 30^{o}C, as described previously, give rise to the α, or monoclinic, crystals, as seen from wide angle x-ray diffraction patterns (figure 9). A comparison of the experimental d-spacings with that reported in the literature by Takahashi et al.,[113] Fisher,[112] and Kuo et al.,[5,119] is shown in table 1.

The unit cell parameters are a = 7.98A, b = 6.29A, c = 8.77A, α and γ = 90^{o}, and β = 102^{o}.[113] The space group is $P2_1/C - C_{2h}$.[112]

TPI crystals surface hydrochlorinated in acetone suspension produce the same x-ray pattern as the α TPI crystals. This indicates that only the amorphous surface regions of the crystal, which do not give a sharp x-ray pattern, have been reacted, having thus, no effect on the x-ray pattern of the crystalline core.

100% hydrochlorinated TPI was obtained by (a) hydrochlorinating TPI crystals in amyl acetate suspension at room temperature, where complete penetration of the HCl into the crystal core occurs,or by (b) hydrochlorinating the polymer in a chloroform solution, at room temperature, and casting a film of the resulting TPI hydrochloride. Both methods give the same x-ray pattern (figure 10), similar to the one found by Bunn and Garner for rubber hydrochloride [114] (see table 2). The crystal lattice is monoclinic with a = 5.83A, b = 10.38A, c = 8.95A, and β = 90°. The symmetry is $P2_1/C$.[114]

When TPI crystals are surface hydrochlorinated in amyl acetate suspension for long periods of time both the α x-ray pattern and the hydrochlorinated TPI pattern are apparently present.

When the hydrochlorinated crystal is dissolved and reprecipitated from any of the liquids mentioned in section III.4, either (a) a new x-ray pattern, identical to the pattern found for 100% hydrochlorinated TPI, but much weaker in intensity, emerges, or (b) the pattern looks very diffused, or cloudy, leading to the conclusion that the polymer is mostly amorphous (figure 11). In the first case, TPI crystals were suspended in amyl acetate and then hydrochlorinated, while in the second case they were suspended in acetone and reacted.

Figure 9: Typical wide angle X-ray diffraction pattern of α TPI crystals and surface reacted α TPI crystals.*

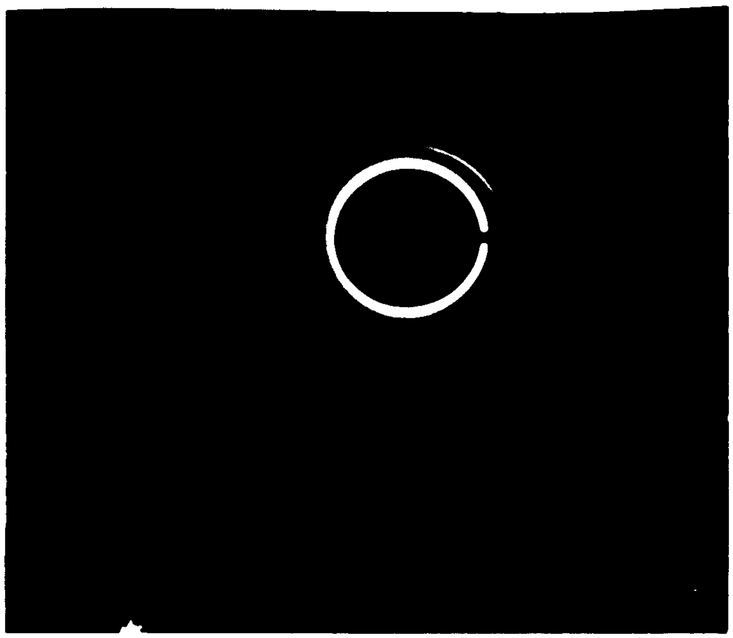

* Unfractionated synthetic TPI lamellas grown from an amyl acetate solution (0.07% W/V), at $T_c = 20^oC$, were used for the above pattern. Irradiation time was 15 hours; voltage and filament current used were 35KV and 15mA, respectively.

Figure 10: Typical wide angle X-ray pattern of 100% hydrochlorinated transpolyisoprene and of recrystallized hydrochlorinated TPI - TPI copolymer that has been hydrochlorinated in amyl acetate suspension.*

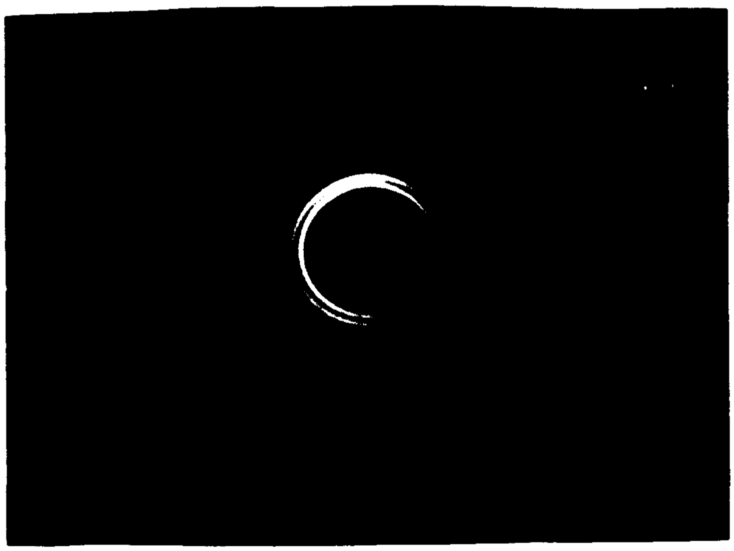

* The sample used in the above pattern was of an unfractionated synthetic TPI containing hedrites grown from an amyl acetate solution (1% W/V), at $T_c = 20^oC$, hydrochlorinated in amyl acetate suspension at 5^oC for 12 days, and reprecipitated from heptane at 20^oC. Irradiation time was 15 hours; voltage and filament current used were 35KV and 15mA, respectively.

Figure 11: Wide angle X-ray diffraction pattern of TPI lamellas hydrochlorinated in an acetone suspension and reprecipitated from 4-methyl-2-pentanone.*

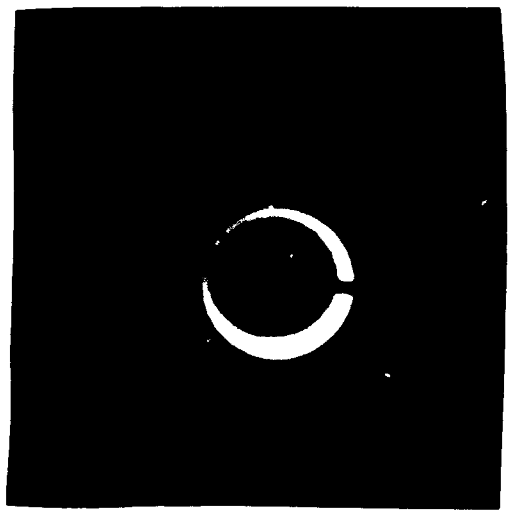

* The TPI lamellas were dilute solution grown from amyl acetate (0.07% W/V), suspended and hydrochlorinated in acetone at $-10^{o}C$ for 6 days, washed and dissolved in heptane to a redissolution temperature of $85^{o}C$, and reprecipitated at $20^{o}C$. Irradiation time was 15 hours; the voltage and filament current used were 35KV and 15mA, respectively.

Table 1: d - spacings of α TPI for the first six lines*

A crystals	B lamellas	C hedrites	D spherulites	E spherulites	F hkl
7.47	7.88	7.79	7.81	7.91	100
4.61	4.90	4.79	4.90	4.95	110
3.77	3.94	3.76	3.90	3.95	200
3.18	3.26	3.04	3.32	3.36	210
2.84	2.87	2.68	2.92	2.95	120
2.64	2.52	2.42	2.70	2.73	121

* d-spacings are given in angstroms (A).

A : unfractionated synthetic α TPI crystals. The d-spacings reported are an average of those from all x-ray patterns obtained. $M_n = 3.5 \times 10^4$. Lamellas were grown in 0.07%(W/V) amyl acetate solution with $T_D = 100^oC$, $T_R = 34^oC$, $T_C = 10, 20, 30^oC$. Hedrites were grown in 1% (W/V) amyl acetate solution with $T_D = 100^oC$, $T_C = 20^oC$.
d-spacings were calculated using the Bragg equation:

$$d = \lambda /2\sin[(\arctan(y/D))/2] \quad \text{equation 7}$$

where y is the experimental diameter of each line: 1.20, 2.00, 2.50, 3.05, 3.50, 3.85 cm (each line is an average value from all diffraction patterns obtained).

D is the diameter of the camera = 5.72cm

is 1.54A^{o}

B : C.C.Kuo, thesis, CCNY, 1985.[5] $M_n = 2.5x10^5$, 1% (W/V) amyl acetate solution. $T_D = 100^oC$, $T_C = 32^oC$.

C : C.C.Kuo, thesis, CCNY, 1985.[5] $M_n = 2.5x10^5$, 1%(W/V) amyl acetate solution. $T_D = 100^oC$, $T_C = 32^oC$.

D : Y. Takahashi et al.[113] Unfractionated Gutta Percha by melt crystallization.

a = 7.98 A, b = 6.29 A, c = 8.77 A, $\alpha = \gamma = 90^o$, $\beta = 102.0^o$

$$1/d^2 = 1/\sin^2 \beta(h^2/a^2 + k^2\sin^2 \beta/b^2 + l^2/c^2 - 2hl\cos\beta/ac) \qquad \text{eq. 8}$$

E : D. Fischer.[112] Unfractionated Gutta Percha.

a = 5.9 A, b = 7.9 A, c = 9.2 A, $\alpha = \beta = 90^o$ and $\gamma = 94^o$; this cell corresponds to the γ-structure proposed by Bunn.[114]

F : Miller indices.

Table 2: x-ray diffraction pattern diameters and d-spacings of 100% hydrochlorinated TPI and of reprecipitated block copolymers of surface hydrochlorinated α TPI crystals in amyl acetate suspension.

experimental[a]			literature[b]		
intensity	diameter (cm)	d-spacing (A)	intensity	d-spacing (A)	Miller index
s	1.90	4.83	vs	5.19	020
				5.08	110
s	2.20	4.22	vs	4.40	111
				4.49	021
m	2.80	3.40	s	3.39	022
				3.36	112
				3.55	102
m	3.50	2.80	s	2.90	200

vs: very strong, s: strong, m: medium

a : The experimental results are an average of all diffraction patterns obtained. The Bragg equation (eq. 4 or 7) was used to calculate the d-spacings.

b : Literature values were obtained from C.W.Bunn and E.V.Garner.[114]

$a = 5.83$ A, $b = 10.38$ A, $c = 8.95$ A, $\beta = 90^{o}$.

III.1.3. Differential Scanning calorimetry

Crystallization from amyl acetate solution by the precooling method at constant crystallization temperature, T_c, of 20 and 30°C yields one crystal form cnly, as evidenced by the appearance of a single DSC endotherm at approximately 58°C. An endotherm in the 56 to 63°C region has been identified previously [120,121] with unfractionated α -TPI . It has been shown that the endotherm value increases with increasing crystallization temperatures.[5] Crystallization by the direct method at constant T_c of 20°C showed a double melting endotherm between 50 and 60°C. The appearance of two peaks is probably due to the presence of a mixture of α and β crystals. Endotherms for β TPI crystals grown by the direct method have been previously identified [116,119] in melting regions slightly below those of α . This is explained further in chapter IV.1.

Surface hydrochlorinated TPI lamellas, grown at 30°C, showed a single endotherm at approximately 58°C. This is the same endotherm found for unreacted α lamellas. Since only the amorphous surface (which does not have an endotherm because of lack of crystallinity) has been reacted, no other endotherm is expected.

When the block copolymer is dissolved and reprecipitated from heptane or $CDCl_3$ no endotherm is seen.

This implies that no crystal ordering is formed upon reprecipitation of the block copolymer. The reprecipitated material is, therefore, amorphous.

Completely hydrochlorinated TPI lamellas cast from chloroform or precipitated from amyl acetate gives a single endotherm at 116^{o}C suggesting crystallinity of the product.

Figures 12-14 show the melting endotherm of TPI hedrites grown by direct crystallization at 20^{o}C, surface hydrochlorinated α TPI lamellas grown at 30 ^{o}C and reacted at -10^{o}C (or unreacted lamellas which give the same endotherm), and completely hydrochlorinated TPI lamellas, respectively.

Figure 12 : DSC scan of TPI hedrites grown from amyl acetate by direct crystallization.*

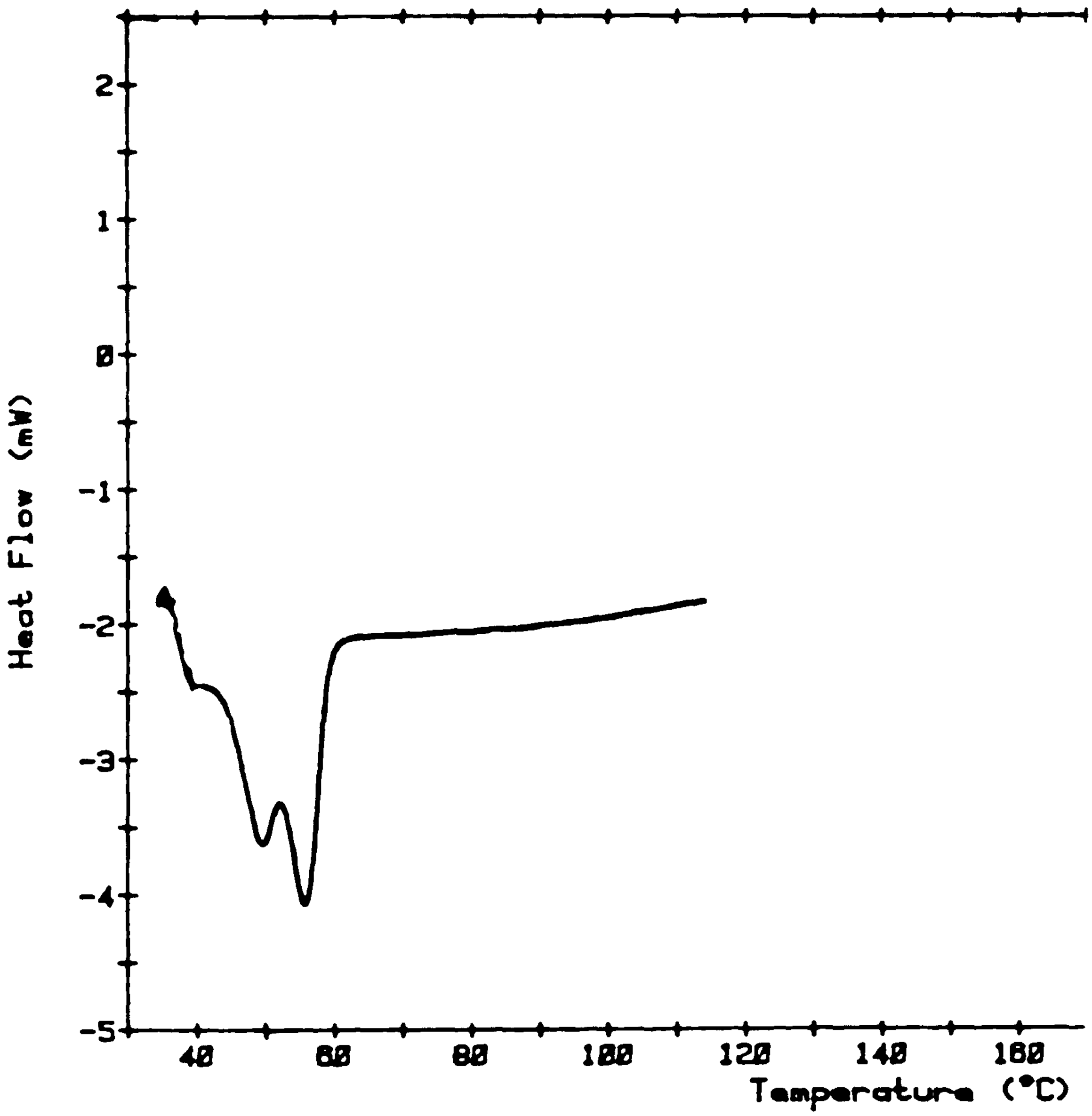

* A 1% (W/V) solution was used. $T_D = 100^oC$; $T_c = 20^oC$.

Figure 13: DSC scan of surface hydrochlorinated α TPI lamellas grown at 30^{o}C.*

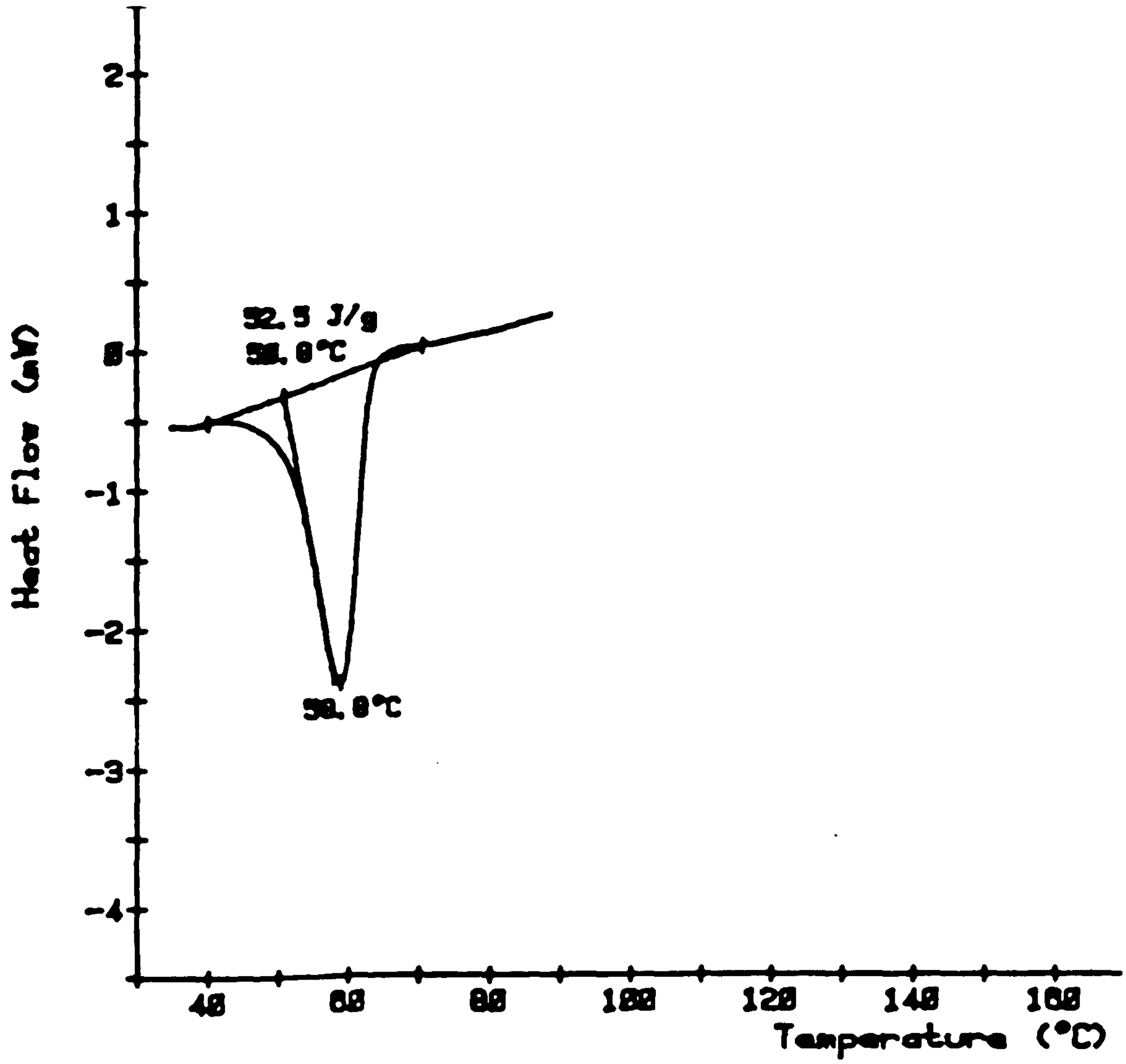

* A 0.07% (W/V) solution was used. T_D = 100^{o}C, T_R = 34^{o}C, T_c = 30^{o}C. The crystal was hydrochlorinated in an amyl acetate suspension at -10^{o}C. An identical thermogram is obtained with unreacted TPI lamellas grown as above.

Figure 14: DSC scan of 100% hydrochlorinated TPI.*

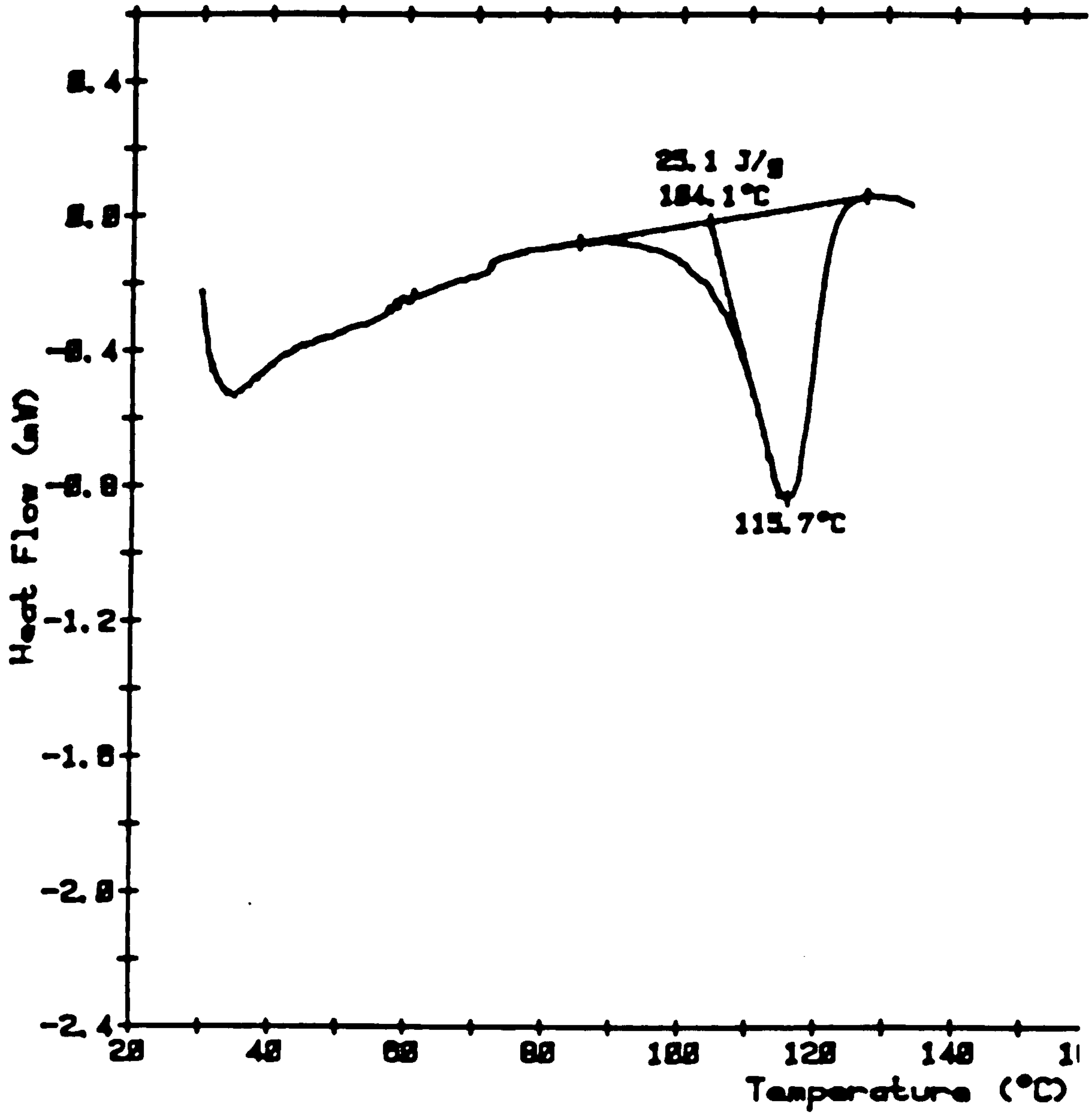

* TPI lamellas were used. They were surface hydrochlorinated in amyl acetate suspension at 20°C, and dried at room temperature.

III.2. Molecular weight determination:

Viscosity measurements:

The viscosities of TPI pellets and TPI crystals grown by the self seeding method at 10, 20 and 30°C were measured using the Ubbelohde viscometer. The results are listed in table 3, below. The pure solvent (toluene) flow time is 95.4 sec..

Table 3: The viscosity average molecular weight of TPI pellets and lamellas grown at different crystallization temperatures.

form	T_C (°C)	M_V *
pellets	-	1.87×10^5
crystals	10	1.90×10^5
crystals	20	1.95×10^5
crystals	30	2.20×10^5

* Each M_V is the average of three experimental results.

T_C represents the crystallization temperature, and M_V, the viscosity average molecular weight.

An example of the experimental results and calculations is given in appendix 6.

III.3. Density:

Density is a macroscopic quantity of a crystal which is linked directly to its unit cell parameters.[111,112,113] For TPI, the pure crystalline density of the α form at 25°C is 1.05 g/cm^3. The amorphous density, at 25°C, is extrapolated from the melt and is 0.905 g/cm^3, as established by dilatometry.[122] The density of the semicrystalline TPI sample increases with increasing crystallization temperature using either the precooling or the direct method. Since these crystals are composed of chain folding lamellas with crystalline and amorphous phases, the increase in density is caused mainly by the decrease in the amount of surface area (noncrystalline phase) in the crystal due to an increase in the crystal thickness. DSC measurements have previously shown [5,119] an increase in the melting endotherms with higher T_c's, indicating that indeed there is an increase in the crystal thickness. An increase in the latter is further shown in this work from ^{13}C NMR calculations on crystalline and amorphous block lengths (chapter III.7). Table 4 shows the density values obtained for lamellas and hedrites grown at different T_c's.

The weight fraction of the crystalline, W_c, and the noncrystalline, $(1 - W_c)$, components can be calculated from equation 9, and are also given in table 4.

$$W_c = \frac{\rho_c\ [\rho_s - \rho_a]}{\rho_s\ [\rho_c - \rho_a]} \qquad \text{equation 9}$$

ρ_s is the sample density obtained experimentally; the amorphous density, ρ_a, and the crystalline density, ρ_c, taken from literature, are 0.905 and 1.05 g/cm^3, respectively.

Table 4: Density, weight fraction of crystalline and noncrystalline components of TPI lamellas and hedrites, in the α form, grown from 0.07 and 1% (W/V) amyl acetate solution, respectively, at crystallization temperatures of 10, 20 and 30°C.

morphology	T_c(°C)	ρ_s	W_c	$1-W_c$
lamella	10	0.963	0.44	0.56
lamella	20	0.969	0.48	0.52
lamella	30	0.978	0.54	0.46
hedrite*	20	0.965	0.45	0.55
hedrite*	30	0.971	0.49	0.51

* note: In addition to the α morphology, hedrites grown here may contain some β TPI crystals. ρ_c for β TPI = 1.02g/cm^3 which would result in slightly higher W_c values.

III.4. Recrystallization / microphase separation

After hydrochlorination of the TPI crystal surfaces, in amyl acetate or acetone suspension, the resulting block copolymer was filtered, washed with a different liquid, and dissolved in that liquid by heating the suspension to its dissolution temperature. Table 5 enumerates the different liquids used. The polymers that dissolved were then cooled at $0^{o}C$ for one hour, heated again, slowly, to their redissolution temperature, and put in an isothermal bath, usually at $0^{o}C$, for a couple of days. The solutions were observed for any precipitation that may be a recrystallization of the copolymer. The redissolution temperatures of the copolymers in the different liquids were compared to the redissolution temperatures of TPI and 100% hydrochlorinated TPI in the same liquids, as shown in table 6.

A drop of the material in the liquid was placed on a glass slide and observed under the optical microscope. No regular features were observed.

The suspensions were further treated with osmium tetroxide, dried, and observed under the electron microscope. Osmium tetroxide reacts with the double bonds of the isoprene units, darkening them, and leaves the hydrochlorinated units unreacted. The electron microscope images again showed no regular patterns, sometimes only an evenly darkened area. The latter suggests that the block lengths are too small (5-17 monomer units, as calculated from ^{13}C NMR experiments) to be observed with the microscope if no regular aggregations occurred.

Wide angle x-ray patterns of the reprecipitated copolymers, that were hydrochlorinated in amyl acetate suspension, show a very weak pattern, containing lines identical to those found for the 100% hydrochlorinated TPI,suggesting a small amount of ordering. These block copolymers are believed to contain highly hydrochlorinated chains due to the 'peeling - off' of the outer layers of the crystals. These chains, in turn, crystallize and show the observed x-ray pattern. The results are further explained in chapter IV. Differential scanning calorimetry results, on the other hand, show no melting endotherm, suggesting, at best, a very disordered crystal.

X-ray analysis of reprecipitated copolymers that have been hydrochlorinated in an acetone media show little or no crystal pattern.

Table 5 : The redissolution temperatures and precipitation temperatures of TPI-hydrochlorinated TPI block copolymers in different liquids.

solvent	T_R (^oC)	T_p(^oC)
acetone	nonsolvent	-
amylacetate	33-34	0
carbon tetrachloride	30	
cyclohexane	RT	-
deuterated chloroform	RT	-
2-ethoxyethanol	nonsolvent	-
heptane	34-35, 85 *	20
hexane	nonsolvent	-
isooctane	80 *	-
methyl alcohol	nonsolvent	-
methyl oleate	120	-
4-methyl-2-pentanone	32	0
tetradecane	120 *	20
toluene	RT	-
water	nonsolvent	-
xylene	RT	-

T_R represents the redissolution temperature; T_p, the precipitation temperature; RT, room temperature.

table 5 ,continuation

* These solutions showed a small quantity of an insoluble residue. It is to be noted also that heptane dissolved the copolymer in two stages: there was an initial partial clearing of the suspension at approximately 35°C, followed by a final clearing at 85°C.

Solvents without a precipitation temperature value did not precipitate at, or above, 0°C. The concentrations used were approximately 1% (W/V).

Table 6 : Redissolution temperature of TPI, 100% hydrochlorinated TPI, and TPI-hydrochlorinated TPI block copolymers with different solvents.

solvent	a T°C	b T°C	c T°C
acetone	NS	NS	NS
amylacetate	34	75	33-34
deuterated chloroform	RT	RT	RT
heptane	39	NS	34-35,85
4-methyl-2-pentanone	49		32

Columns a, b, c represent the redissolution temperatures of TPI, 100% hydrochlorinated TPI, and TPI-hydrochlorinated TPI copolymers, respectively. NS = nonsolvent; RT = room temperature. The concentrations used were approximately 1% (W/V). The temperatures are given in degrees Celsius.

III.5 ^{1}H NMR spectroscopy:

Proton NMR spectra were taken as a qualitative measure of the different types of protons present in the polymer solution. The ratio of the areas under each NMR resonance peak is proportional to the number of similar hydrogens present in the compound.

Chemical shifts for the CH, CH_2, and CH_3 groups in TPI are given in table 7. Also shown are the CH_2 and CH_3 chemical shifts in 100% hydrochlorinated TPI, and the CH, CH_2 and CH_3 block copolymer resonances.

The protons were enumerated, following the backbone of the monomer unit, as follows:

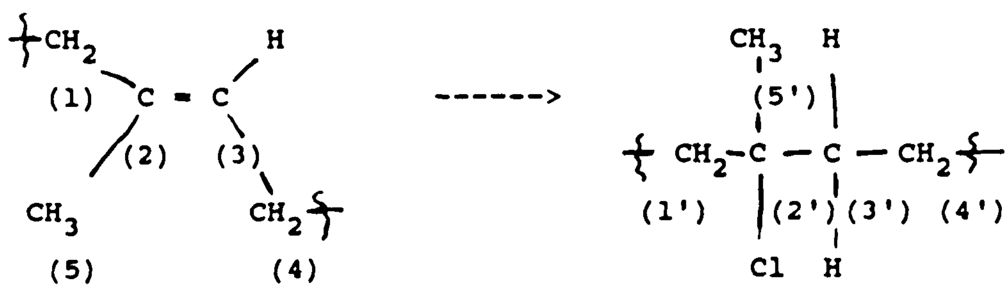

TPI, 100% hydrochlorinated TPI, and HCl-TPI-TPI block copolymer proton NMR spectra are shown in figures 15 - 17.

Table 7 : ^1H NMR chemical shifts for TPI, surface hydrochlorinated TPI, and 100% hydrochlorinated TPI.

		chemical shift (ppm)		
carbon #	Proton	TPI	100% HCl-TPI	HCl-TPI-TPI copolymer
3	CH	5.1	-	5.1
1,4	CH_2	2.0	-	2.0
1',3'	CH_2	-	1.7	1.7
4'	CH_2	-	1.65	1.65
5	CH_3	1.6	-	1.6
5'	CH_3	-	1.5	1.55

Figure 15: 100MHz proton NMR spectrum of unfractionated synthetic 1,4-transpolyisoprene dissolved in $CDCl_3$ (1% W/V).

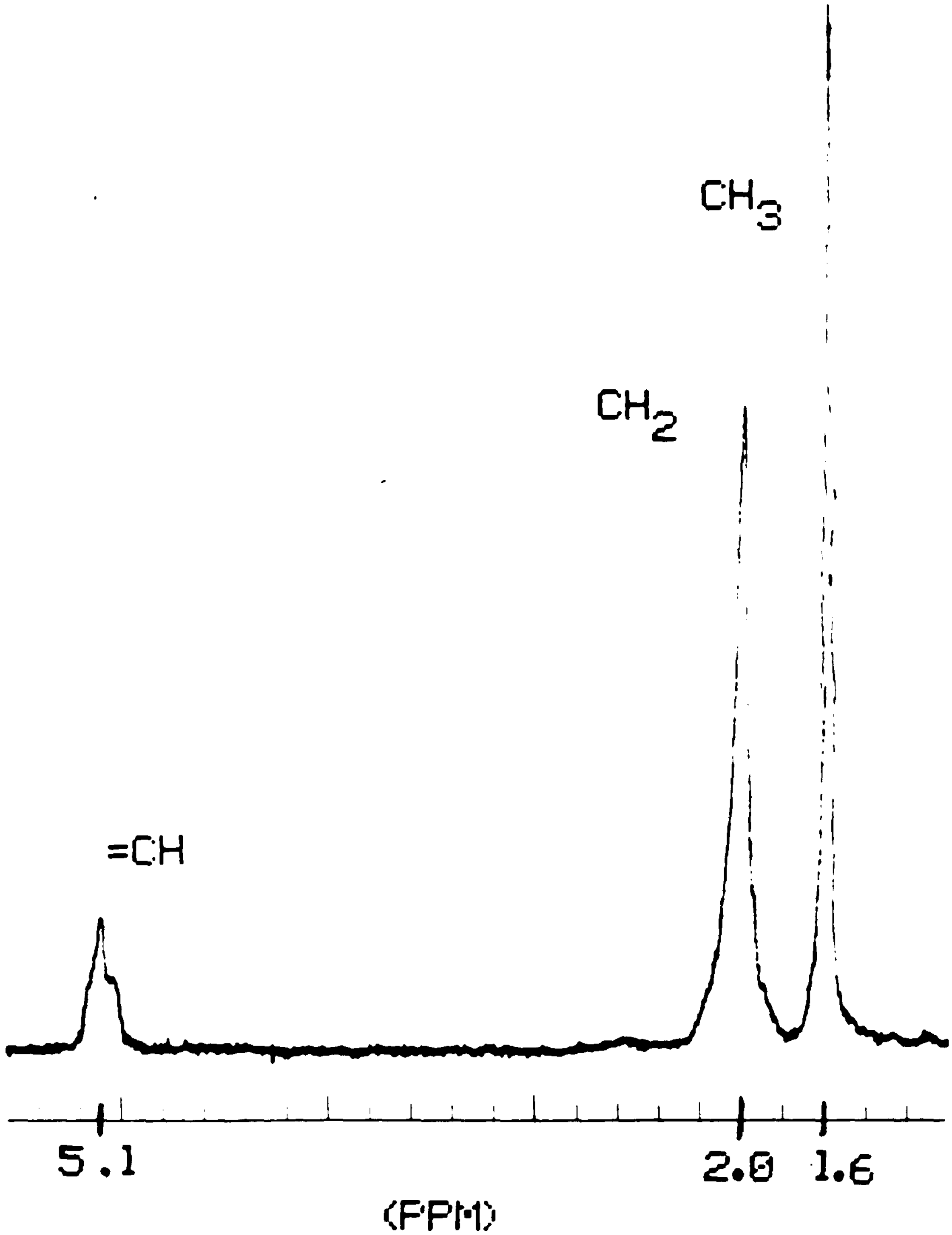

Figure 16 : 200MHz proton NMR spectrum of 100% hydrochlorinated unfractionated synthetic TPI dissolved in $CDCl_3$.

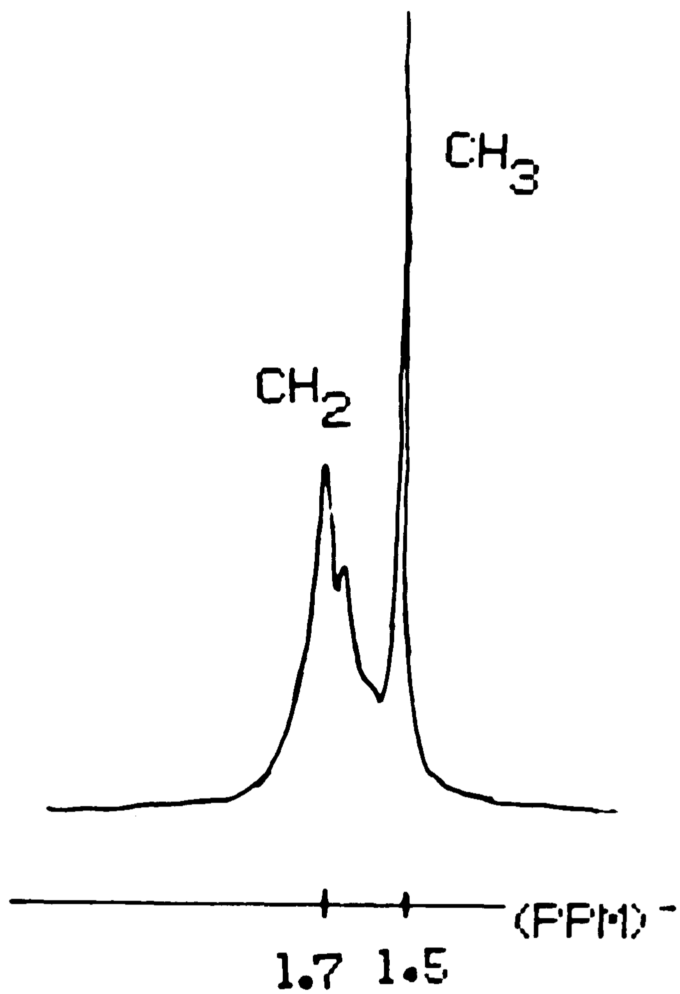

Figure 17 : 200MHz proton NMR spectrum of surface hydrochlorinated TPI block copolymer crystals dissolved in $CDCl_3$.*

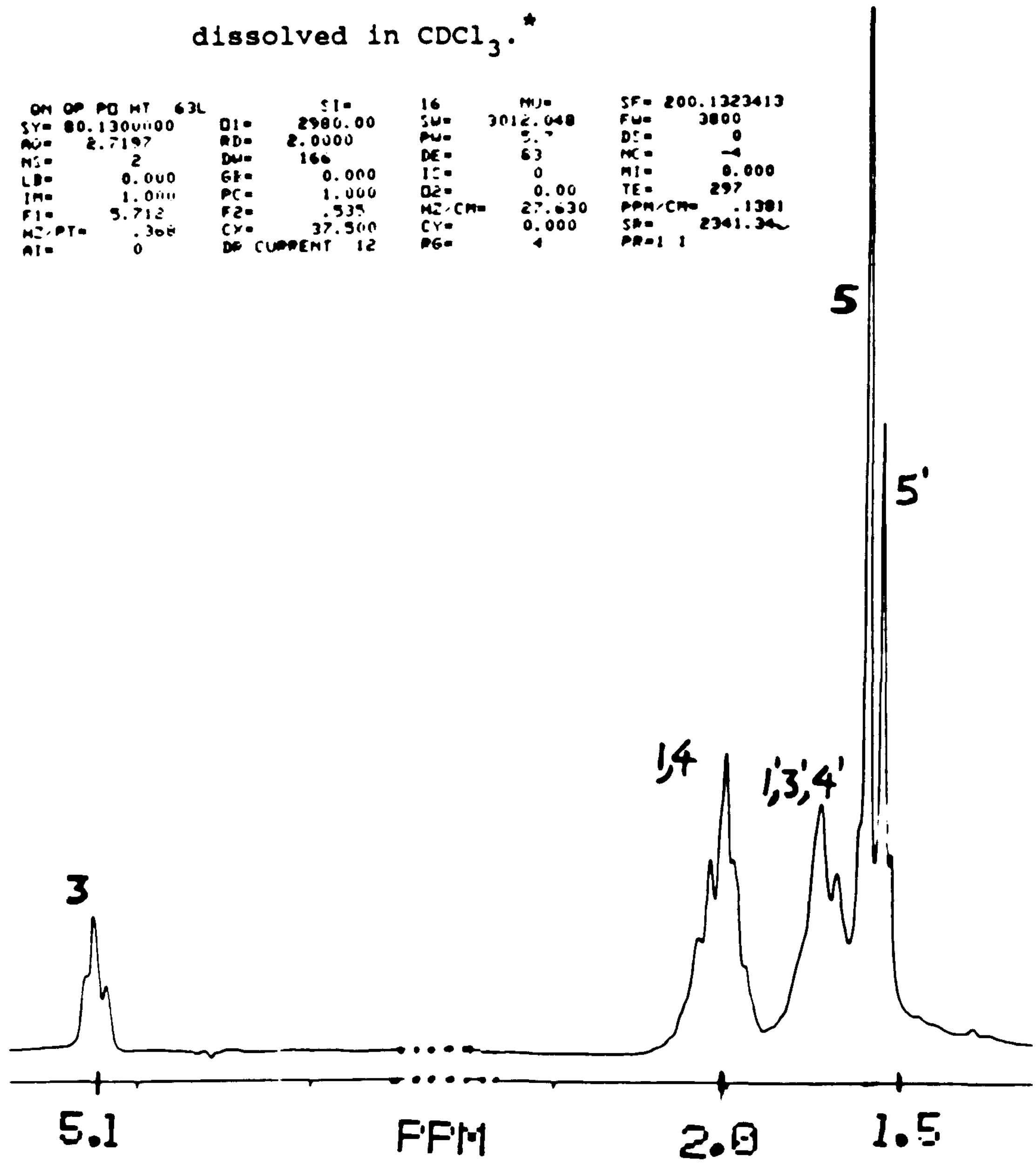

*A 0.07% (W/V) solution was used to grow the lamellas. T_c=20°C; $T_{reaction}$=-10°C in amyl acetate suspension.

While there is an upfield shift of the hydrogens on conversion from sp_2 (unhydrochlorinated) to sp_3 (hydrochlorinated) bonding, there is an opposing force, or a deshielding, due to the introduction of the chlorine atom upon hydrochlorination. A methyl group bonded to an sp2 carbon is shown to shift from 1.7ppm to 1.0ppm when the double bond is replaced with a hydrogen, or to 1.3ppm when the former is replaced with a chlorine atom:[123]

```
                        ------>  C - C - CH3 (1.0ppm)
                                     |
C = C - CH3                          H

     (1.7ppm)
                        ------>  C - C - CH3 (1.3ppm)
                                     |
                                     Cl
```

The result of the two opposing forces in the hydrochlorinated TPI is an overall slight upfield shift of the methyl and of the methylene groups. The former (#5) shifts from 1.6 to 1.5 ppm while the latter goes from 2.0 to 1.65 - 1.7 ppm. The =CH (#3) group converts to an sp3 CH2 upon hydrochlorination, shifting from 5.1 to 1.7ppm. Methylene hydrogens #1 and #4 in TPI show one multiplet at 2.0ppm. This splitting into a multiplet is due to coupling of the nearest hydrogens. The amount of splitting though, is not clearly defined by the spectra. Upon hydrochlorination of two or more consecutive TPI monomer units the newly formed CH2 #3' is now equivalent to

CH_2 #1 shifting upfield by 0.3 ppm. Nonequivalent methylene hydrogens #4' appear, as one peak, separately, at 1.65ppm. Hydrogen atoms at junction points in the polymer (between reacted and unreacted monomer units) may be considered, at first glance, as a possible cause for this peak. However the appearance of the same peak, not just in the copolymer, but in the 100% hydrochlorinated TPI, where there are no junctions, eliminates this conclusion.

Upon close examination of the two methyl peaks (#5 and 5') two extra peaks may be observed. These appear at the baseline upfield of methyl #5' and downfield of methyl #5 in the block copolymer. These extra resonances are absent in TPI and in 100% hydrochlorinated TPI. The upfield region of the block copolymer spectrum is shown in figure 18.

A reasonable explanation for the presence of these two side peaks may be the ability of the spectrometer to distinguish between the methyl protons in the crystalline stem (#5), in the fold region (#5'), and by the junctions between reacted and unreacted monomer units. The observed chemical shifts for A and B can be reasoned by examining their position in the block copolymer chain:

```
  B                       A

 CH3           CH3       CH3
  |             |         |
=C-CH2-CH2-CH2-C-.........C-CH2-CH2-CH=
                |         |
               Cl        Cl

...stem...][.......fold............][...stem......
```

Similar to the chemical shift positions between methyl hydrogens #5 and #5', junction methyl A is more shielded than B since the former is bonded to an sp_3 carbon (-CCl-) while the latter is bonded to an sp_2 carbon (=C). Upon complete hydrochlorination of the polymer the two peaks disappear (see figure 16). This is expected, since no junctions are possible in 100% hydrochlorinated TPI.

Figure 18: Proton NMR spectrum of the methyl region of hydrochlorinated TPI-TPI block copolymers.

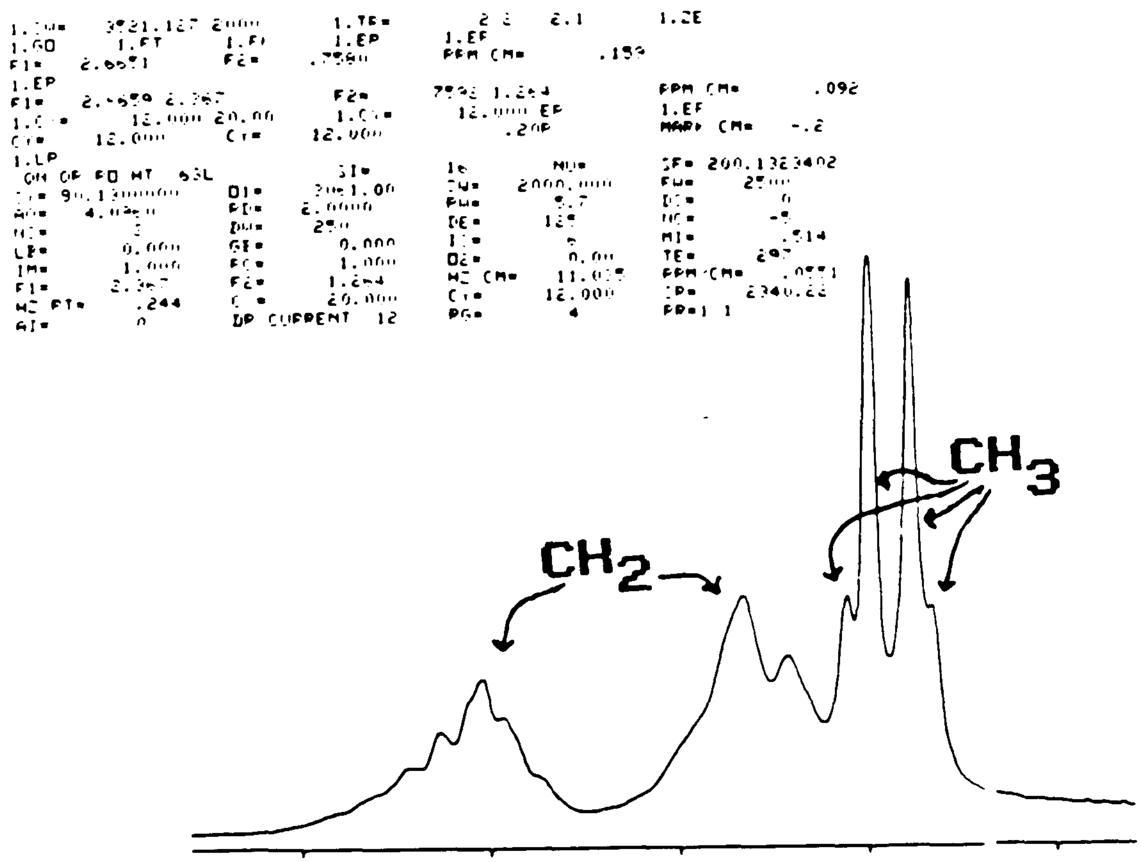

III.6. Carbon -13 NMR spectroscopy

Carbon-13 NMR spectroscopy was used to provide detailed and quantitative information on the block copolymers under study. The principal objective is the determination of the crystalline stem length and the amorphous surface fold length of trans-1,4-polyisoprene crystals grown in solution. The spectra obtained were analysed and compared to similar work done with epoxidized TPI and TPBD in solution and in suspension, solution hydrochlorinated cis- and trans- polyisoprene, and model compounds such as squalene. These are referred to and detailed in the introduction and discussion.

The 50.33 MHz carbon-13 NMR spectra of 100% hydrochlorinated trans-1,4-polyisoprene dissolved in deuterated chloroform is shown in figure 19. Complete hydrochlorination of TPI may be obtained by hydrochlorinating the polymer dissolved in solution or by hydrochlorinating the crystal at room temperature. Both give the same spectra. Figure 20 exemplifies the spectrum of a suspension hydrochlorinated TPI crystal, where all surface folds have been reacted.

figure 19: 50.33 MHz ^{13}C NMR spectral regions of completely hydrochlorinated trans-1,4-polyisoprene.*

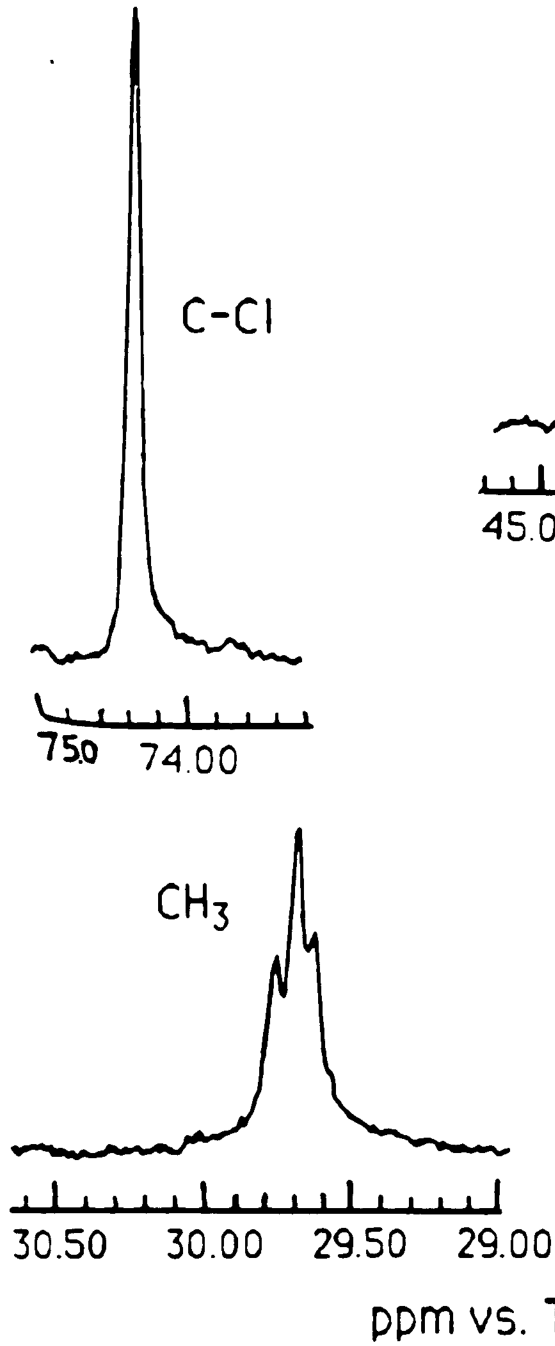

* hydrochlorination in amyl acetate suspension at 20°C.

Figure 20 : 50.33 MHz ^{13}C NMR spectrum of suspension hydrochlorinated trans-1,4-polyisoprene crystals.*

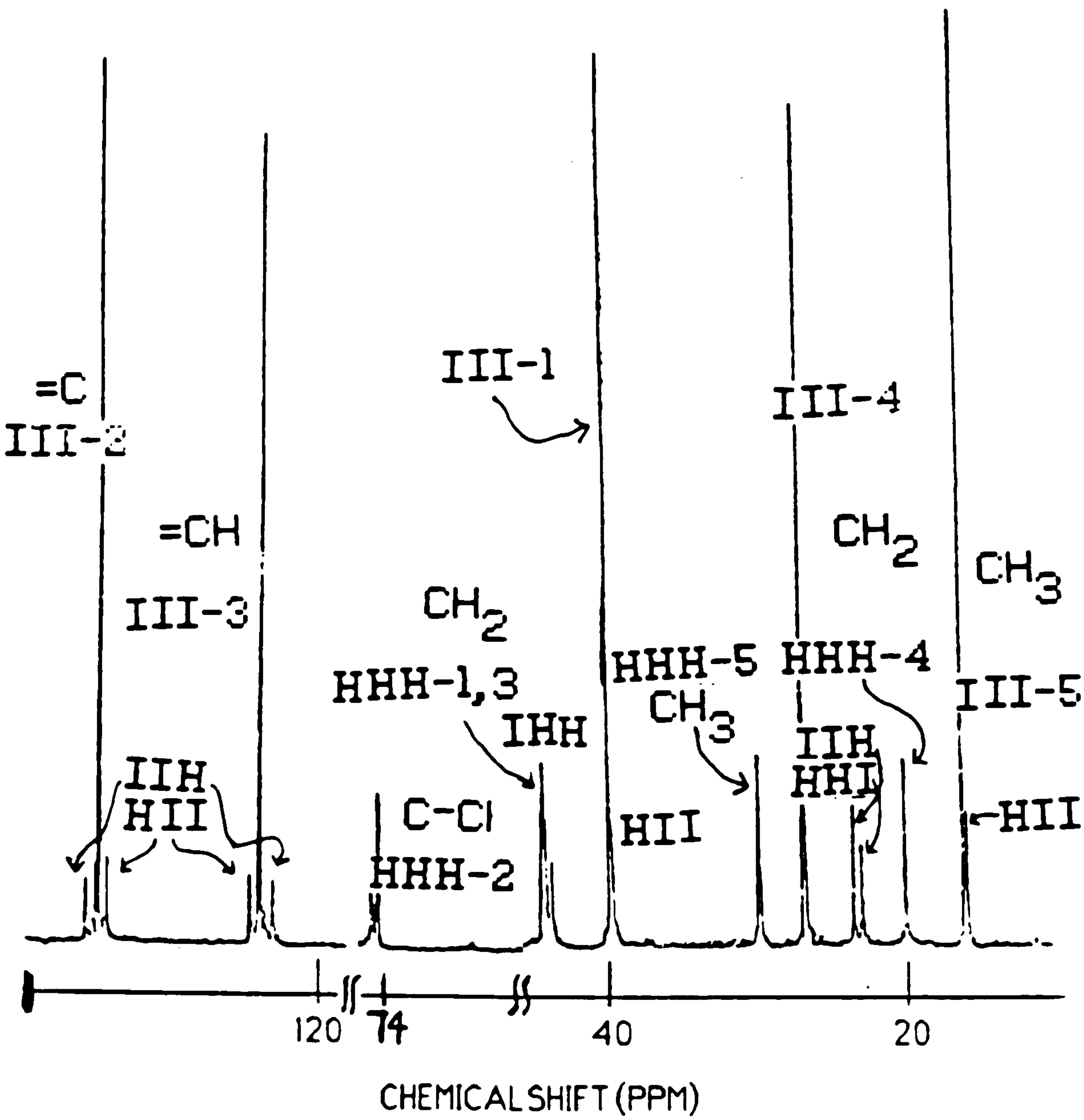

*lamellas grown from amyl acetate (0.07%(W/V)) solution, T_c = 20°C, $T_{reaction}$ = -10°C in acetone suspension.

All peaks are assigned and tabulated with their respective chemical shifts, as shown in table 8. These include results obtained from randomly hydrochlorinated TPI in solution to different degrees of completion, completely reacted TPI, and surface hydrochlorinated TPI crystals in suspension. If I represents an isoprene monomer unit, III designates an isoprene unit between two isoprene units.

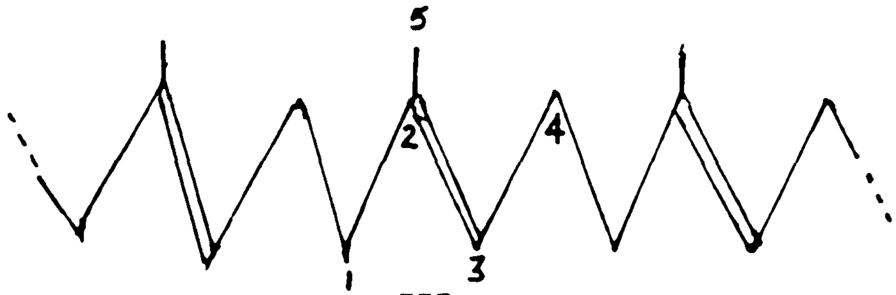

III

Likewise, H represents a hydrochlorinated isoprene monomer unit, while HHH becomes a hydrochlorinated unit between two hydrochlorinated units.

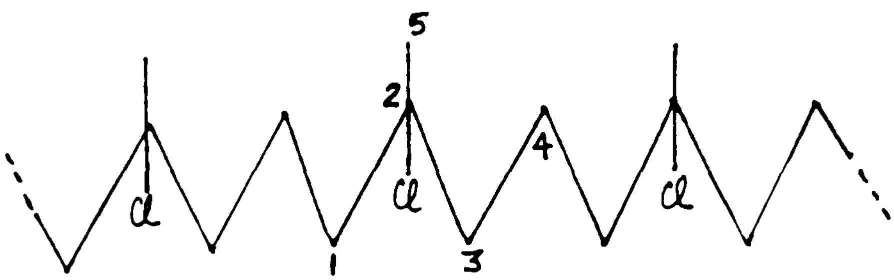

HHH

HHI symbolizes a hydrochlorinated unit with a hydrochlorinated unit on one side and an isoprene unit on the other side. IIH represents a carbon atom in an isoprene unit with an isoprene unit on one side and a hydrochlorinated unit on the other side.

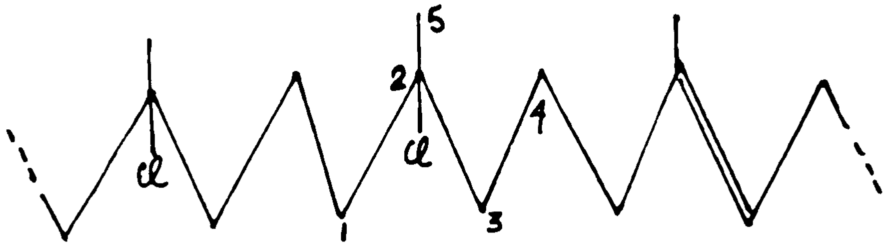

HHI

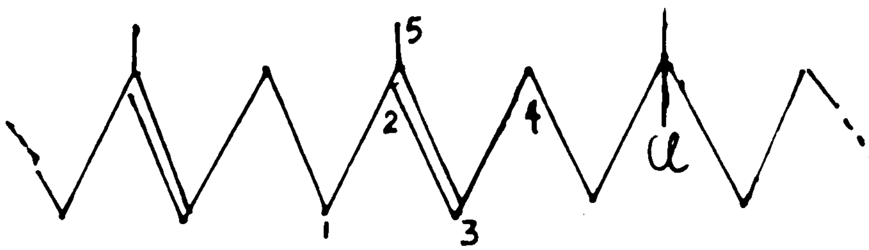

IIH

The enumeration of each carbon in the repeat unit are shown below:

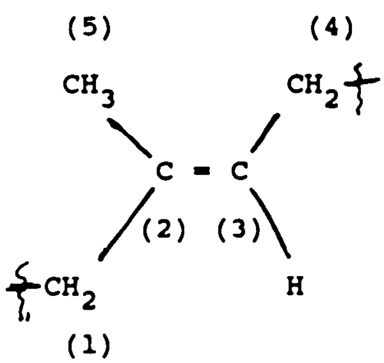

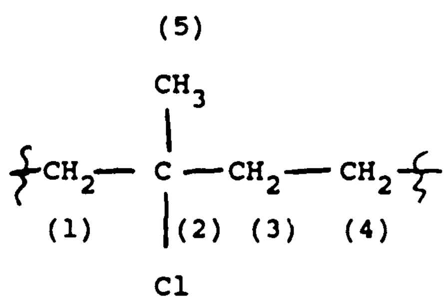

As an example, the region of absorption in the spectrum denoted III-5 refers to the methyl group in an isoprene unit in an isoprene sequence. Likewise, IIH-5 is the methyl group in an isoprene unit with an isoprene unit on one side and a hydrochlorinated unit on the other side.

Table 8 : Carbon - 13 NMR frequencies and assignments for partially and completely hydrochlorinated trans-1,4-polyisoprene.

Assignment	chemical shift (ppm)				
	solution reaction			suspension reaction	
	19%	34%	70%	100%	(28%)
IIH-2	135.70	135.66	135.65	-	135.78
HIH-2	135.30	135.27	135.29	-	-
III-2	134.92	134.92	-	-	134.90
HII-2	134.45	134.46	134.49	-	134.37
HII-3	124.70	124.70	124.60	-	124.81
III-3	124.24	124.17	-	-	124.25
HIH-3	123.82	123.85	123.78	-	-
IIH-3	123.35	123.37	123.33	-	123.29
IHI-2	74.74	74.70	74.66	-	-
IHH-2	74.74	74.70	74.66	-	74.65
HHI-2	74.38	74.33	74.27	-	74.22
HHH-2	74.38	74.33	74.27	74.19	74.22
HHH-1,HHH-3	-	44.29	44.21	44.31	44.25
(r,m)	-	44.10	44.09	44.21	44.13
HHI-1,IHH-3	43.98	43.99	43.97	-	44.00
IHI-3	43.98	43.98	43.97	-	-
IHH-1,HHI-3	43.55	43.56	43.64	-	43.69

table 8, cont.

IHI-1	43.55	43.56	43.64	-	-
III-1,IIH-1	39.75	39.70	39.63	-	39.74
HII-1	39.58	39.59	39.54	-	39.60
HHH-5	-	29.78	29.77	29.78	29.77
(rr,mm,				29.70	29.69
mr,rm)				29.64	29.61
IHI-5	29.78	29.78	29.76	-	-
IHH-5,HHI-5	29.78	29.78	29.76	-	29.77
III-4,HII-4	26.72	26.72	26.54	-	26.73
HIH-4	23.42	23.42	23.41	-	-
IIH-4	23.42	32.42	23.41	-	23.43
IHI-4	22.91	22.90	22.87	-	-
HHI-4	22.91	22.90	22.87	-	22.91
IHH-4	20.04	20.04	20.03	-	20.03
HHH-4	-	20.04	20.03	20.07	20.03
III-5,IIH-5	16.03	16.02	15.96	-	16.03
HIH-5	15.83	15.82	15.83	-	-
HII-5	15.83	15.82	15.83	-	15.80

When two chlorine atoms are present adjacent to each other four isomers are possible. These isomers are shown in figure 21, where a and b form a pair of enantiomers as do c and d. Each of these pairs of mirror images cannot normally be distinguished by NMR without a chiral shift reagent or chiral solvent. The two pairs are, however, diastereomers and these are spectroscopically distinct from each other. A splitting in the resonance peaks is therefore expected. Hydrochlorinated methylene carbons HHH-1,3 show such a doublet, as seen in figure 21. This shows that HHH-1,3 is sensitive only to the chirality of the $C(CH_3)$-Cl in the closest connecting unit. The doublet is seen in partially hydrochlorinated TPI in solution, in surface hydrochlorinated TPI in suspension, and in 100% hydrochlorinated TPI. Both III-1 and III-3 do not show a stereochemical peak, as expected.

Figure 21: 50.33 MHz Carbon-13 NMR spectrum of the methylene HHH-1,3 region of hydrochlorinated TPI and a diagram representing the two diastereomers.

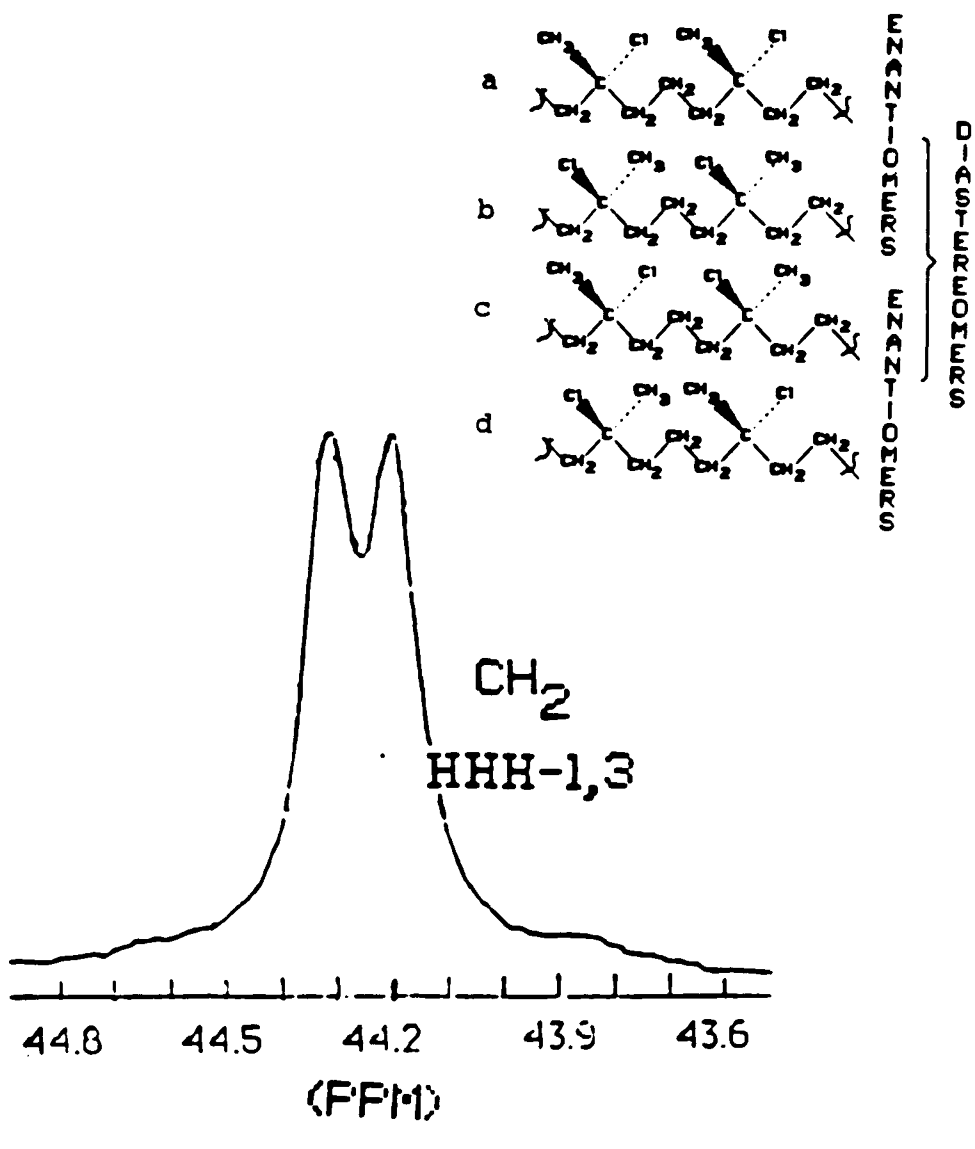

Methyl carbon #5 in hydrochlorinated TPI, designated HHH-5, shows a sensitivity to triad sequences; in other words, the methyl in the middle unit of HHH-5 shows a sensitivity to the chirality of the closest connecting units on both directions on the chain. This is evidenced by the triple resonance observed in the spectrum, as shown in figure 22. When three chlorine atoms are present, in three adjacent monomer units, three spectroscopically distinct combinations are possible: racemic-racemic (rr), meso-meso (mm), meso-racemic (mr) or racemic-meso (rm). The arrows in figure 21 pointing up or down represent the chlorine atom in one of the two possible geometric configurations (i.e. in or out of the plane of the paper, depending on the side of the chlorine attack). The sequence of arrows down-up-down or up-down-up are indistinguishable and gives rise to one peak (rr). Likewise, arrows up-up-up or down-down-down form another indistinguishable peak (mm). Up-up-down or down-down-up (mr) are indistinguishable as are down-up-up or up-down-down (rm). The sequences mr and rm are also spectroscopically unresolved and give one peak with twice the intensity of the rr or the mm resonances. Thus, the expected ratio is 1:2:1 for mm:mr-rm:rr. This is indeed observed (figure 21). The triplet is seen on copolymers in solution and in suspension, and in 100% reacted TPI. Due to lack of chirality, unreacted TPI shows a singlet for the corresponding III-5 sequence, as expected.

Figure 22: 50.33 MHz Carbon-13 NMR spectrum of the HHH-5 region of hydrochlorinated TPI and a diagram representing the observed stereochemical splittings.

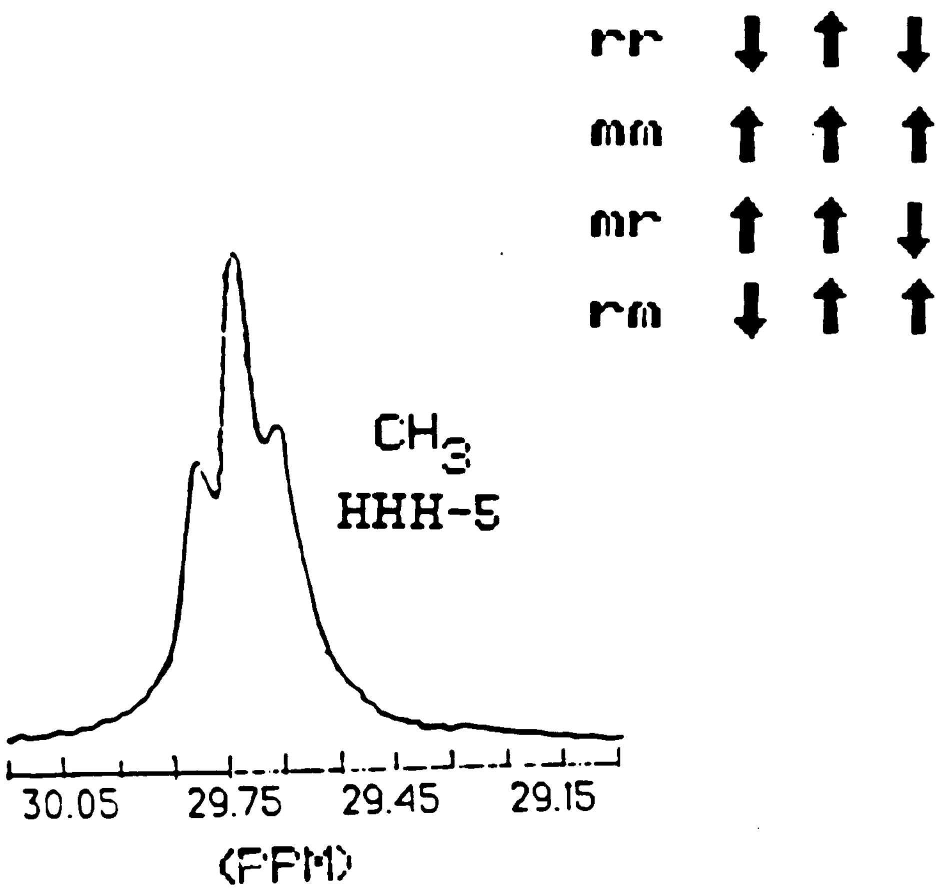

Solution hydrochlorination of TPI to various degrees of completion were studied with NMR in order to help in the identification of all the different junction peaks present, which may also occur in the surface hydrochlorination of the TPI crystals. The completely hydrochlorinated sample is expected to show four regions of absorption: HHH-5, HHH-4, HHH-1,3, and HHH-2. These are found at 20.07, 29.70, 44.26, and 74.19ppm. Partial solution hydrochlorination leads to various new peaks, which include, among the III- and HHH- peaks, junction peaks such as IHH-, HHI-, IIH-, and HII- peaks, which also appear in the hydrochlorinated block copolymer spectra. Also included in the partially solution hydrochlorinated TPI spectra are peaks due to IHI- and HIH- sequences, representing a carbon in an isolated hydrochlorinated unit with unreacted units on either side, or vice versa .

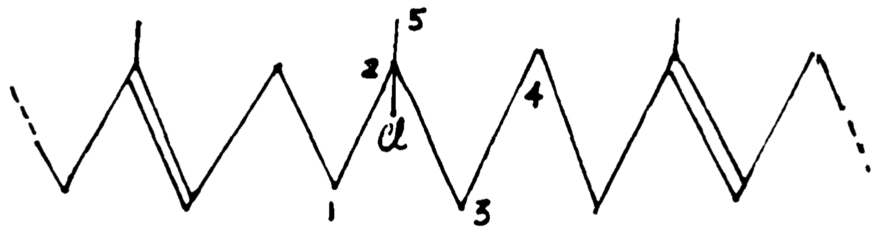

IHI

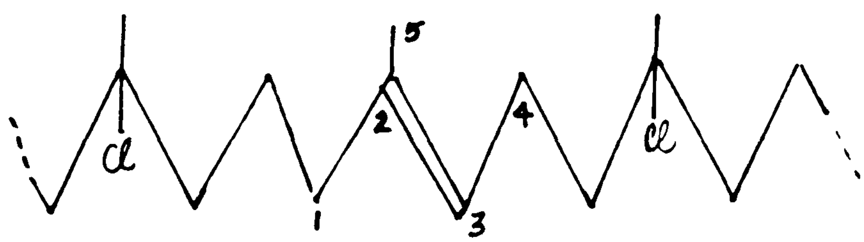

HIH

Such sequences are indicative of random hydrochlorination within the chain. The absence of resonances corresponding to these sequences in the block copolymer confirms that hydrochlorination of the surfaces of the crystal has been complete, and that no reaction of the crystalline core has occurred. Carbons #2 and #3 clearly demonstrate the occurrence of these absorption peaks, as shown in fig. 23.

Figure 23: Sequential splittings in the olefinic carbon region of the 50.33 MHz ^{13}C NMR spectrum of partially hydrochlorinated TPI.

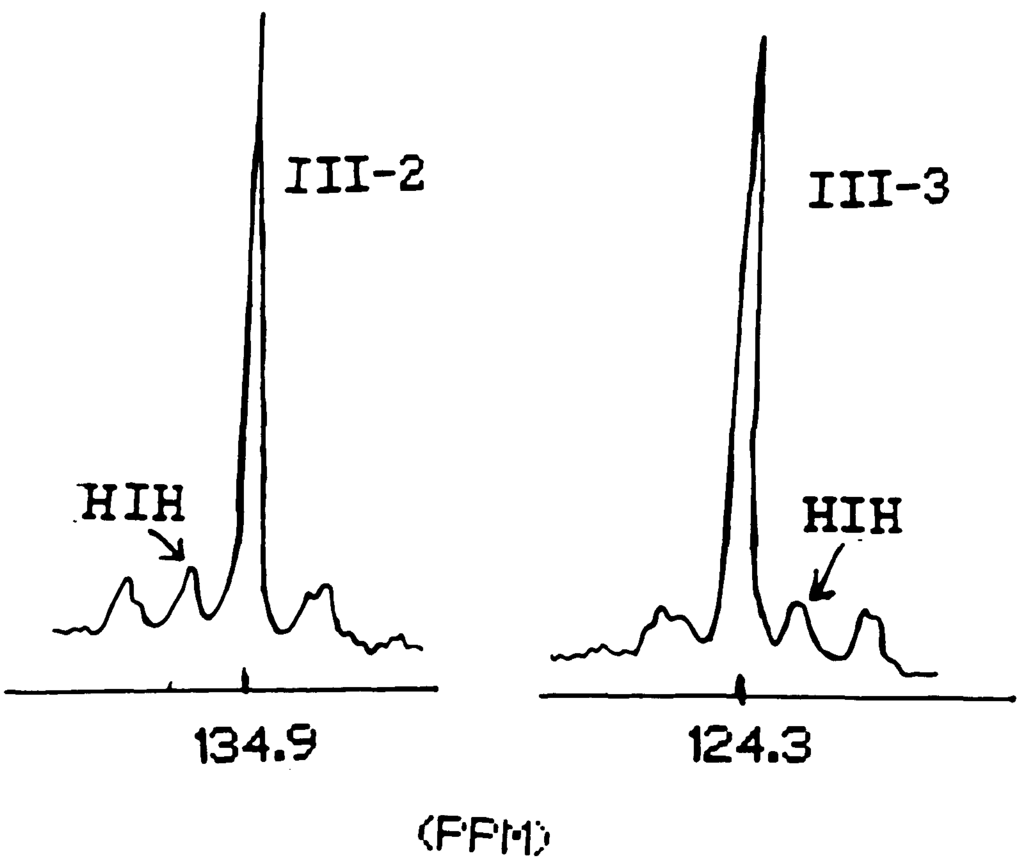

Carbon #2 and #3 in the isoprene unit in the junction with a hydrochlorinated monomer unit (IIH-2 and HII-2, IIH-3 and HII-3) is seen as the outer peaks on either side of the III-2 and III-3 isoprene sequences. These are present in suspension hydrochlorination of TPI crystals, and in different amounts for the various degrees of hydrochlorination in the solution reacted polymer (figure 24). The remaining peak can only be due to the carbon in an isoprene unit surrounded by hydrochlorinated units, the HIH-2 and the HIH-3. These peaks are found, in measurable quantities, only in solution hydrochlorinated TPI, and periodically in suspension hydrochlorinated crystals where amyl acetate was used as the suspending liquid. Figure 23 was obtained from the first type of sample where 19% of the polymer has been reacted. Suspension hydrochlorination in acetone does not show the HIH peak. Figure 24 compares the olefinic and reacted carbon regions of the hydrochlorinated lamellas in acetone suspension to the hydrochlorinated polymer in solution to 19%, 34% and 70%. It can be seen that the block copolymer (spectrum d) shows no measurable quantities of HIH in the unreacted spectral region, or of IHI in the chlorinated region; it shows a small quantity of junction peaks (IIH and HII, and HHI and IHH). The principal resonances are due the III and HHH sequences. At 19% hydrochlorination, most of the sequences are still isoprene units, III-2 and III-3. Junctions are also seen, as explained above. In the hydrochlorinated region, junctions IHI-2 and IHH-2 are more prominent than the HHH-2 (and HHI-2) which are practically absent. At this stage of random reactivity it is rare to find many HHH sequences. At 34% hydrochlorination in solution, the polymer shows four equal resonances for each of the olefinic sequences: IIH-2, HIH-2, III-2, HII-2, and HII-3, III-3, HIH-3, IIH-3. The hydrochlorinated carbon #2 shows 2 peaks, the larger due to IHI-2 and IHH-2, and the much smaller one due to HHI-2 and the hydrochlorinated sequence HHH-2. At 70% hydrochlorination in solution, the III resonances of the olefinic region disappear; the HIH becomes the most prominent peak: the IIH and HII are also very visible. The hydrochlorinated carbon #2 now shows a more pronounced HHH-2 (and HHI-2) resonance peak, approximately equal in intensity to the IHI-2 and IHH-2 peak.

Figure 25 shows the methylene spectral region of the unreacted sequence, III-1, and the hydrochlorinated region of HHH-1,3. The spectra include solution hydrochlorinated TPI to various degrees and crystals surface reacted in acetone suspension. In the block copolymer spectrum, the HHH-1,3 stereochemical splitting is slightly downfield of the satellite junction peaks HHI-1 and IHH-3, and the more clearly defined IHH-1 and HHI-3 peaks. Junction HII-1 appears slightly upfield of the main peak, III-1. The sensitivity of the spectrometer to distinguish the HII-1 resonance suggests that IIH-1 should also be detected. The latter is most probably masked by the III-1 peak. For partial solution hydrochlorination the junction peaks increase relative to the I and H sequences, as expected. In addition, IHI-1 and IHI-3, not found in suspension hydrochlorination, should be included in the total resonance area of the junctions. At 19% solution hydrochlorination, where most H units present are isolated, the HHH-1,3 doublet is absent; only junction peaks appear at this stage.

Chemical shift resonances due to carbon #4 and #5 are also shown in figure 25. At 19% of hydrochlorination the triplet expected for HHH-5 is absent; the singlet observed is due to junction sequences. III-5 and III-4 are large, while HHH-4 is practically absent. Junction sequences due to carbon #4 are relatively large. At 34% of hydrochlorination, the polymer contains an equal amount of III-5 and HII-5, while at 70% the amount of III- sequences found has decreased markedly. Similarly III-4 decreases while HHH-4 increases with an increase in the random hydrochlorination. The IIH-4 and HHI-4 peaks are large, suggesting a truly random hydrochlorination; these are small when the crystal is surface reacted and the only junctions are those between the surfaces and the crystal core.

Figure 24: Olefinic and hydrochlorinated carbon region of the 50.33 MHz ^{13}C NMR spectrum of: a) 19% b) 34% c) 70% solution hydrochlorinated TPI, and d) 28% suspension hydrochlorinated TPI lamellas.

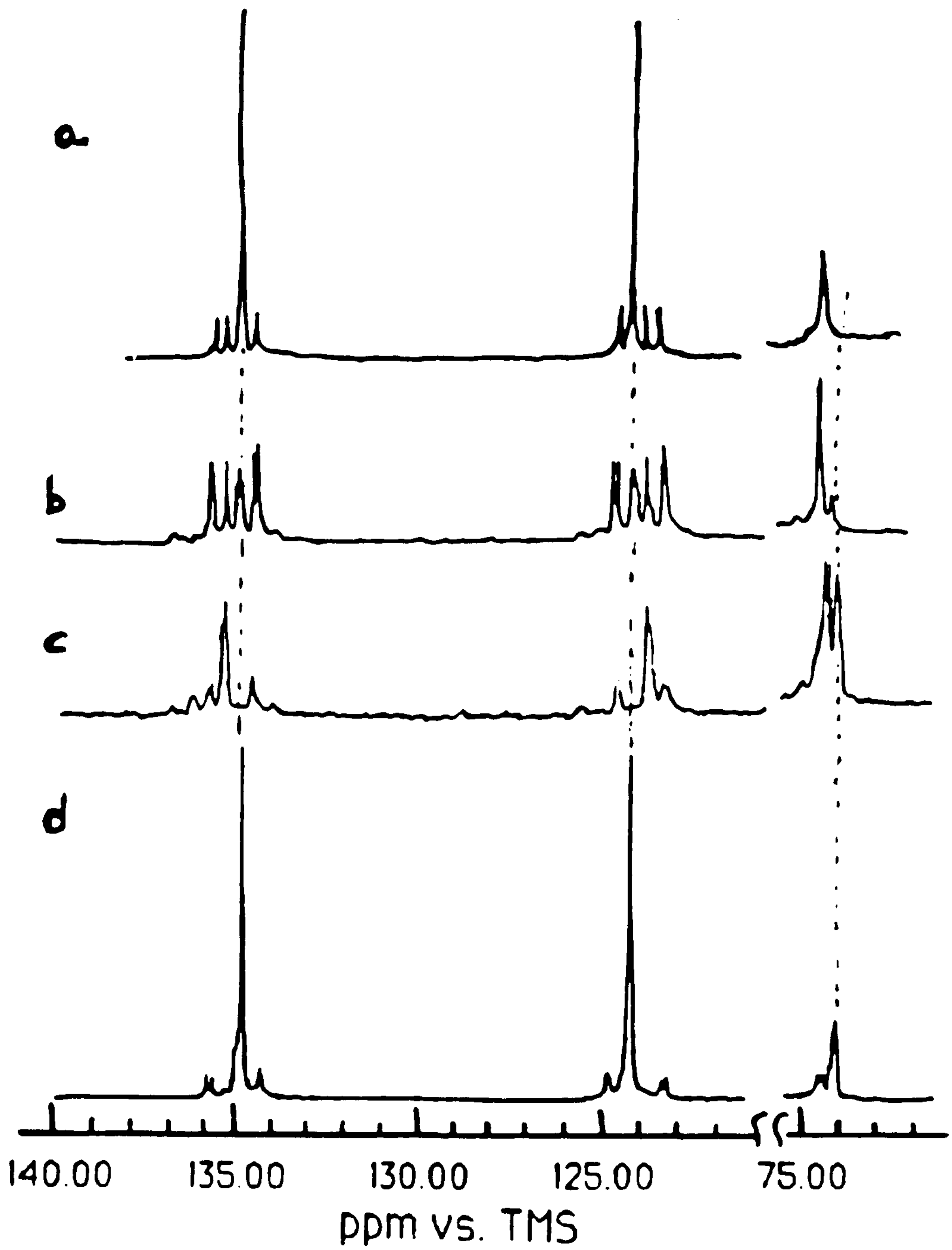

Figure 25: Alkyl carbon region of the 50.33 MHz ^{13}C NMR spectrum of a) 19% b) 34% c) 70% solution reacted TPI and d) 28% acetone suspension reacted TPI lamellas.

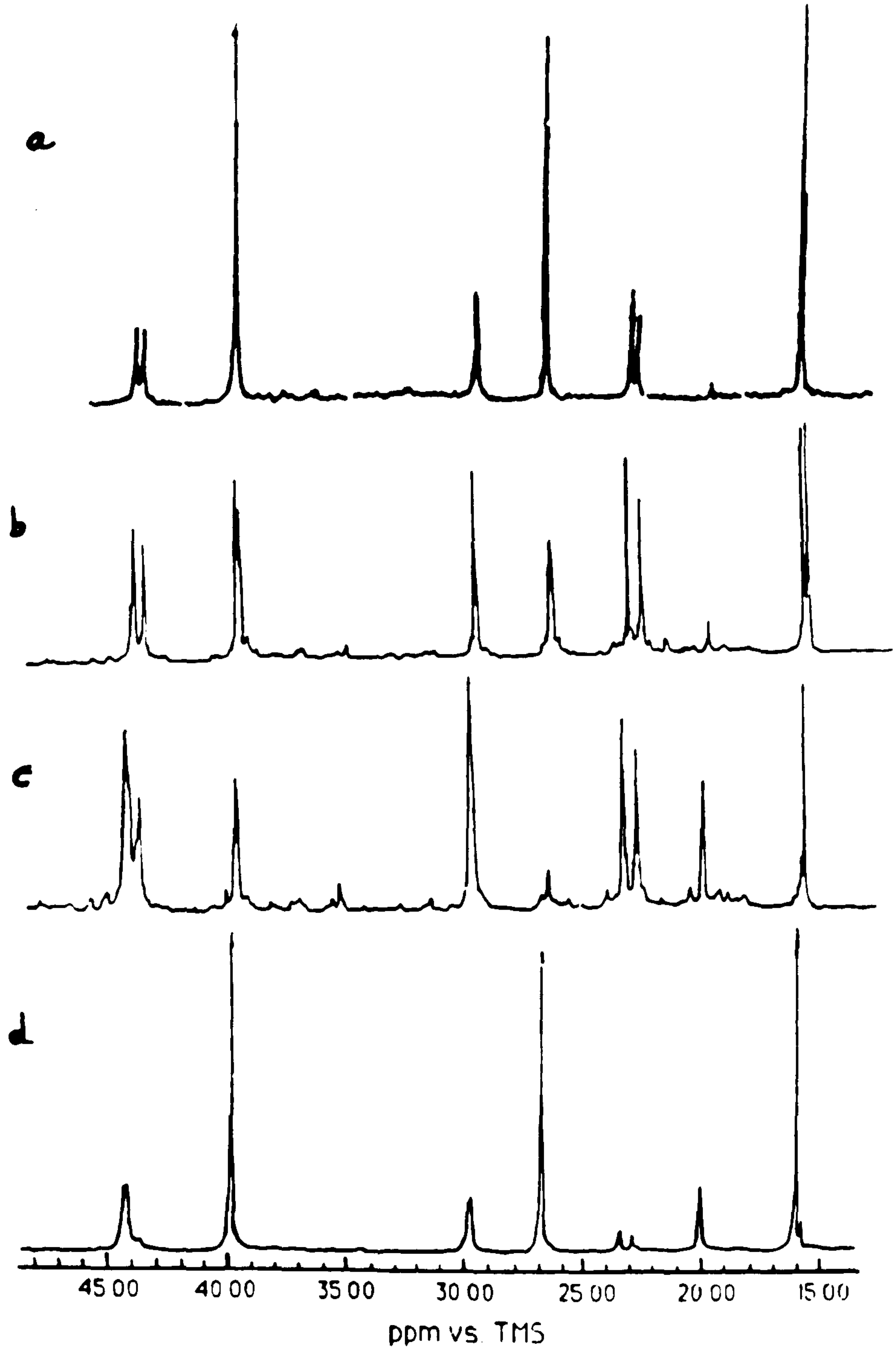

III.7. Hydrochlorination levels and block lengths:

In order to record data quantitatively the appropriate experimental conditions were determined by measuring the carbon-13 spin lattice relaxation (T_1) and by comparing spectra with and without Nuclear Overhauser Enhancement (NOE). In previous measurements [51] T_1's of 0.66, 7.79, 1.31, 0.68, and 3.80 were obtained for polyisoprene for carbons #1, 2, 3, 4, and 5, respectively. Hydrochlorinated TPI shows a decrease in all T_1's: 0.16, 2.2, 0.16, and 0.33 for carbons #1 and 3, #2, #4, and #5, respectively. The resonance for methylene carbon #4 shows a short T_1 value and yields the same block lengths, within experimental error, with and without NOE. Further, its sequential peaks are more separate and distinct than other carbon peaks. As a consequence of the three reasons above, methylene carbon #4 was used preferentially, in the calculations, over the other resonance peaks.

A two-phase spin echo experiment was performed on a sample crystallized by the precooled method at 20°C and hydrochlorinated at 0°C for 4 days. With the proper delay time (0.625/j) all C and CH_2 resonances appear with positive phases, while CH and CH_3 show negative phases. The experiment furnished added information in the distinction and assignment of the different carbons and sequences present.

The amount of hydrochlorination can be established for each sample by a comparison of the graphical integration of the resonances for the I, H, and junction sequences of the alkyl, olefinic, and hydrochlorinated carbons. Each resonance area is proportional to the total number of equivalent carbon atoms present in the sample. For instance, [III-4] is the area under the resonance of methylene carbon, atom #4, in an unreacted TPI unit; [HHH]-4 becomes the area under the resonance for atom #4 in the reacted unit; [J-4] is the average of the areas under the carbon #4 resonances in the junction between the reacted and the unreacted units, i.e.,([IIH-4] + [HHI-4]) / 2. The formation of segmented block copolymers, upon reaction of the crystal surfaces, yields original unreacted blocks and newly formed reacted sections. If they are represented as A and B, respectively, then <A> is the average number of unreacted units per block which includes any irregularities in the crystalline stems or lack of completion of the hydrochlorination in the surface; <B> represents an average number of monomer units in the reacted blocks which includes any variations in the fold lengths, significant amounts of chain ends, and reacted lateral surfaces or HCl penetration into the crystal core. <A> and <B> can be calculated from the resonance areas expressed as a ratio of reacted or unreacted areas and its junctions, as shown in equations 10 and 11, below:

$$\langle A \rangle = ([III] + [J]) / [J] \qquad \text{equation 10}$$

$$\langle B \rangle = ([HHH] + [J]) / [J] \qquad \text{equation 11}$$

The fraction hydrochlorinated, F_H, can be expressed as the ratio of the hydrochlorinated carbon resonance area plus its junction over the sum of all resonances, reacted plus junction, and unreacted plus junction:

$$F_H = \frac{[HHH] + [J]}{[HHH] + [J] + [III] + [J]} \qquad \text{equation 12}$$

The calculations are done using the computer's graphical integration of the resonance areas, as shown in figures 26 and 27 for methylene carbon #4.

Assuming that none of the crystalline blocks have been reacted, that complete surface reaction has occurred, that the number of noncrystalline chain ends and lateral surfaces are small compared to the folds, and that the chain repeat distance, R, of an isoprene unit is 0.439 nm, then:

$$L_s = \langle A \rangle \times R \qquad \text{equation 13}$$

where L_s, the average stem length, is the crystallite thickness along the chain direction. Similarly,

$$U = \langle B \rangle \qquad \text{equation 14}$$

where U is the average number of monomer units per fold.

Figure 26: 50.33 MHz ^{13}C NMR spectral region of carbon #4 in TPI - HCl TPI block copolymer and block length calculations.

$$\langle A \rangle = ([III] + [J]) / [J]$$

$$\langle B \rangle = ([HHH] + [J]) / [J]$$

$$F_H = \frac{[HHI] + [J]}{[HHH] + [J] + [III] + [J]}$$

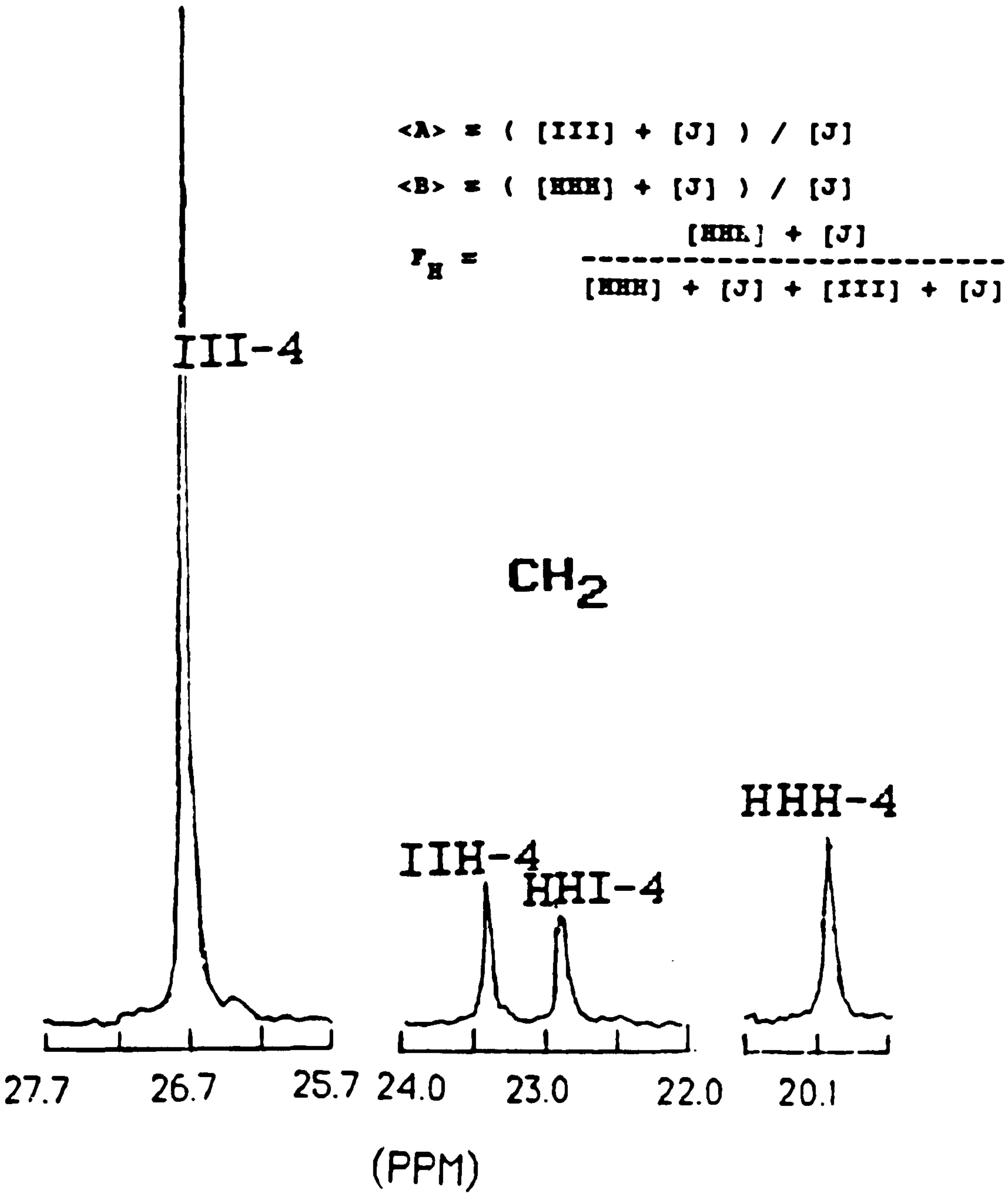

Figure 27 : 50.33 MHz ^{13}C NMR integrals of carbon #4 in TPI-HCl TPI block copolymers and block length calculations.*

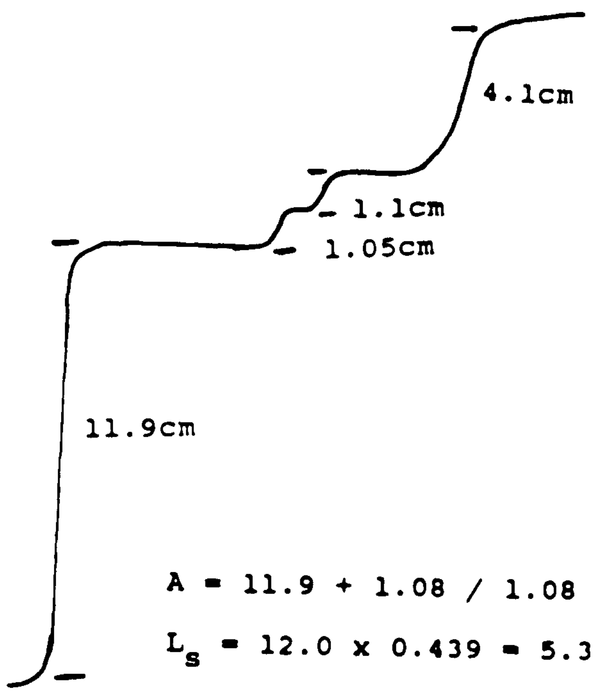

$A = 11.9 + 1.08 / 1.08 = 12.0$

$L_s = 12.0 \times 0.439 = 5.3$

$B = 4.1 + 1.08 / 1.08 = 4.8 = U$

$F_H = (4.1 + 1.08) / (4.1 + 2(1.08) + 11.9) = 0.29$

(scale = 2:1)

* The TPI crystals were grown in amyl acetate solution (0.07% W/V) by the self seeding method at a crystallization temperature of 20°C, and hydrochlorinated for 1 day at -10°C in an acetone suspension.

Hydrochlorination of TPI lamellas and hedrites were carried out at 20, 0, and -7 to $-10^{o}C$ in 1% (W/V) amyl acetate and acetone suspensions. The crystals were grown at crystallization temperatures of 10, 20, and $30^{o}C$ and hydrochlorinated as a function of time. The values of <B>, <A>, L_s, and F_H obtained for the different preparations are given in tables 9 - 17. Also indicated in tables 9 - 17 is the appearance of HIH peaks in any particular preparation. Carbon - 13 NMR measurements were made both with (power gated decoupling, PGD) or without (inverse gated decoupling, IGD) NOE. Most spectral data were collected with the PGD technique unless otherwise indicated (IGD) in the tables. When both methods were used with the same sample, agreement within 6% for <A> and 4% for <B> was observed. In most cases carbon #4 was used for the calculations. When other atoms were used in addition to carbon #4 agreement within 10% was obtained and an average value was used. Unfractionated samples were used (M_n = $3.5x10^4$, M_w/M_n = 4.8) unless otherwise specified (high, medium, or low molecular weight: HMW, MMW, LMW, respectively). Values of <A> and <B> are given in monomer units, while L_s is given in nanometers.

Table 9: Results of hydrochlorination of TPI lamellas (T_c = 20^oC) in amyl acetate suspension at 0^oC.

Time (days)	<B>	<A>	L_s	F_H	HIH	comments
3	5.1	4.3	1.9	0.53		
3	4.3	10.9	4.8	0.30	*	
4	5.4	16.9	7.4	0.25	*	
4	5.0	6.6	2.9	0.43		
4	3.8	3.0	1.3	0.57	*	HMW
4	9.3	8.7	3.8	0.52		MMW
4				1.0		$T_{reaction}=20^oC$
7	5.6	7.1	3.1	0.44		
7	6.7	3.9	1.7	0.65		HMW
12	12	11.8	5.2	0.50	*	
14	5.1	2.5	1.1	0.68		
18	8	4.5	2.0	0.69	*	
28	6.1	3.6	1.6	0.63	*	
	5.7	3.6	1.6	0.58	*	IGD
28				1.0		

Table 10: Results of hydrochlorination of TPI lamellas (T_c = 10°C) in amyl acetate suspension at -7 to -10°C.

Time (days)	<B>	<A>	L_s	F_H	HIH comments
3	5.2	3.4	1.5	0.60	*
5	6.7	3.2	1.4	0.68	*
6	3.9	5.7	2.5	0.40	*
12	11	3.9	1.7	0.74	
20				1.0	

Table 11: Results of hydrochlorination of TPI lamellas (T_c = 20°C) in amyl acetate suspension at -5 to -10°C.

Time (days)	<B>	<A>	L_s	F_H	HIH comments
0.063	2.6	6.6	2.9	0.27	*
0.20	4.1	10	4.5	0.29	
0.33	3.5	7.3	3.2	0.34	*
0.50	3.8	9.5	4.4	0.28	*
1	5.1	12.5	5.5	0.29	
1	4.7	10.5	4.6	0.31	*
2	3.8	5.9	2.6	0.39	*
2	5.8	15.0	6.6	0.28	* poor resolution
3	2.1	8.9	3.9	0.20	poor resolution
5	5.1	11.4	5.0	0.31	
6	3.9	3.4	1.5	0.53	*
12	5.2	6.1	2.7	0.54	*
16	5.9	7.5	3.3	0.44	poor resolution
18	6.0	5.9	2.6	0.50	*
25	13	5.5	2.4	0.66	*
30	6.6	11.2	4.9	0.38	* poor resolution
40	9.4	7.3	3.2	0.62	*

Table 12: Results of hydrochlorination of TPI hedrites (T_c = 20°C) in amyl acetate suspension at -5 to -10°C.

Time (days)	<B>	<A>	L_s	F_H	HIH comments
0.042	2.4	22	9.4	0.099	*
0.18	5.2	18	8.0	0.26	*
0.50	5.4	15	6.8	0.26	*
1	5.9	17	7.2	0.26	
2	6.7	15	6.6	0.31	
4	8.1	21	9.3	0.28	
5	7.7	11	5.4	0.41	
7	6.9	17	7.2	0.29	
8	6.3	15	6.7	0.31	
9	5.6	12	5.5	0.31	poor spectrum
10	6.6	15	6.5	0.31	
12	7.1	19.4	8.5	0.27	poor spectrum
14	13	8.1	4.1	0.62	* poor spectrum
15	13	12	5.3	0.52	
18	21	10	4.6	0.67	*

Table 13:Results of hydrochlorination of TPI lamellas (T_c = 30^{o}C) in amyl acetate suspension at -7 to -10^{o}C.

Time (days)	<B>	<A>	L_s	F_H	HIH	comments
0.063	3.8	19	8.0	0.17	*	
0.083	4.3	19	8.2	0.19		
0.17	3.8	9.7	4.3	0.28		
0.21	4.9	18	7.8	0.21		
1	3.1	5.5	2.4	0.36	*	
1	5.1	17	7.3	0.23		
1	4.9	14	6.3	0.26		IGD
1	4.0	12	5.4	0.25		HMW
2	3.4	8.1	3.5	0.30		
2.3	4.2	10	4.5	0.29		
3	4.9	16	7.1	0.23		
4	6.1	19	8.2	0.25		
6	5.7	17	7.3	0.26		
9	4.9	14	6.0	0.26		
	6.1	16	7.0	0.28		IGD
12	3.8	7.5	3.3	0.29		
12	3.3	6.0	2.6	0.36		
12	4.1	9.3	4.1	0.31		
21	5.3	14	5.9	0.28		

Table 14: Results of hydrochlorination of TPI lamellas (T_c = 10°C) in acetone suspension at -7 to -10°C.

Time (days)	<B>	<A>	L_s	F_H	HIH comments
2	3.9	9.1	4.0	0.30	IGD
2	5.0	7.5	3.9	0.40	* IGD
3	4.6	12	5.3	0.28	
6	3.9	9.1	4.0	0.30	IGD
6	5.1	8.3	3.6	0.40	* IGD
8	5.1	14.5	6.4	0.26	
13	5.2	7.6	3.3	0.41	
17	7.0	7.1	3.1	0.42	* IGD poor scan
18	4.0	7.4	3.3	0.35	
average	4.5 +/-0.5	10 +/-2	4.3 +/-0.9	0.38 +/-0.05	

Table 15: Results of hydrochlorination of TPI lamellas (T_c = 20°C) in acetone suspension at -7 to -10°C.

Time (days)	<B>	<A>	L_s	F_H	HIH	comments
0.083	3.0	12	5.3	0.20		
0.71	4.0	9.9	4.3	0.29		
1	4.8	12.0	5.2	0.30		
2	4.1	9.6	4.2	0.30		
4	4.8	14	6.1	0.25		
5	4.8	9.3	4.1	0.29		
10	5.3	15	6.6	0.26		
17	5.1	11	4.9	0.31		
20	5.5	13.4	5.9	0.29		
average	4.8 +/-0.5	11 +/-2	5.0 +/-0.9	0.29 +/-0.1	(0.71 to 20 days used)	

Table 16: Results of hydrochlorination of TPI hedrites (T_c = 20°C) in acetone suspension at -7 to -10°C.

Time (days)	<B>	<A>	L_s	F_H	HIH comments
0.23	2.2	2.2	9.7	0.089	
0.79	5.1	14	6.1	0.26	
1	4.8	17	7.5	0.22	
1.75	6.0	17	7.5	0.27	
5	4.5	19	8.3	0.18	
6.7	5.6	18	7.9	0.24	
10	4.7	18	8.1	0.20	
11	6.1	16	7.0	0.28	
14	5.1	17	7.5	0.23	
16.8	5.1	17	7.5	0.23	
average:	5.3 +/-0.5	17 +/-1	7.4 +/-0.5	0.24 +/-0.03	(0.79 to 16.8 days)

Table 17: Results of hydrochlorination of TPI lamellas (T_C = 30°C) in acetone suspension at -7 to -10°C.

Time (days)	<B>	<A>	L_s	F_H	HIH comments
0.13	3.9	19	8.5	0.17	* IGD
1	4.6	19	8.2	0.20	IGD
2	4.9	19	8.4	0.20	IGD
3	5.2	15	6.6	0.25	
	5	15	6.6	0.26	IGD
6	4.6	17	7.4	0.21	IGD
6	5.3	19	8.3	0.22	IGD
7	5.0	17	7.3	0.23	IGD
21	5.5	17	7.3	0.25	IGD
average:	5.1 +/-0.5	17 +/-2	7.5 +/-0.5	0.23 +/-0.02	(1 to 21 days used)

Tables 9-17 and figures 28 -32 below, indicate that <A> and <B> values depend on many factors including the amount of time and temperature of hydrochlorination, the liquid used as the reacting medium, as well as the crystallization temperature.

When lamellas (grown at $T_c = 20^oC$) are hydrochlorinated in amyl acetate suspension at temperatures of 0^oC or higher, <A> and <B> values obtained show a very large deviation between different preparations, and do not follow any pattern with time (table 9). Furthermore, HIH sequences are observed frequently, suggesting random hydrochlorination of the crystal. Complete hydrochlorination of the lamellas is sometimes observed, suggesting penetration of the HCl molecules into the inner core of the crystal.

At lower reacting temperatures of approximately -10^oC both lamellas and hedrites crystallized at 20^oC and reacted in amyl acetate suspension for various time periods contain three regions of interest, as seen in figure 28. The plot of <B> vs. time shows, in the first region ending at 0.5 days of hydrochlorination, an upward slope where the surface folds are in the process of being reacted. This region usually contains HIH sequences, as expected. There is a slower increase with time up to 10 days in the second region and a much larger rate of increase at longer reaction times, in the third region. NMR sequences due to

HIH are still observed for various preparations. <A> values show a continuous increase with time and, like the values observed for <B>, never reach an equilibrium value. In general, <A> values calculated for hedrites are larger than those for the lamellas by approximately 5 or 6 monomer units, also shown in figure 28, where PC represent precooled TPI lamellas and D are the direct - grown multi-lamellar hedrites.

When acetone is used as the reacting medium on lamellas grown at a crystallization temperature of $20^{\circ}C$ <A> and <B> become constant after approximately 1 day of hydrochlorination. An average value for <B>, <A>, L_s, and F_H are calculated using preparations obtained after equilibrium is established (after 0.71 day of hydrochlorination). These are, respectively, 4.8 +/- 0.5, 11 +/- 2, 5.0 +/- 0.9, and 0.29 +/- 0.1. <B> values found for hydrochlorinated hedrites, also grown at $T_c = 20^{\circ}C$ and reacted in acetone suspension, agree, within experimental error, with those of the lamellas. The <A> values of the former are, on the other hand, approximately 50% larger than those found for the lamellas grown at the same crystallization temperature. A plot of <A> and <B> vs. time comparing lamellas and hedrites reacted in acetone medium is shown in figure 29. Average values of <B>, <A>, L_s, and F_H calculated for the hedrites are 5.3 +/- 0.5, 17 +/- 1, 7.4 +/- 0.5, and 0.24 +/- 0.03, respectively.

Lamellas grown at 20^{o}C and reacted in amyl acetate and acetone suspensions are compared in figure 30, where Ac = acetone, and AA = amyl acetate. <A> is usually lower in the former, while its <B> values grow much above the ones reacted in the acetone media. As a result, the reacted fraction, F_H, in amyl acetate reacting medium exceed those of acetone by approximately 60%.

Lamellas grown at crystallization temperatures of 30^{o}C and reacted in amyl acetate suspension exhibit slightly larger <B> values, compared to the same crystals hydrochlorinated in acetone suspension. <A> is approximately the same for both instances. A large fluctuation in values is noticed for the amyl acetate reacting medium compared to acetone but not as large as those found for lamellas grown at T_c = 20^{o}C. Also noticeable is a greater instance of NMR resonances attributed to HIH in lamellas grown at 20^{o} compared to the 30^{o}C for reaction in amyl acetate. The average values obtained for lamellas grown at 30^{o}C and reacted in acetone media are 5.0 +/- 0.4, 18 +/- 2, 7.7 +/- 0.5, and 0.22 +/- 0.02 for <B>, <A>, L_s, and F_H, respectively. The average was taken using values obtained after 1 day of reaction, when the surface reaction seems to reach completion. <A> and <B> results as a function of time are plotted in figure 31 comparing amyl acetate and acetone as the suspension liquids.

For lamellas prepared at crystallization temperatures of 10°C, hydrochlorination in amyl acetate at -7 to -10°C leads to 74% reaction after 12 days and 100% reaction after 20 days. In addition, most NMR spectra contain HIH resonance peaks. Lamellas hydrochlorinated in acetone suspension, under the same conditions, react to 29 +/- 1% from 2 to 8 days and increase to 41 +/- 1% after a 13 day time period. <A> decreases from 11 +/- 2 to 7.5 for the above time periods, while <B> remains approximately the same throughout, at 4.5 +/- 0.5. Some of these samples also show HIH sequences.Tables 10 and 14 enumerate the <B>, <A>, L_s, and F_H results, while figure 32 plots <A> and <B> as a function of time for amyl acetate and acetone as the hydrochlorinating media.

It is evident from the above tables and figures that the level of hydrochlorination, F_H, changes with time the same way that <B> does. This is most clearly seen for reactions in amyl acetate suspension in figure 33 , where F_H is plotted vs time for lamellas and hedrites hydrochlorinated in amyl acetate. The values calculated for <B> remain the same, within experimental error, for lamellas and hedrites grown at various crystallization temperatures and hydrochlorinated in acetone. This suggests that the nature of the fold is similar for the different crystals used, giving a mean value of 4.8 monomer units. The lamellar crystalline stem increases from 11 to 18 monomer units as the crystallization temperature increases from 20 to 30°C. This trend has been noted previously[5,115] using microscopy and small angle diffraction. <A> values for hydrochlorinated lamellas grown at 10°C also show the same trend, ranging from 8 to 11 monomer units. This values are, however, less reliable since the lamellar structure is smaller and therefore subject to more defects and easier destruction.This is evidenced by the observation of HIH sequences in the NMR spectra. The crystal stem found for hedrites grown at a T_c = 20° are approximately 50% higher than the lamellas grown in the same conditions.

The average crystalline stem length, the average number of monomer units per fold, and the hydrochlorinated fractions, are summarized in table 18 for lamellas grown at different crystallization temperatures and hydrochlorinated in acetone. Also given are the noncrystalline fractions obtained from density measurements. These differ by as much as 50% from the F_H values obtained from NMR spectroscopy. Table 19 compares lamellas grown at T_c = 20°C and hydrochlorinated in acetone, hedrites under the same conditions, and lamellas grown at T_c = 20°C and epoxidized in 2-ethoxyethanol. The latter work is being carried out by Woodward and Elkayam, and agrees, within experimental error, with the results on hydrochlorinated lamellas.

Table 18: Noncrystalline fraction and parameters obtained by hydrochlorination of trans-1,4-polyisoprene lamellas [a].

T_c (^oC)	$1 - W_c$ [b]	F_H [c]	U [d]	<A> [e]	L_s [f]
10	0.56	0.32 +/-0.05	4.5 +/-0.5	10 +/-2	4.3 +/-0.9
20	0.52	0.29 +/-0.01	4.8 +/-0.5	11 +/-2	5.0 +/-0.9
30	0.46	0.23 +/-0.02	5.1 +/-0.5	17 +/-2	7.5 +/-0.5

[a] grown from 0.07% (W/V) amyl acetate solution at crystallization temperature, T_c, after precipitation at 0^oC and redissolution at 34^oC using unfractionated polymer, hydrochlorinated in acetone at -7 to -10^oC

[b] noncrystalline fraction from density measurements

[c] fraction available for hydrochlorination

[d] average number of monomer units per fold

[e] average number of monomer units in crystalline traverse

[f] average crystallite thickness along chain direction (nm)

Table 19 : Epoxidation and hydrochlorination results for trans-1,4-polyisoprene lamellas and hedrites.*

	U	<A>	L_s (nm)	F_H
epoxidized lamellas	5.4 +/-0.8	12 +/-1	5.4 +/-0.30	0.30 +/-0.02
hydrochlorinated lamellas	4.8 +/-0.5	11 +/-2	5.0 +/-0.9	0.29 +/-0.01
hydrochlorinated hedrites	5.3 +/-0.5	17 +/-1	7.4 +/-0.5	0.24 +/-0.03

* grown from amyl acetate solution at 20^{o}C using unfractionated polymer

Figure 28 : Average block lengths, <A> (unreacted) and <B> (reacted), vs. log time for trans-1,4-polyisoprene lamellas and hedrites hydrochlorinated in amyl acetate suspension.

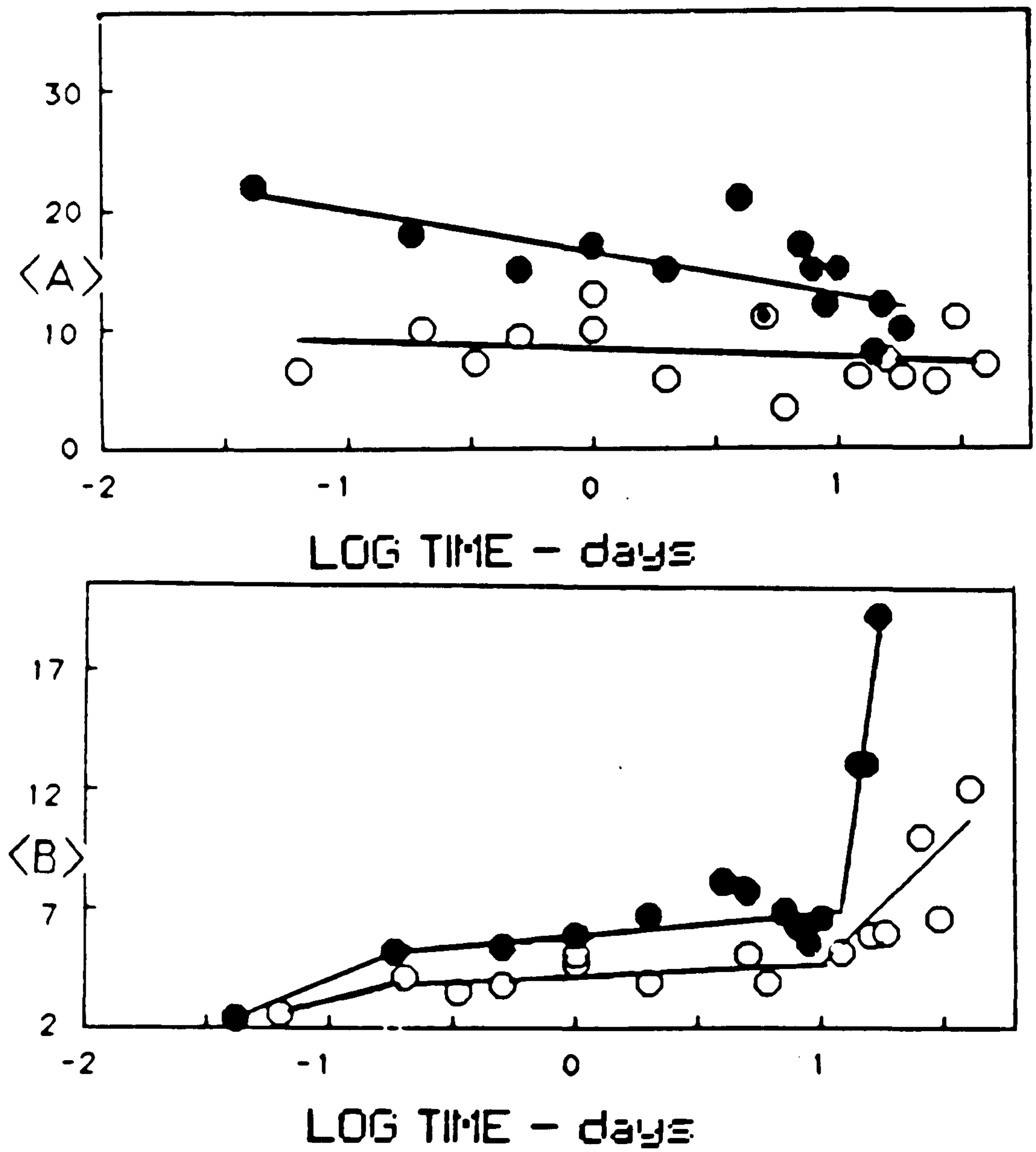

o PC ● D $T_c = 20^{\circ}C$ $T_{reaction} = -7$ to $-10^{\circ}C$

Figure 29: Average block lengths, <A> (unreacted) and <B> (reacted), vs. time for trans-1,4-polyisoprene lamellas and hedrites hydrochlorinated in acetone suspension.

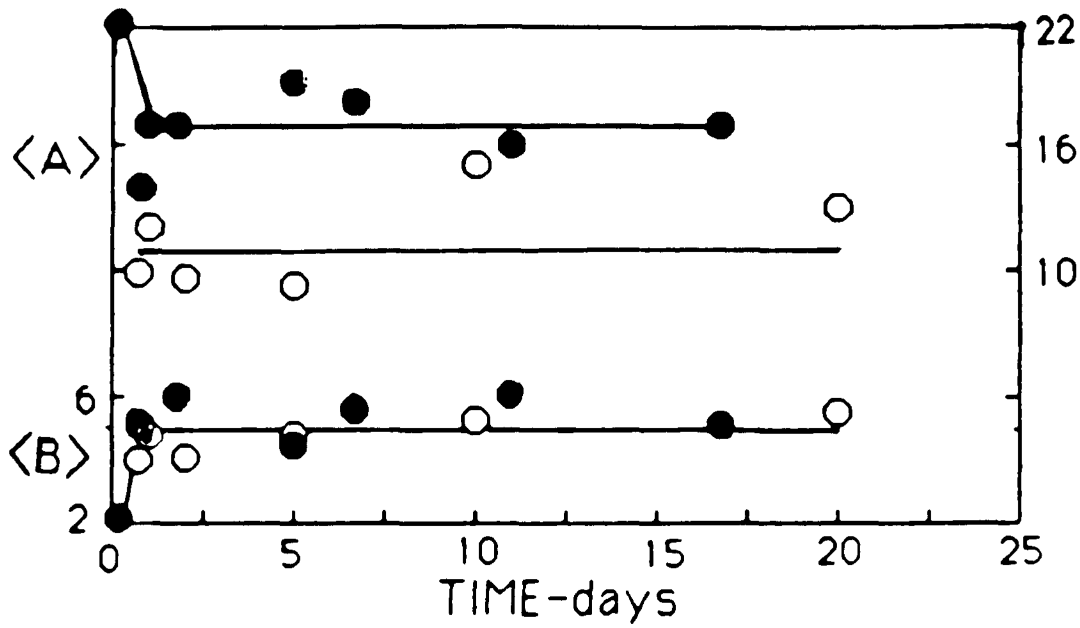

O PC ● D T_c = 20 °C $T_{reaction}$ = -10°C

Figure 30: Average block lengths, <A> (unreacted) and <B> (reacted), vs. time for trans-1,4-polyisoprene lamellas crystallized at 20°C and hydrochlorinated in amyl acetate and in acetone suspensions.

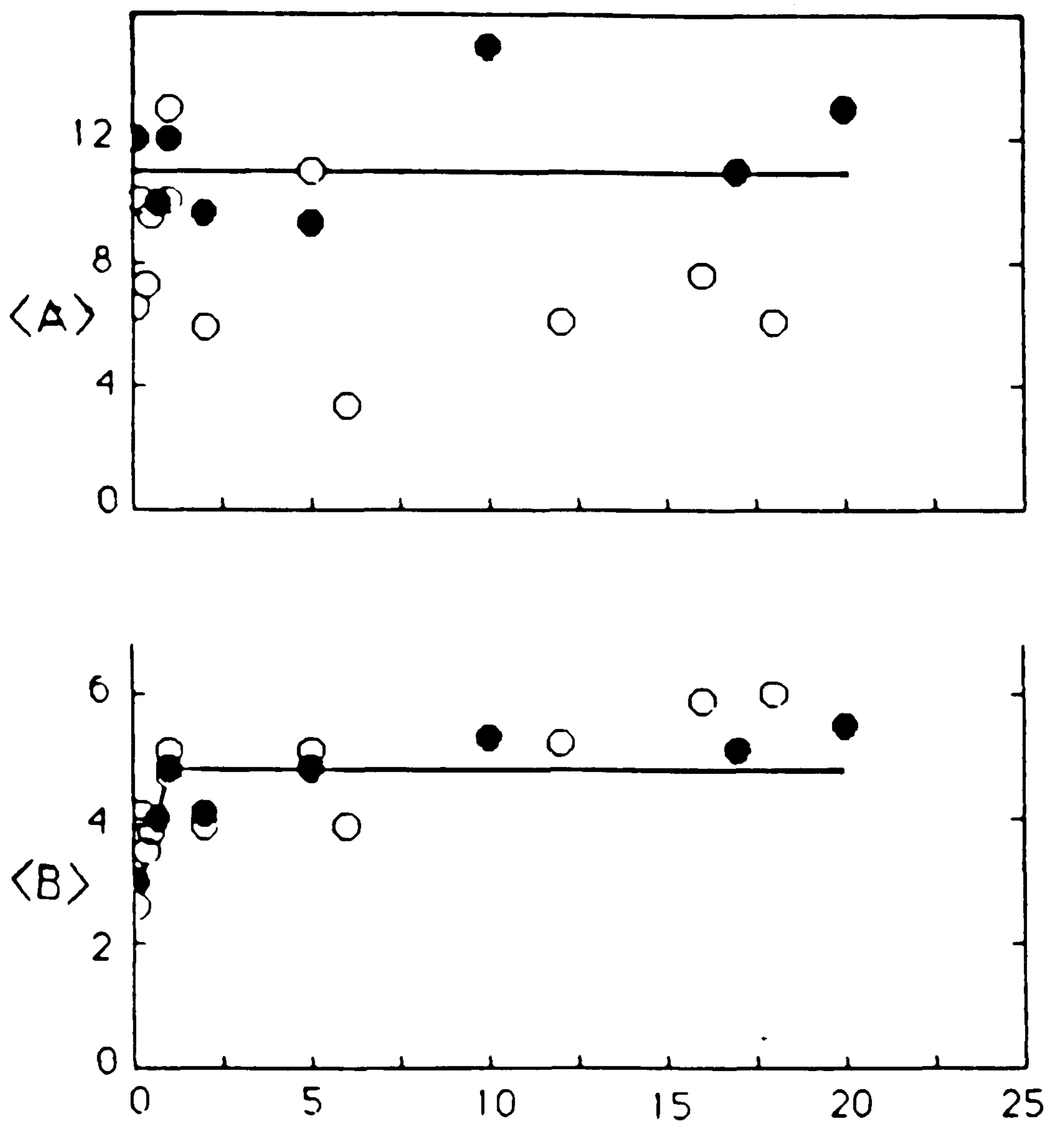

○ AA ● AC $T_{reaction} = -10°C$

Figure 31: Average block lengths, <A> (unreacted) and <B> (reacted), vs. time for trans-1,4-polyisoprene lamellas crystallized at 30°C and hydrochlorinated in acetone suspension.

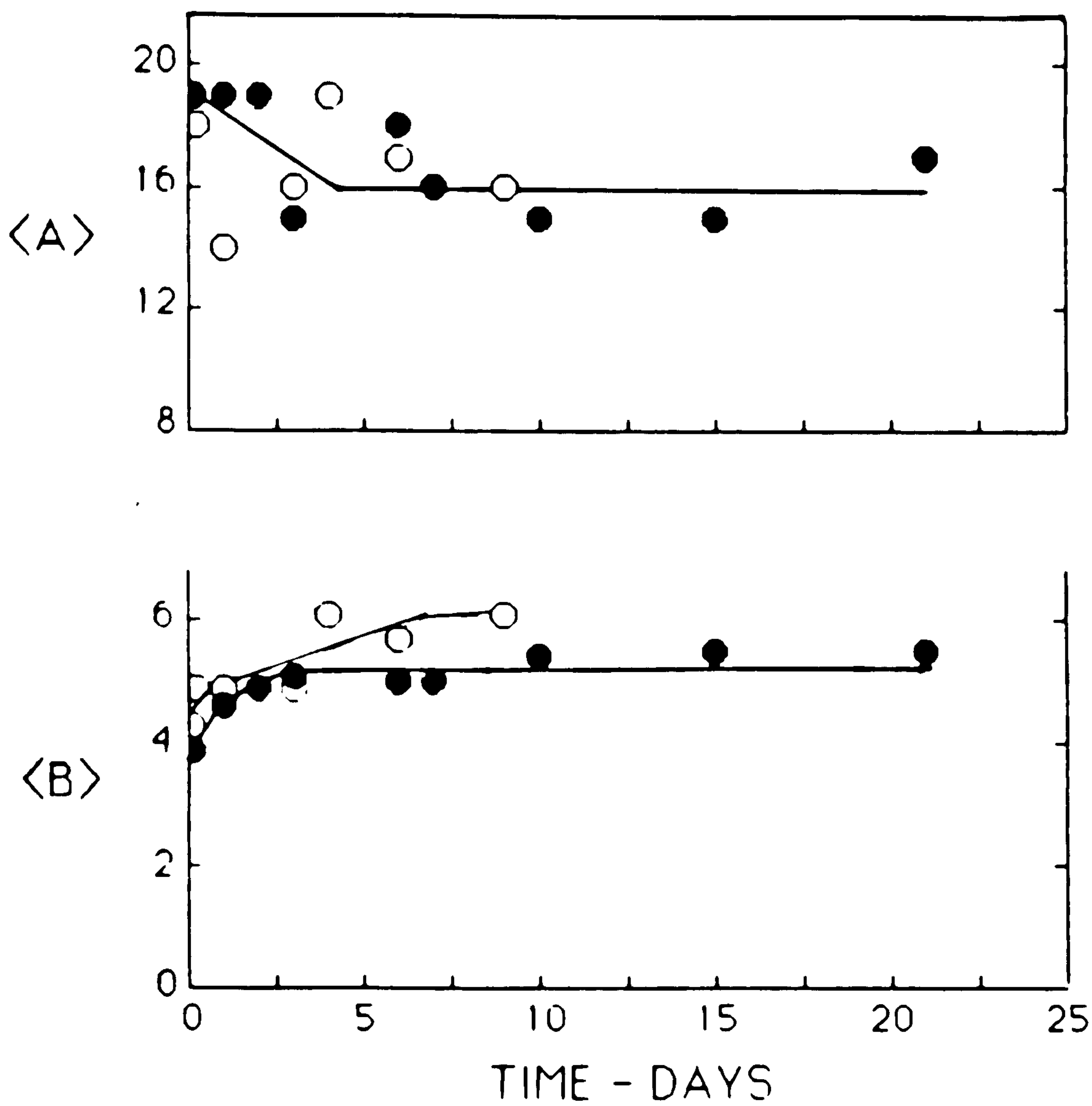

○ AA ● AC $T_{reaction} = -10^{\circ}C$

Figure 32 : Average block lengths, <A> (unreacted) and <B> (reacted), vs. time for trans-1,4-polyisoprene lamellas crystallized at 10°C and reacted in amyl acetate and acetone suspensions.

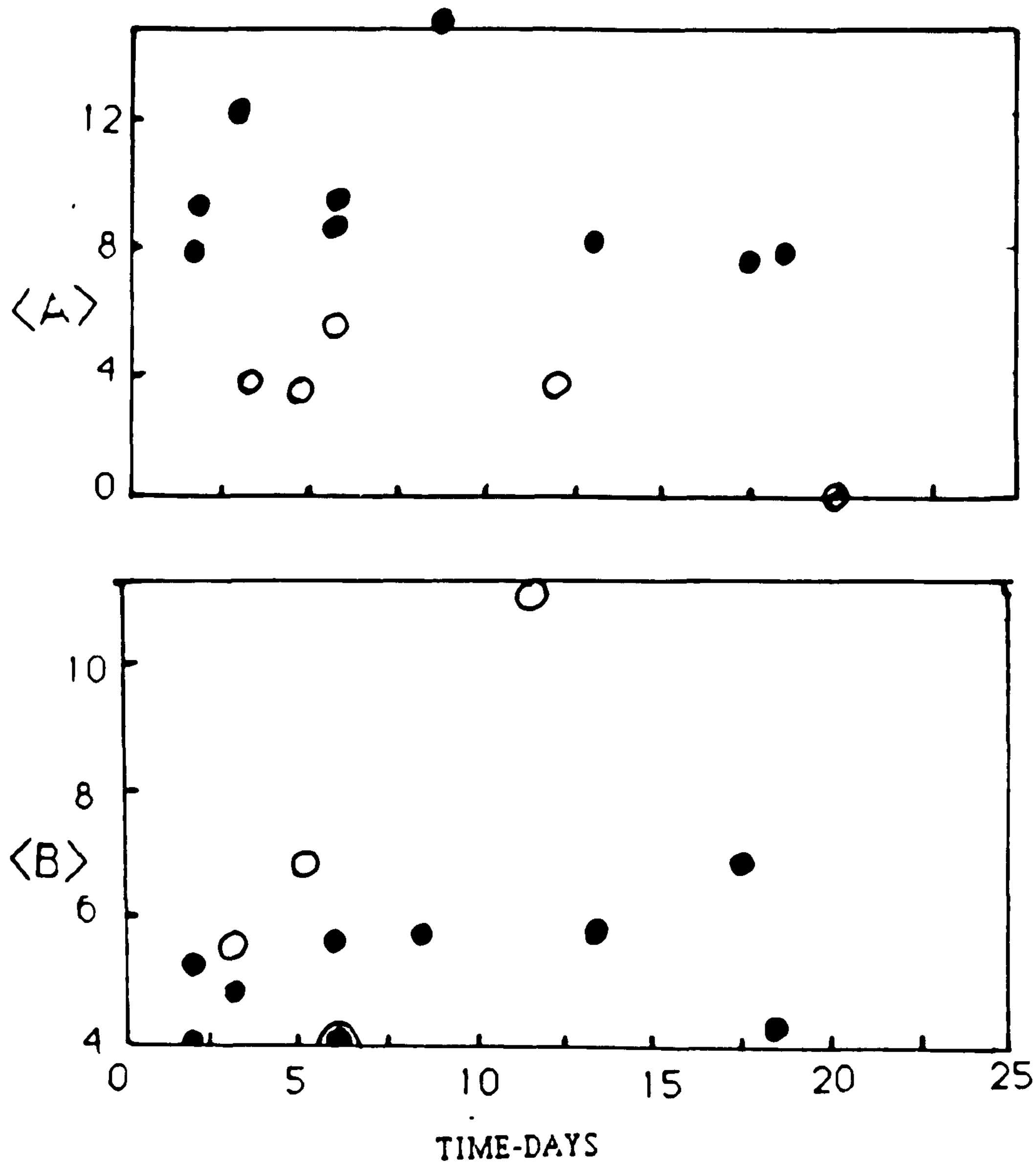

o AA ● AC $T_{reaction} = -10^{o}C$

Figure 33: Hydrochlorinated fraction, F_H, vs log time for trans-1,4-polyisoprene lamellas and hedrites hydrochlorinated in amyl acetate suspension.

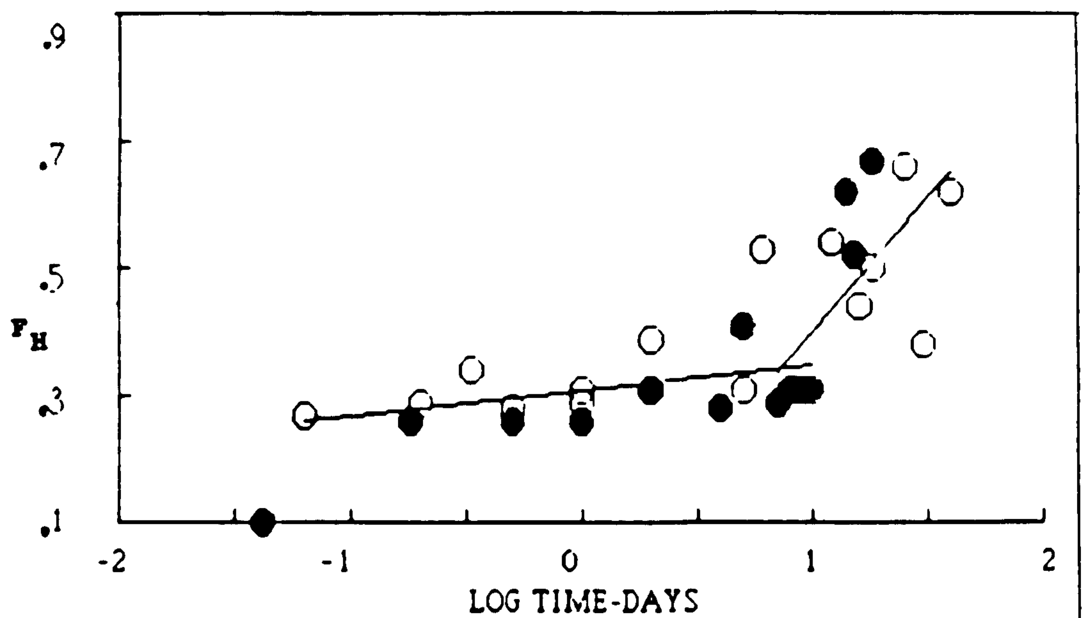

O PC ● D $T_c = 20^oC$ $T_{reaction} = -7$ to -10^oC

IV. Discussion

IV.1. The TPI lamella

Chain folded TPI lamellas, as grown here, are composed of crystalline and amorphous phases. The chain folds, at the surface of the lamellas, encompass most of the amorphous phase. Thus, the surface hydrochlorination of the crystal results in regular block copolymers where the folds are hydrochlorinated while the crystalline core remains unreacted. This is schematically represented in figure 34.

The principal objective of this study is the determination of the number of monomer units present per crystalline section and noncrystalline fold. These numbers, as well as the hydrochlorination level, will be dependent on many factors, including, (1) the crystallization temperature used in the preparation of the crystal, (2) the crystal morphology, (3) the suspension liquid used as the hydrochlorinating medium and (4) the reaction temperature used during the hydrochlorination.

Figure 34 : Schematic representation of reacted, B, and unreacted, A, units in a chain folded lamella.

<A> = avg. # of A units/stem

<B> = avg. # of B units/fold

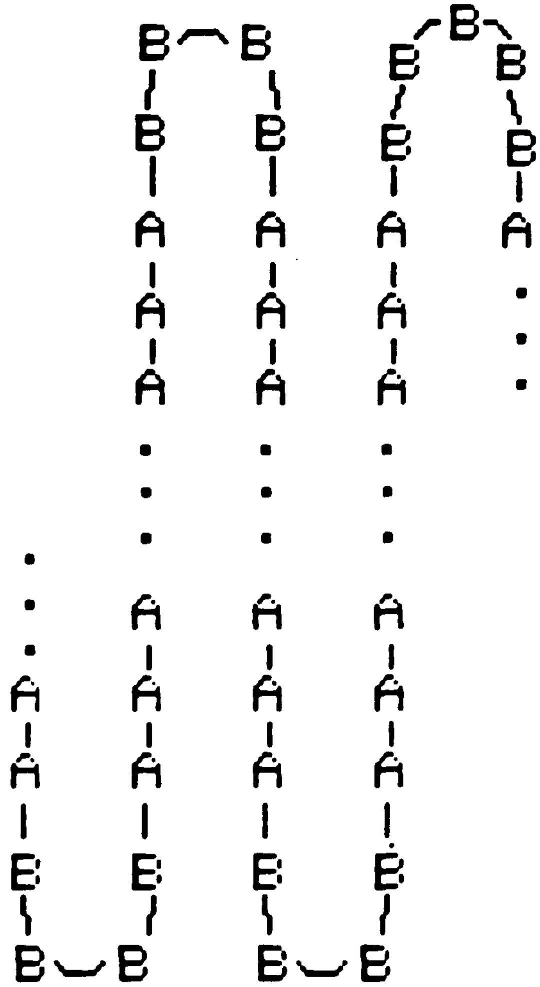

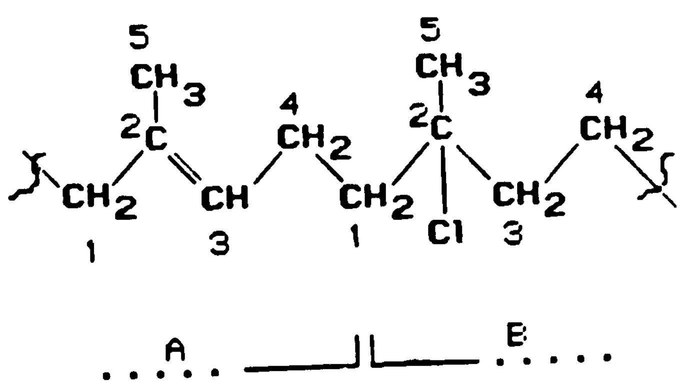

While being a good absorbent of HCl gas, acetone is essentially a nonsolvent for both TPI and hydrochlorinated TPI. These qualities make acetone a good suspension liquid for the hydrochlorination of TPI crystals. The <A> and <B> values obtained remain constant after an initial short period for crystals grown at 20 and 30^{o}C, as seen in tables 15 - 17, and in figures 29 and 31. This indicates that penetration of the HCl into the crystal core does not occur. The crystalline stem length along the chain direction, L_s, can be calculated from the average number of unreacted monomer units,<A>. This is done by multiplying <A> by the chain repeat distance, R, where R = 0.439 nm for α TPI, as given by Takahashi, Sato, Tadokoro, and Tanaka.[113] The average number of reacted monomer units, <B>,is equated to the average number of monomer units in the chain fold, U. This assumes that not only is reaction in the crystal core negligible, but also reaction of the lateral surfaces, interlamellar links, and noncrystallizing chain ends are small compared to the folds. The lateral surface area has been previously estimated [50] to be approximately 2% or less, depending on the preparation, and can therefore, be neglected. The crystallinity calculated from density measurements (table 4) shows little, if any change with a change in TPI morphology from hedrites to single overgrown lamellas at constant molecular weight and crystallization temperature. This suggests that any interlamellar links present in the multilamellar structures contain about the same average number of monomer units as found in a fold.[5] The chain ends, or cilia, are also found to be negligible from calculations based on work done by Woodward et al.[55] These calculations are briefly mentioned in the introduction. To expand on those equations, let:

$$C = (L_s/R) - 2 \qquad \text{equation 15}$$

where C represents the average length of two cilia,and L_s is the crystalline thickness obtained from ^{13}C NMR measurements. Two units are subtracted from C since the chemical shifts of the carbon nuclei in the two terminal units of each chain can be demonstrated [54] to fall outside the resonances used. The number of folds per number average chain, F_n, is related to the total number average chain length, M_n/M_o and the hydrochlorinated fraction,F_H, obtained from ^{13}C NMR:

$$F_n = (R/L_s)[(M_n/M_o)(1 - F_H) - 1] \qquad \text{equation 16}$$

The total number of isoprene units per number average chain at the surface of the crystal is given by $B(F_n +1)$, where B includes both the folds and cilia. Two cilia per chain can be counted as one fold , and

$$U = (B(F_n + 1) - C)/F_n \qquad \text{equation 17}$$

Using equations 15, 16, and 17 the values for C, F_n, and U are obtained, and shown in table 20. Values for L_s and F_H for each lamellar crystallization temperature is given in table 18. Table 20 also compares the U value thus obtained, i.e., corrected for cilia, with the values obtained from ^{13}C NMR analysis.

Table 20 : Comparison of U and B.

T_c	C	F_n	U	B	B - U
10	7.79	35.63	4.3	4.5	0.2
20	9.39	31.99	4.7	4.8	0.1
30	13.94	24.15	4.8	5.2	0.4

It can be seen from column 6 that the difference between U and B is negligibly small, within experimental error. The cilia does not need to be considered, and U = B. It is interesting to note that with an increase in the crystallization temperature the amorphous fold seems to also increase, though slightly. Therefore, the length of the noncrystallizing chain ends should also increase. The discrepancy between B, obtained directly from NMR measurements, and U, obtained from the above equations which subtracts the cilia, are therefore larger with the increase in T_c.

A slight increase in the density measured for TPI crystals is observed (table 4) with an increase in the crystallization temperature. This is due to the increase in the crystalline : amorphous content ratio as T_c increases. A large discrepancy exists, however, between the fraction available for hydrochlorination, F_H, as obtained for crystals in suspension from ^{13}C NMR analysis, and the non-crystalline fraction, $(1 - W_c)$, as obtained by density measurements on dried mats (table 4). It was also found for TPBD lamellas[54,55] grown from solution and epoxidized in suspension that the reacted fraction is generally smaller than $(1- W_c)$. These results can be explained as due to one or more of the following: (1)density measurements may show a higher ratio of the noncrystalline component due to lamellar collapse and rearrangement upon drying (2)a failure of the two component model employed in the density method: ρ_c is obtained from x-ray results while ρ_a is extrapolated from values for the melt (3)the presence of a significant fraction of noncrystalline material not available for chemical reaction. Evidence for (1) [124] and (2) [125,126] has been given for polyethylene lamellas. Experimental results [125] and calculations using space filling models for polyethylene [126] suggest that ρ_a, as extrapolated from the melt, is larger than the fold surface density. However, it has been shown that the crystallinity derived from solid state ^{13}C NMR spectra of TPBD lamellas [67] agree with that from density measurements, eliminating possibility (2). Comparison of the solid state carbon-13 NMR spectra taken after epoxidation of TPBD with those taken before suggests that the *noncrystalline* component reacts completely,[67] eliminating explanation (3). The most likely explanation for the discrepancy between carbon-13 NMR and density results is the lamellar collapse of the lamellas during the drying process, increasing the noncrystalline component present during density measurements. Recent evidence for molecular collapse has been found by Elkayam and Woodward:[127] $F_{reacted}$ was obtained from surface epoxidized low molecular weight TPI lamellas using carbon-13 NMR spectroscopy. $F_{reacted}$ shows a better agreement with (1 $-W_c$) values than for higher molecular weight samples. Low molecular weight samples are believed [50] to contain fewer folds and a greater number of chain ends. This reduction in the number of folds suggests that there is less strain in the crystal avoiding much collapse of the latter upon drying. The resulting higher crystallinity of such samples lowers (1 $-W_c$) to a better agreement with $F_{reacted}$, which in turn increases in value due to the presence of chain ends, thus proving (1) as the viable explanation.

The surface fraction available for hydrochlorination, F_H, depends upon two factors: the crystalline thickness and the number of monomer units per fold. The lamellar thickness is seen to increase with increasing crystallization temperature (table 18), as calculated from carbon-13 NMR spectroscopy. This effect is also seen for various other polymers, including polyethylene,[1] TPBD,[73] and isotactic polystyrene.[128] The fold length seems to remain constant, within experimental error, lowering the F_H values with an increase in the T_C. The number of monomer units per fold averaged to 4.8 for TPI lamellas which falls within the range found previously for TPBD (U =3.0, 5.0, 5.6) using ^{13}C NMR spectroscopy.[54] It also agrees with ^{13}C NMR work being done presently [52,127] on the epoxidation of TPI lamellas (U =5.4). Three different types of folding of polymer single crystals have been proposed, as mentioned in the introduction (p.2-3): (1) irregular adjacent reentry (loose folds) (2) regular adjacent reentry (tight folds) (3) switch board or nonadjacent reentry folds. Molecular models of the fold surfaces for α TPI using the crystal structures given by Takahashi et al.[113] and by Fischer [112] can be constructed. A tight adjacent reentry fold model is found to contain three and four monomer units, respectively, assuming 110 folding.[50] These values suggest that indeed considerable adjacent reentry occurs with some fold looseness or occasional nonadjacent reentry. This conclusion is in agreement with earlier work on TPBD preparations including epoxidation,[58,129] bromination,[59] broad-line ^{1}H NMR in the presence of CS_2,[130] and infra red spectroscopy.[57,131] Figure 35, below, is a schematic representation of regular reentry folding of a crystal with some deviations such as nonadjacent reentry, cilia, etc.

Figure 35: Possible departures from strictly regular folding, plus defects, in a single crystal.

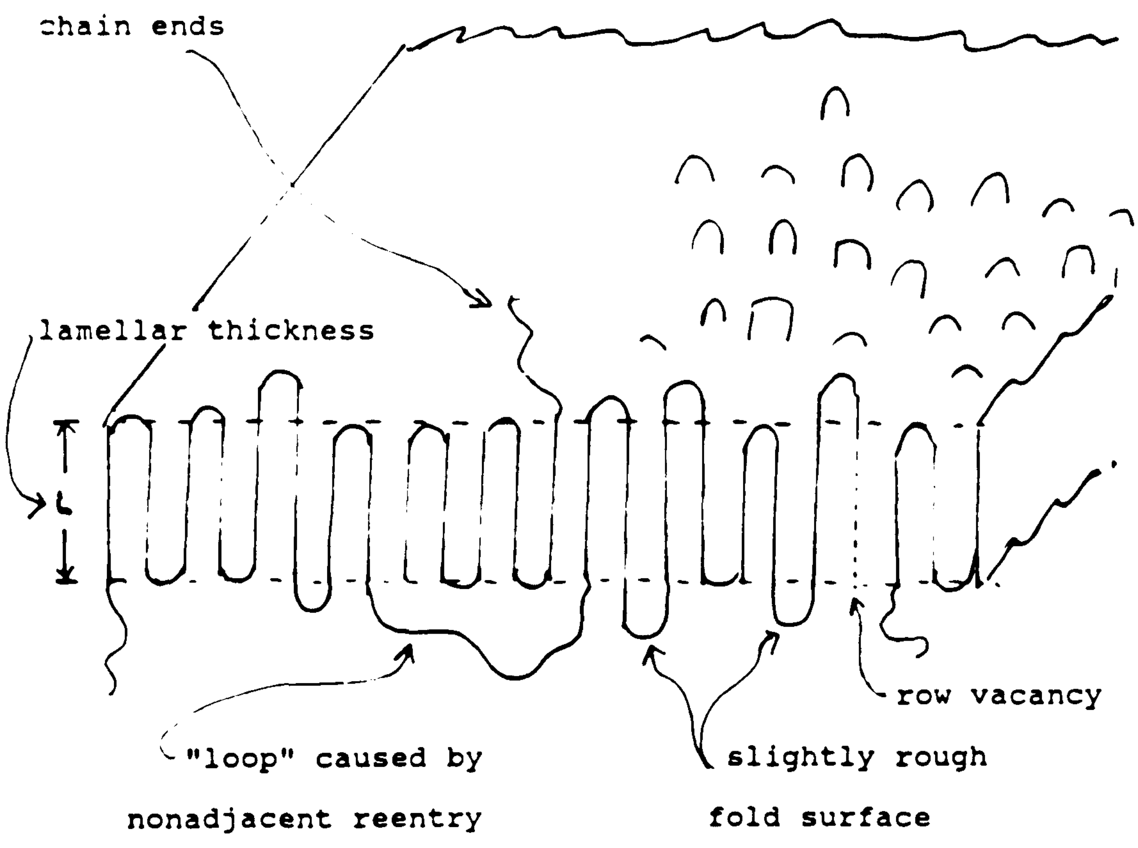

Recent work[52] on the epoxidation of TPI in 2-ethoxyethanol suspension yielded values of 0.30, 5.4, and 12 for $F_{reacted}$, U, and <A>, respectively. The reactions were carried out at $0^\circ C$ using unfractionated synthetic TPI samples crystallized at $20^\circ C$ from 0.1% amyl acetate by the precooling method. The results agree, within experimental error, with those obtained in this work. In an earlier study,[51] epoxidation was carried out in amyl acetate suspension for 20 days using a fractionated TPI sample ($M_n = 2.9 \times 10^5$) crystallized at $20^\circ C$. Values for <B> of 7.4 and for <A> of 11 were found. Although the <A> values agree within experimental error, the <B> values are much higher. It is now believed that the latter is due to the choice of amyl acetate as the epoxidation medium, which apparently leads to a mixture of completely epoxidized chains in addition to the block copolymers. Chang, Siegmann and Hiltner[132] observed a similar behavior in the chlorination of polyethylene crystals. Based on electron microscopy and infrared spectroscopy of these chlorinated single crystals, it is proposed that beyond the initial chlorination of the lamellar surfaces, the reaction proceeds through the lamellar side faces from the periphery inward. Thus, two major phases coexists: the undamaged interior region of the lamellas and the surrounding chlorinated material.

When TPI crystals were hydrochlorinated in amyl acetate suspension at -7 to -10^{o}C the <A> values calculated were lower while <B> and F_H were higher than the results obtained with acetone as the suspending liquid (see tables 10 - 17 and figures 28 - 32). The results show large fluctuations with the tendency of a decrease in the <A> values and an increase in the <B> values with time. This suggests that HCl penetration into the crystal is occurring while the reaction is allowed to proceed. Further, HIH sequences were frequently observed, which can only be present if HCl is allowed occasionally beyond the amorphous surface. The presence of HIH sequences also lowers both <A> and <B> since the former is added to the junction resonance peaks. Two stages, therefore are present, in the hydrochlorination of TPI in amyl acetate suspension: In the initial stage of the reaction block copolymers are formed with unreacted sections inside surrounded by completely hydrochlorinated chains. In the second stage one or two of the following processes may be occurring: penetration of the HCl molecule into the inner core of the crystal through the folds may occur if favorable solvent - polymer contact loosens the folds. Alternatively, the partial or complete solvation of the hydrochlorinated outer layers of the crystal may occur, exposing new inner layers which in turn react with the HCl. The latter process leads to a smaller block copolymer core with unreacted sections of the same length as before. Amyl acetate dissolves hydrochlorinated

TPI at a lower temperature than it does TPI, thus allowing the second stage to occur. This latter 'peeling - off' effect is demonstrated in figure 36.

Figure 36a shows the schematic of a cross section the unhydrochlorinated TPI crystal revealing the crystal core, the noncrystalline folds and the chain ends. The darker, or thicker, lines in figure 36b represent the hydrochlorination of the monomer units in the folds, cilia and lateral surfaces of the crystal. The crystalline core remains unreacted. In figure 36c the chain is seen to be partially solvated by the amyl acetate. The outer lateral layer is loosened from the crystal, either partially or entirely, exposing a new inner layer of unreacted chains. These, in turn, are reacted, as shown in figure 36d. The process may continue until the entire crystal is reacted.

Figure 36 : The 'peeling-off' effect of surface hydrochlorinated TPI crystal chains as a result of solvation in amyl acetate as the suspending liquid.

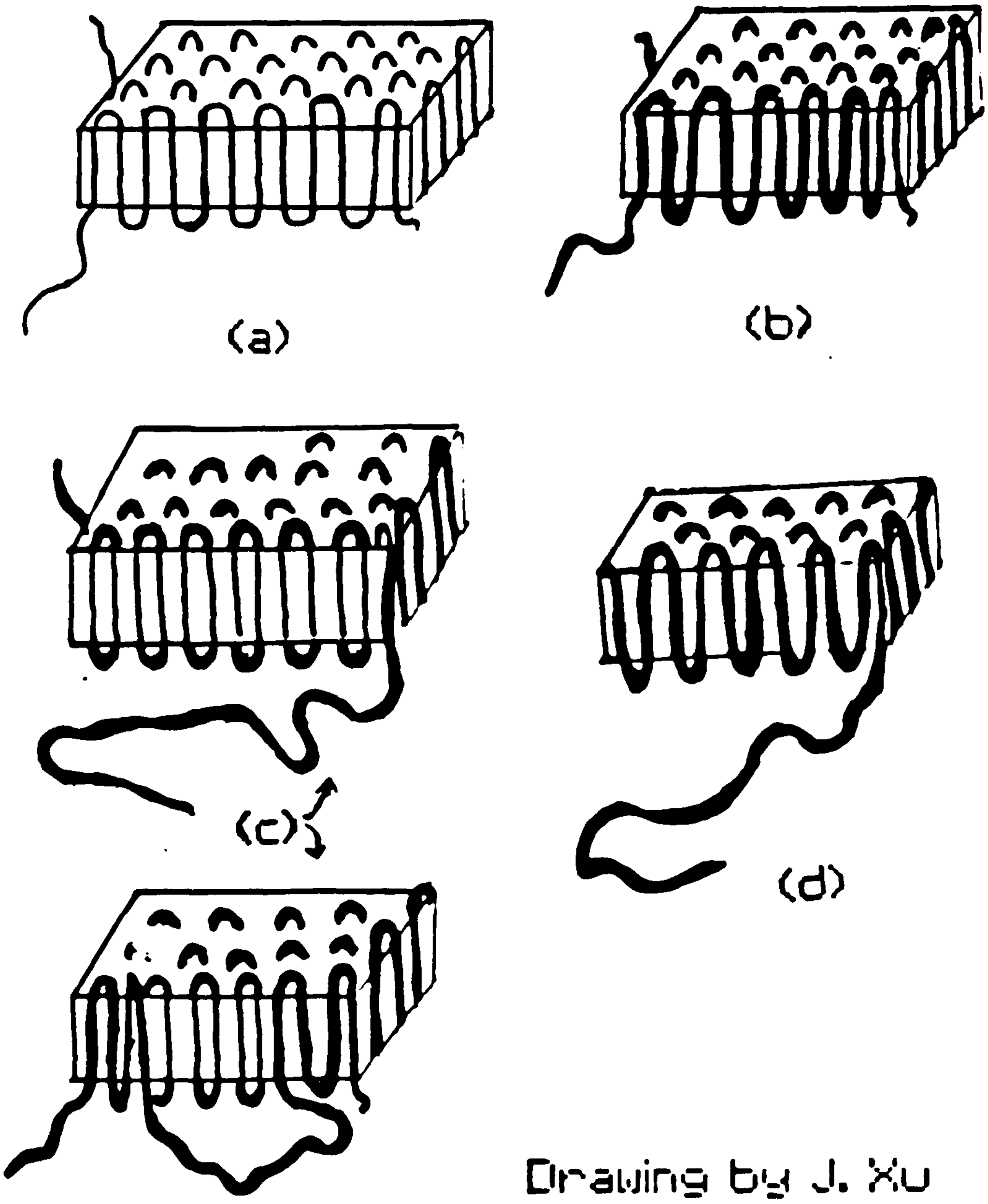

The mixture of block copolymers and highly hydrochlorinated chains is sometimes observed as mixed x-ray patterns of α TPI and hydrochlorinated TPI. Such a pattern is not observed for crystals reacted in acetone suspension where only the α TPI x-ray pattern is seen.

The presence of highly hydrochlorinated chains resulting from the peeling - off of the crystal is, however, not seen when subjected to a DSC analysis. The hydrochlorinated units may not crystallize significantly, thus escaping detection. Completely hydrochlorinated TPI, however, does exhibit an x-ray pattern and a melting endotherm, and therefore does crystallize to some extent. It is interesting to note, that carbon-13 NMR results conclusively show that hydrochlorinated TPI is an atactic product due to stereochemical multiplet resonances observed (figures 21 -22). Further, both possible stereoisomers are present in equal amounts showing equal probability for the site of the HCl attack. The roughly equal sizes of the methyl and the chloro substituent may lead to their accommodation in the same unit cell. It can be concluded, therefore, that although hydrochlorinated TPI is atactic it can exhibit a crystalline x-ray pattern and an endotherm. Also of interest is the x-ray pattern found for hydrochlorinated crystals that have been dissolved and reprecipitated. For crystals reacted in acetone suspension no pattern is seen after reprecipitation. When the crystals are reacted in amyl acetate, however, the reprecipitation of the block copolymer leads to the hydrochlorinated TPI crystal structure pattern, though very diffuse. The TPI - hydrochlorinated TPI ratio for these block copolymers are usually between 70/30 and 75/25. The crystal structure, being of the lesser compound, is probably due to the stronger polarity of that component.

A further important observation in this work is the decrease in the lamellar crystalline length along the chain direction from 7.5 to 5.0 to 4.3 nm with a decrease in the crystallization temperature from 30 to 20 to 10^oC, respectively. With a decrease in T_c, and therefore an increase in the supercooling, the lamellas also become more susceptible to defects, penetration and reaction, and destruction. Defective unreacted lamellas, grown at 10^oC can also be seen with the electron microscope, as shown in figure 7c. Lamellas crystallized at 10^oC and reacted in acetone suspension sometimes show HIH peaks. When the lamella or the hedrite is reacted in amyl acetate suspension the above changes are more pronounced. Lamellas grown at $T_c = 10^oC$ reach 100% hydrochlorination after approximately 12 days of reaction and show penetration (HIH peaks) throughout (figure 32, table 10). At $T_c = 20^oC$ there is a slight continuous increase in F_H until approximately 10 days of reaction in both lamellas and hedrites. After 10 days there is a sharp increase reaching 70% reaction after

18 days (figure 33, tables 11,12). HIH resonance peaks are observed frequently in lamellas and periodically in hedrites. At $T_c = 30^oC$ hydrochlorination in amyl acetate suspension is more stable and HIH peaks are seldom noticed with the NMR (figure 31, table 13).

Increasing the temperature at which the reaction is occurring also plays a role in the observed products. Lamellas grown at $T_c = 20^oC$ and reacted in amyl acetate suspension at 0^oC or higher show much fluctuation in $\langle B \rangle$ and $\langle A \rangle$ (table 9).HIH resonances are also present.

Although some fractionated samples (high, medium, and low molecular weight) have been used, most of this work was done with unfractionated samples. The effect of molecular weight has been studied previously, and is presently under study, by Woodward and coworkers [52,116,119,127,133] using TPI and epoxidized TPI. Here some fractionated TPI samples were used for the hydrochlorination of lamellas at temperatures of 0^oC or higher in amyl acetate suspension. No conclusion was obtained for the molecular weight dependence since (1) very few samples were used and (2) the solvent and $T_{reaction}$ have been proven above to cause destruction (such as penetration and peeling-off) of the crystal.

Viscosity measurements were obtained for TPI pellets and for TPI lamellas grown at $T_c = 10$, 20, and 30^oC (table 3). A slight increase in the molecular weight is observed with an increase in T_c. The latter seems, therefore, to fractionate the polymer chains to a certain extent, eliminating the lower molecular weight chains as the temperature is increased.

An average <A> value of 17 monomer units is found for hedrites grown at a crystallization temperature of 20°C. This is much higher than the value of 11 found for lamellas grown at the same T_c. A double melting endotherm was found for the above hedrites, as shown in figure 12. Although x-ray analysis shows the presence of the α form exclusively any β form would be masked by the α crystal diffraction pattern. Table 21 compares the first few d-spacings of α TPI obtained in this research (see also table 1) with those reported for β TPI crystals.

Table 21: d-spacings of α and β TPI for the first few lines

α TPI lamellas (A)	β TPI aggregates of curved lamellas (A)*	β TPI spherulites** (A)
7.47		
4.61	4.59	4.69
3.77	3.69	3.89
3.18	3.04	2.94
2.84	2.72	2.76

* Reported by Kuo,[5] $M_n = 2.5 \times 10^5$, 1% (W/V) amyl acetate solution, $T_D = 100°C$, $T_c = 0°C$

** Reported by Bunn,[111] unfractionated Gutta Percha

X-ray analysis is, therefore, inconclusive in this case in determining the presence of any β crystal form with the α TPI. Previous studies by Kuo et al.[5,116,119] indicate, however, that α and β TPI crystals may indeed be present for directly crystallized samples. In one set of experiments crystallization of synthetic TPI not in contact with a liquid was carried out at slow cooling rates after slow heating of the samples. A study of DSC thermograms showed that only the α form is nucleated when the starting sample temperature is 70°C. As the starting temperature is increased, an endotherm characteristic of the β form appears and increases in relative size. Quenching to 0°C from a starting temperature of 80°C resulted in only the crystallization of the β form. The melting endotherm reported by the author for β TPI falls in the range of 47 - 55°C. This agrees with the smaller of the double peaks observed in the present work and suggests that, here too, a mixture of α and β crystals are present.

Hedrites, spherulites, and overgrown lamellas in the β form have been reported by Kuo et al.[119] to have a significantly higher crystallinity than hedrites or overgrown lamellas in the α form for the same crystallization temperature. This suggests that the lamellar thickness for TPI crystals in the β form is larger than those in the α form. The measured thickness for β lamellas grown from the melt using unfractionated TPI were also reported by Davies and Long [153] to be larger than those for the α form grown at the same T_c. The <A> values obtained for hedrites in the present work is larger than those obtained for the overgrown α lamellas suggesting that (along with the DSC evidence) β crystals are indeed present in the directly crystallized hedrites. Further work must be done, however, before any conclusion can be made for certainty on the morphology of these TPI hedrites grown by the direct method of crystallization.

The amorphous content obtained for hedrites in the present work agree, within experimental error, with those of the lamellas, proving, again, that the nature of the fold is the same for both lamellas and hedrites grown at different crystallization temperatures.

IV.2. Recrystallization / microphase separation

Phase separation has been studied for a number of different AB, ABA, and irregular $(AB)_x$ type block copolymers, where A and B are alternating sections which may be flexible and/or rigid, hydrophobic and/or hydrophilic, crystallizable and/or noncrystallizable or cocrystallizable. AB type block copolymers have been prepared with ethylene oxide or ε-caprolactone as the crystallizable section, and butadiene, ethylmethacrylate or styrene in the amorphous portions.[66,134-136] Lamellar crystallization of the former section occurs upon cooling to low temperatures in the presence of a liquid. The resulting structure depends on the solubility of the amorphous part by the liquid, the molecular weight and nature of the two blocks, the concentration, solvent and crystallization temperature. Heatly and Begun [137] performed carbon-13 NMR relaxation experiments on a styrene-butadiene-styrene triblock copolymer (PS-PBd-PS) as a function of solvent and temperature. They show that the motions of the PBd block become increasingly hindered as the solvent is changed from chloroform to toluene to dimethoxyethane to ethyl acetate. Kaplan and O'Malley [138] have used solid state proton T_1 and T_2 measurements to study phase separation in a polystyrene-polyethylene oxide (PS-PEO) diblock copolymer. The PS phase is hydrophobic and glassy, whereas the PEO component is hydrophilic and semicrystalline. The T_1 and T_2 data show individual homopolymer transitions, indicative of phase separation. The data also shows that substantial phase mixing must occur at the PS-PEO phase boundaries. Assink and Wilkes [139] have also used pulsed solid state proton NMR to study phase separation in polystyrene-polybutadiene-polystyrene triblock copolymers. The free induction decays clearly show the presence of two components: the PS with its rapid decay (i.e., rigid material), and the PBd with its long decay (i.e., the mobile component). AB and ABA type block copolymers of isoprene have been prepared by ionic polymerization with monomers such as styrene, vinyl-2-pyridine, vinyl-4-pyridine and methylmethacrylate. A review of such preparations and investigations of their different properties, including microphase separation, is given by Gallot.[66] Microdomain formation in isoprene-styrene amorphous block copolymers has been observed in solution, in films cast from solution, in the melt, and in polymer blends.[66,140-144] The morphologies found include dispersed spheres, lamellar structures and hexagonally packed cylinders. Segmented polyurethane block copolymers (irregular $(AB)_x$) are made up of irregular sized hard and soft segment lengths composed from a diisocyanate, an intermediate molecular weight glycol and a short glycol.[145] Phase separation in these systems has been studied and models for the ordering in the hard segment domains have been given.[145,146] The extent of microphase separation in regular $(AB)_x$ type copolymers has not been investigated to date. Their properties are expected to differ, though, from those of the AB and ABA type due to the much shorter block length of the former. So far it has been found,[66,147,148] at least for the AB and ABA type copolymers, that microphase separation becomes more difficult, i.e. occurs at larger solvent-polymer interaction parameters (χ), as the number of blocks in the copolymer increases at constant total composition and molecular weight. For a regular $(AB)_x$ type block copolymer of moderate molecular weight, such as hydrochlorinated trans-1,4-polyisoprene - trans-1,4-polyisoprene treated here, the number of A or B blocks can be 100 or greater.

The reprecipitation of these regular block copolymer (i.e. copolymers derived from the hydrochlorination of TPI crystals in acetone suspension) did not show any sign of recrystallization or microphase separation. Microscopy and differential scanning calorimetry results were negative. X-ray results also seemed negative. It can also be seen from table 5 in chapter III that very few solvents are capable of reprecipitating the block copolymers.

IV.3. Proton NMR spectroscopy

^1H NMR results clearly indicates that hydrochlorination of TPI crystals is a simple Markownikoff addition, uncomplicated by side reactions and alternative routes, such as cyclization, isomerization, or degradation. Antimarkownikoff addition, for instance, would reveal a -CH(Cl)- resonance peak. Such peak has not been found. Instead, the presence of sharp singlet methyl resonances indicates that all methyl groups are attached to carbons bearing a double bond or a chlorine atom. Although cyclization, as another example, is a common side reaction, it is understandable that a tight reentry model of crystallization, and a hydrochlorination of the crystal at low temperatures, should not allow for such mobility of the chain. At high temperatures of 313-353K, Golub and Heller [80] have observed the presence of 8-17% cyclized double bonds in fully hydrochlorinated hevea (cis-1,4-polyisoprene) and balata (trans-1,4-polyisoprene) in benzene. Polyisoprenes are also known to undergo cyclization when treated with strong acids at temperatures near 333-353K.[149] If cyclization had indeed occurred, it would be evident at a resonance of approximately 1.0-1.5ppm. For example, one cyclization product might be similar to:

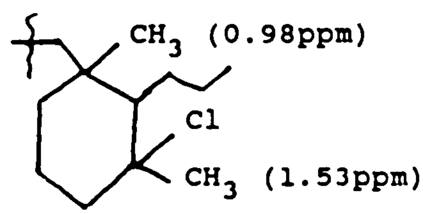

The possibility of some cyclization as an explanation for the extra peaks found by the methyl peaks (approx. 1.5ppm) may be ruled out. The peaks do not appear in the spectrum of totally hydrochlorinated TPI where any cyclization would have persisted. The resonances of the two heterosteric methyl groups in the 3,4-hydrochlorinated polyisoprene may also appear in the region of these small peaks, according to Markownikoff's rule, e.g., [102]

```
-CH2 - CH-
        |
  CH3- C -CH3
        |
        Cl
```

It has been reported[80] that hydrogen chloride reacts with 3,4-polyisoprene to give a product with a predominantly monocyclic structure.[80] Such a cyclization would involve the presence of two consecutive 3,4 units. This situation is not favored in the present polyisoprene which contains only 1% of monomer units other than the trans-1,4 to be distributed randomly along the polymer chain.[92] Furthermore, as mentioned above, the two peaks in question disappear in the spectrum of fully hydrochlorinated TPI, and can only be interpreted as junction signals.

IV.4. ^{13}C NMR Spectroscopy

Along with the help of literature values of model compounds, the assignments were based on prediction rules based on α, β, and γ effects:
The methyl group in HHH-5 is shifted downfield relative to its position in the unreacted III-5. This is due to the deshielding effect of the chlorine on the methyl group. In general, the spectral signals for carbon bound to electron withdrawing atoms, such as the chlorine atom, will shift to lower fields relative to the unchlorinated carbon.

For example, the carbon of methane, 2.3ppm, will shift to 22.8ppm upon substitution of one of its hydrogens with a chlorine.[123] The methyl group below, as another example, shifts from 13.3 to 40.9ppm as one of its hydrogens is replaced by a chlorine atom. A downfield shift is also seen for the olefinic carbons, from 118.6 to 123.1ppm, and from 131.6 to 138.9ppm.[151,151]

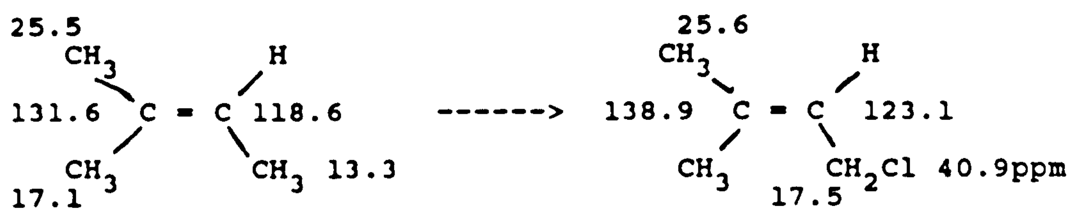

Methylene III-1 appears downfield of methylene III-4 due to the deshielding effect of the methyl group in the β position of carbon #1. III-4 is however, downfield of its corresponding hydrochlorinated units, HHH-4. Unsaturation of the α carbon causes a deshielding of the carbon in question relative to a sp_3 carbon. Furthermore, a γ effect of the chlorine on the HHH-4 shifts the latter 2 or 3ppm upfield. The position generates the opposite effect of that expected from the electron withdrawing rule which normally deshields the carbon.

Contrary to β methylene #4, HHH-1 appears downfield of III-1 because of the effect caused by the chlorine atom. Unreacted sp_2 carbon III-3, at 124.25 ppm, shifts upfield when the double bond is replaced by hydrogen chloride. The resulting HHH-3 becomes equivalent to HHH-1 and both appear as a single peak at 44.25 - 44.13 ppm the peak is split into a doublet due to stereochemistry).

Although chlorine deshields a carbon, its effect is smaller than the effect of a double bond on that carbon. III-2 is found, therefore, downfield of HHH-2.

The best defined of the junction peaks are the IIH-4 and the HHI-4. The latter resonance appears upfield of the former by 0.5 ppm. This deshielding is the result of the α effect of the double bond on methylene #4 of the isoprene unit in question (in the IIH resonance) which is absent on the HHI resonance. Similar reasonings, based on α, β, and γ effects, can be used to explain the positions of the other junctions.

The resonance splittings denoted as stereochemical appear not only in the TPI - HCl TPI block copolymer spectra but also in the completely hydrochlorinated TPI. The observed splittings in the latter confirms that the extra peak cannot be caused, as an alternate explanation, by a junction. It further shows that both possible stereoisomers are present in equal amounts and, therefore, attack from either side is equally possible. However, the chirality effect clearly depends on the chain conformation since the resonances for the different carbon atoms are either not split at all, split into a doublet, or into a triplet. Substituted carbons #2 and #4 show singlets. The 1:1 doublet splitting for the equivalent #1 and #3 methylene carbons shows that they are only sensitive to the chirality of the $C(CH_3)$-Cl in the closest connecting unit. The 1:2:1 triplet splitting of carbon #5 in a reacted sequence shows that the methyl group is affected by the chirality of the nearest groups in both directions.

Similar stereochemical splittings have already been identified in model compounds such as partially and completely epoxidized 3,7-decadiene,[54] as discussed in the introduction. Such interpretation confirmed the observation of similar splittings in epoxidized transpolybutadiene,[54] also mentioned in the introduction. In the oxirane ring carbon resonances, for instance, the chirality splitting of each OOO sequence (where O designates an oxirane unit) is sensitive to its nearest neighboring ring only. This is clearly seen in the spectrum of solution epoxidized TPDB where the OOO sequence is dominant. Both squalene,[51] which has previously been used as a model compound for the epoxidation of TPI, and epoxidized TPI,[51,52,127,152] also show diastereomeric splittings for different carbons (see introduction and appendices 2-4). Both alkyl carbons C5 and C9 in 50 to 100% epoxidized squalene show doublets, displaying a clear sensitivity to the chirality of the neighboring oxirane units. C4 and C8 also split, but to a lesser extent than C5 and C9. This difference in magnitude of the splitting indicates that different carbons in a sequence show different sensitivities to diastereomers. Similar behavior is found for hydrochlorinated TPI where, as mentioned earlier, carbons #2 and #4 do not split at all, while carbons #1,3 and #5 do split. The preservation of the trans geometry is also evidenced from C5 and C9 resonances of squalene. No cis C5 and C9 resonances appeared at 32ppm as would be expected based on the carbon-13 NMR spectrum of solution epoxidized cispolyisoprene.[81] The sensitivity of the methyl carbons C6' and C10' in epoxidized squalene to the chirality of neighboring oxiranes is also demonstrated by pairs of resonances. Carbon C2 as well as C3 also show doublets while C7 and C11 become nonequivalent when considering triads of oxirane units resulting in at least eight resonances which were resolved. This shows that NMR spectroscopy is sometimes sensitive not only to diad, but also to triad stereosequences. The olefinic region of epoxized TPI both in solution and in suspension have been shown to contain fine splittings due to its sensitivity to pentad sequences. Oxirane carbon C2 and CH_2 carbons show doublets reflecting the chiral relationship with only the nearest neighbor unit. The C3 oxirane and the methyl carbon are sensitive to neighbors in both directions along the chain. They are, thus, each split into a four line pattern produced by the four possible diastereomers. The epoxidized squalene and TPI spectra are further detailed in the introduction.

Sequential resonance peaks obtained for partially hydrochlorinated TPI can also be compared to similar previous work. The olefinic region of partially epoxidized TPI shows a similarity in the appearance of satellite peaks due to HII and IIH sequences on either side of the unreacted sequences. However, in the partial hydrochlorination of TPI these peaks are not symmetrically placed due to the asymmetry of the substitution. HIH resonances are also clearly present at low amounts of hydrochlorination while for epoxidation the equivalent resonances can only be observed for high degrees of reaction in the absence of the III resonance.

V. Conclusions

The following conclusions have been drawn from the above investigation:

1. Surface hydrochlorination of TPI lamellas or hedrites result in block copolymers of the $(AB)_x$ type, as calculated from carbon-13 NMR spectroscopy.

2. The suspension liquid used as the medium for hydrochlorination plays an important role in the resulting reaction: Acetone is a nonsolvent for both TPI and hydrochlorinated TPI allowing the reaction to reach completion at the surface without HCl penetration of the inner core. When amyl acetate is used as the suspension liquid penetration of the crystal core occurs.

3. Thinner TPI lamellas are more susceptible to defects, penetration, reaction, and destruction.

4. The degree of hydrochlorination of the crystals is a function of the reaction temperature. At low temperatures only a surface reaction occurs (in acetone media).

5. The crystalline stem length increases with an increase in the crystallization temperature, from carbon-13 NMR analysis.

6. The number of monomer units per fold remains constant,

within experimental error, for lamellas and hedrites grown at $T_c = 10 - 30^{o}C$. A mean value of 4.8 monomer units is obtained by carbon-13 NMR analysis.

7. Considerable adjacent reentry folding occurs in TPI lamellas with occasional fold looseness or occasional nonadjacent reentry.

8. Stereoisomeric splittings are found for certain carbons in hydrochlorinated TPI.

9. There is a discrepancy between the non-crystalline fraction $(1 - W_c)$, as obtained from density measurements on dried mats, and the fraction available for hydrochlorination, F_H.

10. Completely hydrochlorinated TPI is atactic with evidence of crystallinity being observed.

VI. Appendix

Appendix 1.

Possible isomers of partially epoxidized 3,7-decadiene (ignoring the cis,cis (Z,Z) diene and its epoxidation products). D = double bond, O = oxirane ring (epoxy unit), Z and E = cis and trans double bonds, c and t = cis and trans oxirane rings.

(i) OD-EE

(ii) OD-ZE

(iii) OD-tE

(iv) OD-tZ

(v) OD-cE

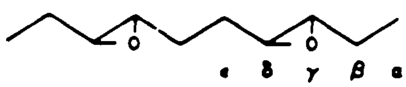

(vi) OO-tt

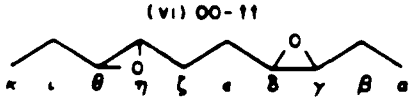

(vii) OO-ct

Appendix 2.

Olefinic carbon region of the 50.3-MHz ^{13}C spectra of (a) 25% and (b) 90% solution-epoxidized and (c) crystal-epoxidized 1,4-*trans*-polyisoprene. Observed in $CDCl_3$ at 40 °C.

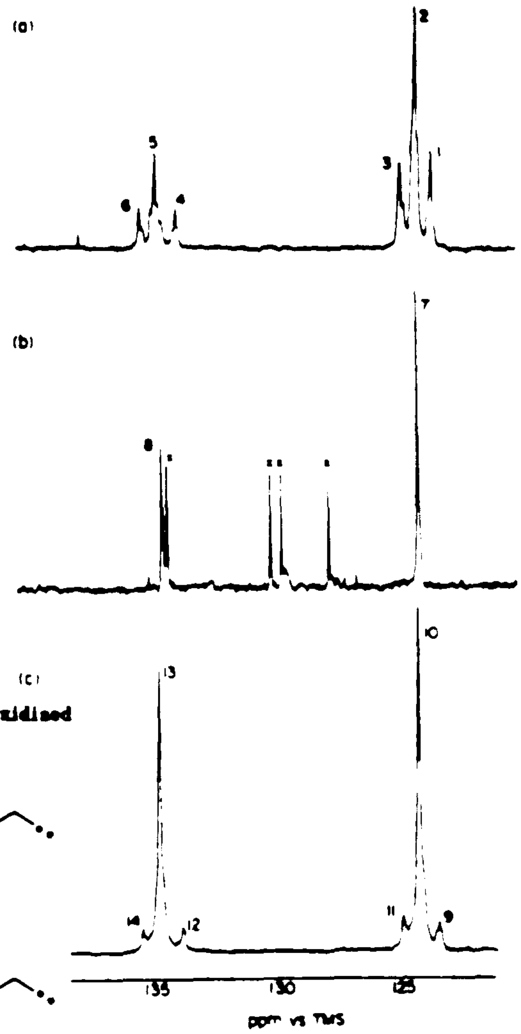

^{13}C Chemical Shifts of Olefinic Carbons in Epoxidized 1,4-*trans*-Polyisoprene *

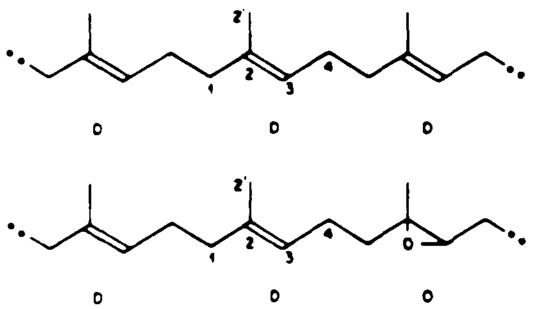

peak desig	assign-ment	chem shift: 25% solution-epoxidized TPI	90% solution-epoxidized TPI	crystal-epoxidized TPI
1, 9	DDO-C3	123.75		123.53
2, 10	DDD-C3	124.43		124.33
3, 11	ODD-C3	125.01		125.00
4, 12	ODD-C2	134.09		133.93
5, 13	DDD-C2	134.95		134.87
6, 14	DDO-C2	135.55		135.58
7	ODO-C3		124.29	
8	ODO-C2		134.72	

*Structural formulas of two representative sequences are shown

The peaks labeled "x" result from an apparent side reaction in TPI epoxidized to 90% at 20 °C. It is probable that the MCBA is reacting with oxirane to form an ester linkage and a secondary alcohol.

Appendix 3.

Figure 5. Oxirane carbon region of the 50.3-MHz ^{13}C spectra of (a) 25% and (b) 90% solution-epoxidized and (c) crystal-epoxidized 1,4-*trans*-polyisoprene. Observed at $CDCl_3$ at 40 °C. ("x" indicates residual amyl acetate.)

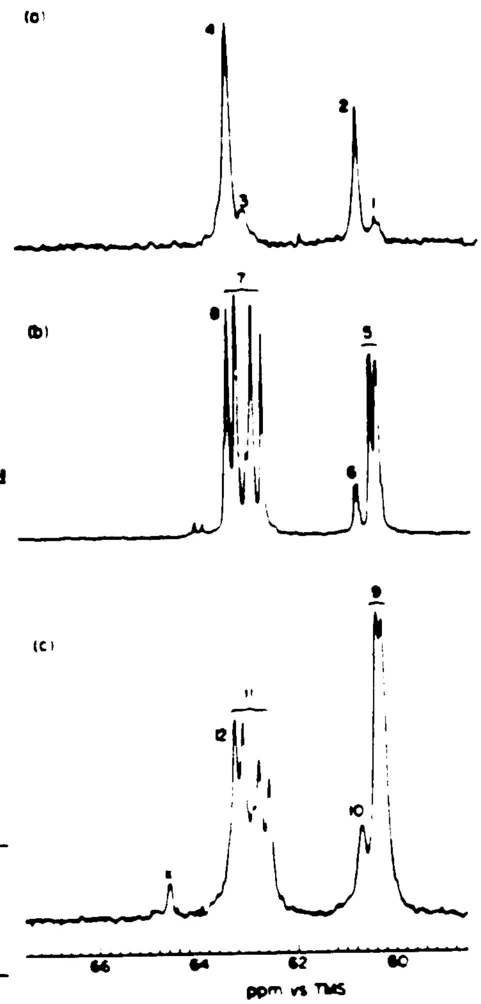

^{13}C Chemical Shifts of Oxirane Ring Carbons in Epoxidized 1,4-*trans*-Polyisoprene[a]

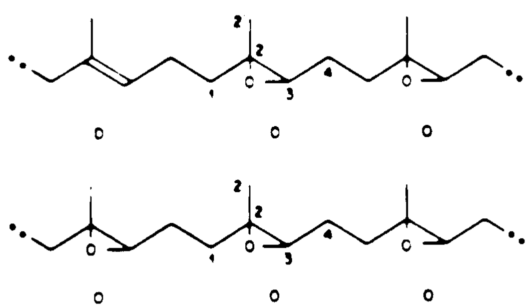

peak desig	assignment	chem shift: 25% solution-epoxidized TPI	90% solution-epoxidized TPI	crystal-epoxidized TPI
1, 5, 9	OOD-C2 (m,r)	60.22	60.32	60.21
		60.31	60.44	60.33
2	DOD-C2	60.69		
2, 6, 10	DOO-C2	60.69	60.70	60.66
			60.76	
3, 7, 11	DOO-C3	62.94	62.63–63.31	62.53–63.20
		62.99		
4	DOD-C3	63.09		
4, 8, 12	OOD-C3	63.09	63.31	63.20
5, 9	OOO-C2 (m,r)		60.32	60.21
			60.44	60.33
7, 11	OOO-C3 (mm, mr,rm,rr)		62.63	62.53
			62.82	62.74
			63.14	53.05
			63.31	53.20

[a]Structural formulas of two representative sequences are shown.

Appendix 4.

. Alkyl carbon region of the 50.3-MHz ^{13}C spectra of (a) 25% and (b) 90% solution-epoxidized and (c) crystal-epoxidized 1,4-*trans*-polyisoprene. Observed in $CDCl_3$ at 40 °C. ("x" indicates residual amyl acetate.)

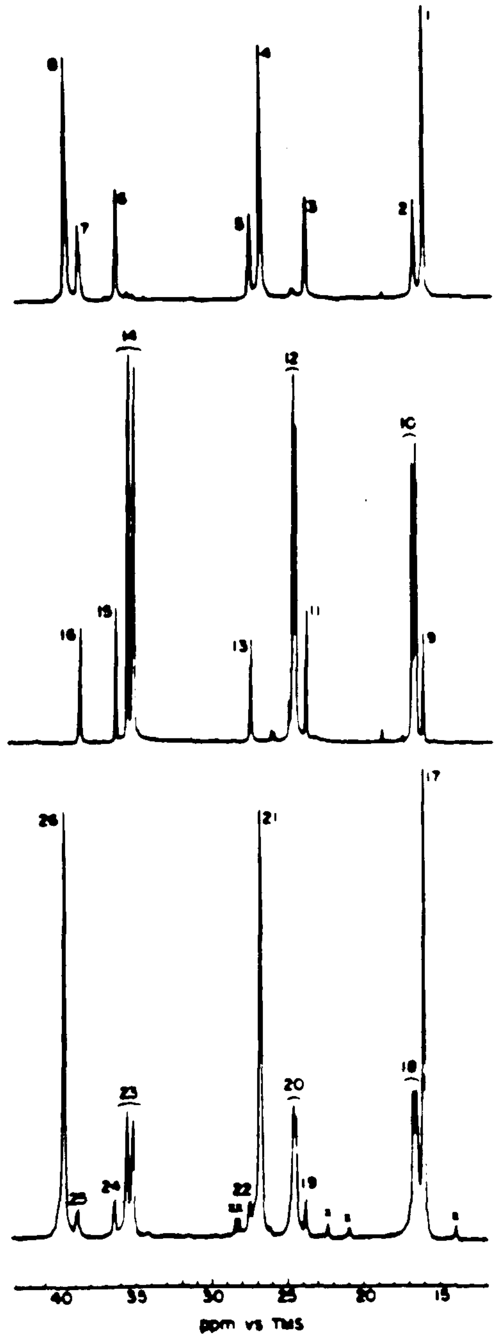

^{13}C Chemical Shifts of Alkyl Carbons in Epoxidized 1,4-*trans*-Polyisoprene[a]

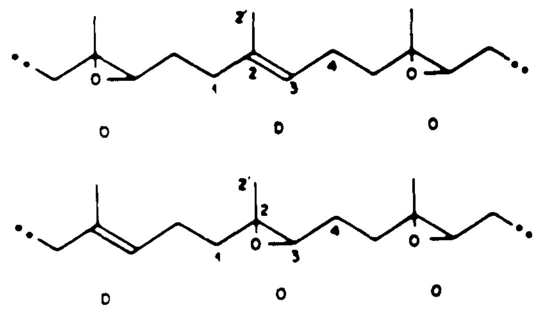

peak desig	assign-ment	chem shift: 25% solution-epoxidized TPI	90% solution-epoxidized TPI	crystal-epoxidized TPI
1, 17	DDD-C2'	16.10		16.03
	ODD-C2'			
	DDO-C2'			
2	DOD-C2'	16.72		
3, 19	DDO-C4	23.86		23.76
4, 21	DDD-C4	26.88		26.77
	ODD-C4			
5	DOD-C4	27.57		
6, 24	ODD-C1	36.46		36.33
7	DOD-C1	38.98		
8, 26	DDD-C1	39.85		39.75
	DDO-C1			
9	ODO-C2'		16.06	
10, 18	OOD-C2'		16.56	16.47
	DOO-C2'		16.78	16.69
	OOO-C2'			
	(m,r)			
11	ODO-C4		23.80	
12, 20	DOO-C4		24.49	24.42
	OOO-C4		24.66	24.57
	(m,r)			
13, 22	OOD-C4		27.44	27.48
14, 23	OOD-C1		35.24	35.17
	OOO-C1		35.61	35.54
	(m,r)			
15	ODO-C1		36.40	
16, 25	DOO-C1		38.74	38.78

[a] Structural formulas of two representative sequences are shown.

Appendix 5.

Molecular structures of Trans-1,4-Polyisoprene.

(A) β -structure from Bunn.

(B) α -structure from Bunn.

(C) α -structure from Takahashi et al.

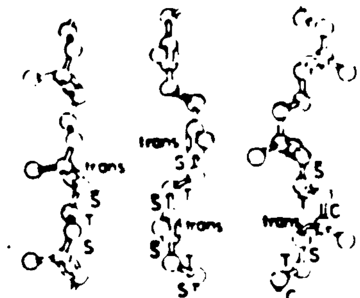

(A) (B) (C)

Appendix 6.

Viscosity measurement:

Example, shown bellow: TPI lamellas were grown at $T_c = 10^oC$ and dried. Sample size = 0.020011 grams / 0.025 liter of toluene = 0.008 = C_1.

Table 22: Flow time, t (sec), of TPI lamellas dissolved in toluene at different concentrations.

trial #	15ml of C_1	toluene increments +5ml (C_2)	+5ml (C_3)	+5ml (C_4)	+5ml (C_5)	+5ml (C_6)
1	256.6	206.4	179.2	162.6	151.1	143.0
2	256.6	206.4	179.0	162.4	151.15	143.1
3	256.6	206.4	179.2	162.5	151.1	144.0*
avg	256.6	206.4	179.1	162.4	151.1	143.1

* disregard

(continued next page)

(appendix 6. continuation)

$\eta_i = (t_i/t_o) - 1$ where t_o = 95.4 sec = flow time of the pure solvent (toluene).

$C_i = C_1$ (initial volume/total volume)

Table 23: Concentration vs flow time of TPI dissolved in toluene.

C_i	η_i/C_i
0.008	211.21
0.006	193.9
0.0048	182.8
0.004	175.8
0.0034	171.7
0.003	166.7

$[\eta] = K M^a$

where $K = 3.34 \times 10^{-2}$ and

$a = 0.686$ (from literature)

$[\eta]$ = intercept of C vs η/C from least square analysis

= 140.8 (correlation = 0.99949)

therefore,

$\underline{M = 1.9 \times 10^5}$

VII. REFERENCES

(1) Wunderlich, B. "Macromolecular Physics" vol.1, Academic Press, 1973.

(2) Blundell, D.J.; Keller, A. **J. Macromol. Sci. Phys.** 1968, **B2**, 301.

(3) Smets, G.; Hart, R. **Adv. Polymer Sci.**, 1960, **2**, 173.

(4) Keith, H.D. **J. Polym. Sci.**, 1964, **A2**, 4339.

(5) Kuo, C.C. **Thesis**, CCNY, 1983.

(6) Keller, A. **Phil. Mag.**, 1957, **2**, 1171.

(7) Fischer, G.W. **Z. Naturforsch**, 1957, **12a**, 753.

(8) Till, P.H. **J. Polym. Sci.**, 1957, **24**, 301.

(9) Geil, P.H. "Polymer Single Crystals", Wiley, N.Y., 1963.

(10) Bunn, C.W. **Trans. Faraday Soc.**, 1939, **35**, 482.

(11) Bank, M.I.; Krimm, S. **J. Polym. Sci.: A2**, 1969, **7**, 1785.

(12) Yoon, D.Y.; Flory, P.J. **Polymer**, 1977, **18**, 509.

(13) Fischer, E.W.; Stamm, M.; Dettermaier, M.; Herchenroder, P. **Polym. Preprints**, 1979, **20**, **(1)**, 219.

(14) Voegel, R.; Sillescu,H. **Macromoleculse**, 1979, **12**, 162.

(15) Bassett, D.C.; Hodge, A.M. **Polymer**, 1978, **19**, 469.

(16) Bassett, D.C.; Hodge, A.M. **Proc. Roy. Soc.**, 1978, **A 359**, 121.

(17) Bassett, D.C.; Hodge, A.M.; Olley, R.H. **Discussions Faraday Soc.**, 1978, **68**, 218.

(18) Bassett, D.C.; Hodge, A.M. **Proc. Roy. Soc.**, 1981, **A 377**, 25.

(19) Bassett, D.C.; Hodge, A.M. **Proc. Roy. Soc.**, 1981, **A 377**, 39.

(20) Bassett, D.C.; Hodge, A.M. **Proc. Roy. Soc.**, 1981, **A 377**, 61.

(21) Keith, H.D.; Padden, F.J. **Polymer**, 1984, **25**, 28.

(22) Khoury, F. **Discussions Faraday Soc.**, 1979, **68**, 404.

(23) Kuo, C.C. **Thesis**, CCNY, 1983, p.15.

(24) Mandelkern, L. **J. Polym. Sci.: Polym. Revs.**, 1975, **50**, 457. **Acc. Chem. Res.**, 1976, **9**, 8.

(25) Harrison, I.R.; Runt, J.; Stanislow, L.J.; Bell, D.A. **J. Polym. Sci.: Polym. Phys. Ed.**, 1979, **17**, 63.

(26) Illers, K.H.; Kanig, G. **Colloid & Polymer. Sci.**, 1982, **260**, 564.

(27) Cheam, T.C.; Krimm, S. **J. Polym. Sci.: Phys. Ed.**, 1981, **19**, 423.

(28) Jing, X.; Krimm, S. **J. Polym. Sci.: Polym. Phys. Ed.**, 1982, **20**, 1155.

(29) Udagawa, Y.; Keller, A. **J. Polym. Sci.: A2**, 1971, **9**, 437.

(30) Ergoz, E.; Mandelkern, L. **J. Polym. Sci.: Polym. Phys. Ed.**, 1972, **10**, 631.

(31) Blundell, D.J.; Keller,A.; Connor, T.M. **J. Polym. Sci.**, 1967, **A2**, **5**, 991.

(32) Fischer, E.W.; Peterlin, A. **Makromol. Chem.**, 1964, **74**, 1.

(33) Bergmann, K.; Nawotki, K. **Kolloid Z. U. Z. Polymers**, 1972, **250**, 1094.

(34) Fischer, E.W.; Lorenz, R. **Kolloid Z.**, 1963, **189**, 97.

(35) Jacksonn, J.B.; Flory, P.J.; Chiang, R. **Tran. Faraday Soc.**, 1963, **59**, 1906.

(36) Hoffman, J.D.; Davis, G.T. **J. Res. Nat'l Bur. Stand. Soc.**, 1975, **79A**, 613.

(37) Keller, A.; Udagawa, Y. **J. Polym. Sci.**, 1971, **A2**, **9**, 1793.

(38) Priest, D.J. **J. Polym. Sci.**, 1971, **A2**, **9**, 1777.

(39) Patel, G.N.; Keller, A. **J. Polym. Sci.: Polym. Phys. Ed.**, 1975, **13**, 2259.

(40) Keller, A.; Martuscelli, E.; Priest, D.J.; Udagawa, Y. **J. Polym. Sci.**, 1971, **A2**, **9**, 1807.

(41) Keller, A.; Matreyek, W.; Winslow, F.H. **J. Polym. Sci.**, 1962, **62**, 291.

(42) Harrison, I.R.; Baer, E. **J. Polym. Sci.**, 1971, **A2**, **9**,1305.

(43) Equiluz, M.; Ishida, H.; Hiltner, A. **J. Polym. Sci.: Polym. Phys. Ed.**, 1979, **17**, 893; 1980, **18**, 2295.

(44) Harrison, I.R.; Butler, J.S.; Runt, J.P. **Org. Coatings & Plastics Chem. Reprints**, 1981, **44**, 176.

(45) Guzman, J.; Fatou, J.G.; Perena, J.M. **Makromol. Chem.**, 1980, **181**, 1051.

(46) Chang, B.H.; Siegmann, A.; Hiltner, A. **Bull. Am. Phys. Soc.**, 1983, **28**, 272.

(47) Bassett, D.C. **Polymer**, 1964, **5**, 457.

(48) Tsuboi, K. **J. Macromol. Sci. - Phys.**, 1968, **B2**, 603.

(49) Harrison, I.R.; Baer, E. **J. Colloid & Interfacial Sci.**, 1983, **31**, 176.

(50) Anandakumaran, K.; Herman, W.; Woodward, A.E. **Macromol.**, 1983, **16**, 563.

(51) Schilling,F.C.; Bovey, F.A.; Anandakumaran, K.; Woodward, A.E., **Macromol.**, 1985, **18**, 2688.

(52) Elkayam, A.; Xu, J.; Woodward, A.E. **Macromol.**, submitted for publication.

(53) Taylor, M.; Woodward, A.E., unpublished results, see A.E. Woodward, Modification of Polymers, J.A. Moore and C.E. Carraher, Jr., Eds. Plenum 1983.

(54) Schilling, F.C.; Bovey, F.A.; Tseng, S.; Woodward, A.E. **Macromol.**, 1983, **16**, 808; **Polym. Preprints**, 1983, **24**- 1, 235.

(55) Tseng, S.; Herman, W.; Woodward, A.E., Newman, B.A. **Macromol.**, 1982, **15**, 338.

(56) Tseng, S.; Woodward, A.E. **Macromol.**, 1982, **15**, 343.

(57) Hendrix, C.; Whiting, D.A., Woodward, A.E. **Macromol.**, 1971, **4**, 57.

(58) Stellman, J.M.; Woodward, A.E. **J. Polym. Sci.**, 1969, B7, 755; **J. Polym. Sci.**, 1971, **A2**, **9**, 59.

(59) Wichacheewa, P.; Woodward, A.E. **J. Polym. Sci.: Polym. Phys.**, 1978, **16** 1849.

(60) Marchetti, A.; Martuscelli, E. **J. Polym. Sci.: Polym. Phys.**, 1976, **14**, 151.

(61) Xu, J.; Woodward, A.E., unpublished results.

(62) Jelinski, L.W.; Schilling, F.C.; Bovey, F.A. **Macromol.**, 1981, **14**, 581.

(63) Williams, E.A.; Cargioli, J.D.; Hobbs, S.Y. **Macromol.**, 1977, 10, 782.

(64) Klesper, E.; Gronski, W.; Barth, V. **Makromol. Chem.**, 1970, **139**, 1.

(65) Komoroski, R.A.; Horne, S.E.; Carman, C.J. **J. Polym. Sci.: Polym. Chem. Ed.**, 1983, **21**, 89.

(66) Gallot, B.R.M. **Adv. Polym. Sci.**, 1978, **29**, 85.

(67) Schilling, F.C.; Bovey, F.A.; Tonelli, A.E.; Tseng, S.; Woodward, A.E. **Macromol.**, 1984, **17**, 728.

(68) Mazur, S. **Organic Coatings & Plastics Preprints**, 1982, **45**, 79.

(69) Tatsumi, T.; Fukushima, T.; Imada, K>; Takayanagi, M. **J. Macromol. Sci. - Phys.**, 1967, **B1**, 459.

(70) Evans, H.; Woodward, A.E. **Macromol.**, 1976, **9**, 88.

(71) Ng, S.B.; Stellman, J.M.; Woodward, A.E. **J. Macromol. Sci. - Phys.**, 1973, **B7**, 533.

(72) Marchetti, A.; Martuscelii, E. **J. Polym. Sci.: Polym. Phys. Ed.**, 1976, **14**, 323.

(73) Finter, J.; Wegner, G. **Makromol. Chem.**, 1981, **182**, 1859.

(74) U.S. Pats. 1, 495, 580 (1924) 1, 544, 531, 535 (1925) E. Gebawer - Fuelnegg (to Marbo Patents inc.), U.S. Pat. 2, 072, 255 (1937).

(75) Le Bras, J.; Delante, A. "Les Derives Chimiques du Caoutchouc Naturel", Dunod, Paris, 1950, p.31.

(76) Bloomfield, G.F.; Farmer, E.H. **J. Soc. Chem. Ind.**, 1934, **53**, 435, 475.

(77) Bloomfield, G.F. **J. Chem. Soc.**, 1944, 114.

(78) Von Amerongen, G.J.; Koningsberg, C. **J. Polym. Sci.**, 1950, **6**, 653.

(79) Van Veersen, G,J. **Proc. Second Rubber Technol. Conf.**, London, 1948, 87.

(80) Golub, M.A.; Heller, J. **J. Polym. Sci.**, 1964, **B2**, 523.

(81) Gemmer, R.V.; Golub, M.A. **J. Polym. Sci.: Polym. Chem.**, 1978, **16**, 2985.

(82) Hayashi, D.; Takahashi, T.; Kurihara, H.; Veno, H. **Polym. Journal**, 1981, **13-3**, 215.

(83) Duch, M.W.; Grant, D.M. **Macromol.**, 1970, **3**, 165.

(84) Araki, Y.; Yoshimoto, T.; Imanari, M.; Takeuchi, M.; **Kobunski Kagaku**, 1972, **29**, 397.

(85) Furukawa, J.; Kobayashi, E.; Kawagoe, T.; Katsuki, N.; Imanari, M. **J. Polym. Sci.: Polym. Let. Ed.**, 1973, **11**, 239.

(86) Randall, J.C. "Polym. Sequence Determination, Carbon-13 NMR Method" ,Academic Press, NY, NY ,1977.

(87) Furukawa, J.; Kobayashi, E.; Katsuki, N.; Kawagoe, T. **Makromol. Chem.**, 1974, **175**, 237.

(88) Clague, A. D. H.; Van Broekhoven, J. A. M.; Blaauw, L.P. **Macromol.**, 1974, **7**, 348.

(89) Tanaka, Y.; Sato, H.; Ogawa, M.; Hatada, K.; Terawaki, Y. **J. Polym. Sci.: Polym. Let. Ed.**, 1974, **12**, 369.

(90) Tanaka, Y.; Sato,H.; Hatada, K.; Terawaki, Y.; Okuda, H. **Makromol. Chem.**, 1977, **178**, 1823.

(91) Katritzky, A.R.; **Weiss**, D. E. **J. Chem. Soc. Perkin Trans**, 1974, **2**, 1542.

(92) Tanaka, Y.; Sato, H.; Ogura, A.; Nogoya, I. **J. Polym. Sci.: Polymer Chem. Ed.**, 1976, **14**, 73.

(93) Tanaka, Y.; Sato, H.; Seimiya, T.; **Polym J**, 1975, **7**, 264.

(94) Tanaka, Y.; Sato, H. **Polyms**, 1976, **17**, 413.

(95) Sato H.; Ono, A.; Tanaka, Y. **Polymer**, 1977,**18**, 580.

(96) Gronski, W.; Murayama, N.; Cantoro, H. J.; Miyamoto, T. **Polymer**, 1976, **17**, 358.

(97) Tanaka, Y.; Sato, H. **Polymer**, 1976, **17**, 113.

(98) Cameron, G.G.; Chishti, S.A.A.; Ebdon, J.R.; Heatley, F. **Eur. Polym. J.**, 1979, **15**, 203.

(99) Shahab, Y.A.; Basheer, R.A. **J. Polym. Sci.: Polym. Chem. Ed.**, 1979, **17**, 919.

(100) Randall, J.C. **J. Polym. Sci.: Polym. Phys. Ed.**, 1975, **13**, 901.

(101) Sievers, R.E. " Nuclear Magnetic Shift Reagents", Academic Press, NY, 1973.

(102) Tran, A.; Prud'homme, J. **Macromol.**, 1977, **10**, 149.

(103) Dorman, D.E.; Jautelat, M.; Roberts, J.D. **J. Organic Chem.**, 1971, **36**, 2757.

(104) Breitmaier, E.; Haas, G.; Voelter, W. "Atlas of Carbon-13 NMR Data", Heyden & Son, Inc., Philadelphia, 1979.

(105) Levitt, M.H.; Freeman, R. **J. Magn. Res.**, 1979, **33**, 473.

(106) De Haan, J.W.; Van de Ven, L.J.M. **Org. Magn. Res.**, 1973, **5**, 147.

(107) Grant, D.M.; Paul, E.G. **J. Am. Chem. Soc.**, 1964, **86**, 2984.

(108) Lindemann, L.P.; Adams, J.Q. **Anal. Chem.**, 1971, **43**, 1245.

(109) Pegg, D.T.; Doddrell, D.M.; Bendall, M.R. **J. Chem. Phys.**, 1982, **77**, 2745.

(110) Sorenson, O.W.; Ernst, R.R. **J. Magn. Res.**, 1983, **51**, 477.

(111) Bunn, C.W. **Proc. Phys. Soc., London**, 1942, **A180**, 40.

(112) Fischer, D. **Proc. Phys. Soc., London**, 1953, **66**, 7.

(113) Takahashi, Y.; Sato, T.; Tadokoro, H.; Tanaka, Y. **J. Polym. Sci.**, 1973, **11**, 233.

(114) Bunn, C.W.; Garner, E.V. **J. Chem. Soc.**, 1942, 654.

(115) Anandakumaran, K. **Thesis**, CCNY, 1984.

(116) Anandakumaran, K.; Kuo, C.C.; Mukerji, S.; Woodward, A.E. **J. Poly. Sci.: Polym. Phys. Ed.**, 1982, **20**, 1669.

(117) Salzberg, H.M.; Morrow, J.I.; Cohen, S.R.; Green, M.E. "Physical Chemistry Laboratory, Principles and Experiments", MacMillan Publishing co., 1978, p.118.

(118) Blundell, D.J.; Keller, A.; Kovacs, A.J. **J. Polym. Sci.**, 1966, **B4**, 481.

(119) Kuo, C.C.; Woodward, A.E. **Macromols.**, 1984, **17**, 1034.

(120) Keller, A.; Martuscelli, E. **Makromol. Chem.**, 1972, **151**, 189.

(121) Lovering, E.G.; Wooden, D.C. **J. Polym. Sci.**, 1971, **A-2**, **9**, 175.

(122) Mandelkern, L.; Quinn, J.A.; Roberts, D.E. **J. Am. Chem. Soc.**, 1956, **78**, 926.

(123) Silverstein, R.M.; Bassler, G.C.; Morriel, T.C. "Spectrometric Identification of Organic Compounds", p.159-229, Wiley & Sons, 1974.

(124) Fanconi, B.; Sarazin, D. **Polym Preprints**, 1984, **25** **(2)**, 173.

(125) Harrison, I.R.; Runt, J. **J. Macromol. Sci., Phys.**, 1980, **B17**, 83.

(126) Harrison, I.R.; Juska, T. **J. Polym. Sci., Polym. Phys. Ed.**, 1980, **17**, 491.

(127) Elkayam, A.; Woodward, A.E., unpublished results.

(128) Jones, D.H.; Zatham, A.J.; Keller, A.; Girolamo, M. **J. Polym. Sci.: Polym. Phys.**, 1973, **11**, 1759.

(129) Newman, B.; Stellman, J.M.; Woodward, A.E. **J. Polym. Sci.: Polym. Phys. Ed.**, 1972, **10**, 2311.

(130) Eng, S.B.; Woodward, A.E. **J. Macromol. Sci., Phys.**, 1974, **B10**, 627.

(131) Oyama, T.; Shiokawa, K.; Murata, Y **Polym. J.**, 1974, **6**, 549.

(132) Chang, B.H.; Siegman, A.; Hiltner, A. **J. Polym. Sci., Polym. Phys. Ed.**, 1984, **22**, 255.

(133) Xu, J.; Woodward, A.E. **Macromol.**, 1986, **19**, 1114.

(134) Gervais, M.; Gallot, B. **C.R. Acad. Sci. (Paris)**,1970, **C270**, 784.

(135) Gervais, M.; Gallot, B. **Makromol. Chem.**, 1977, **178**, 1577.

(136) Herman, J.J.; Jerome, R.; Teyssie, P.; Gervais, M.; Gallot, B. **Makromol. Chem.**, 1978, **179**, 1111.

(137) Heatley, F.; Begun, A. **Makromoml. Chem.**, 1977, **178**, 1205.

(138) Kaplan, S.; O'Malley, J.J. **Polym. Prepr. Div. Polym. Chem., Am. Chem. Soc.**, 1979, **20(2)**, 266.

(139) Assink, R.A.; Wilkes, G.L. **Polym. Eng. & Sci.**, 1977, **17**, 606.

(140) Gallot, B.; Mayer, R.; Sadron, C. **Rubber Chem. Tech.**, 1967, **40**, 932.

(141) Inoue, T.; Soen, T.; Hashimoto, T.; Kawai, H. **J. Polym. Sci.**, 1969, **A2**,7, 1283.

(142) Uchida, T.; Soen, T.; Inoue, T.; Kawai, H. **J. Polym. Sci.**, 1972, **A2**,10, 101.

(143) Hashimoto, T.; Nagatsoshi, K.; Todo, A.; Hasegawa, H.; Kawai, H. **Macromol.**, 1973, **7**, 364.

(144) Pedemont, E.; Turturro, A.; Bianchi, U.; Devetta, P. **Polym.**, 1978, **14**, 144.

(145) Bonart, R.; Morbitzer, L.; Hentze, G. **J. Macromol. Sci.-Phys.**, 1969, **B3**, 337.

(146) Koberstein, J.T.; Stein, R.S. **J. Polym. Sci.: Polym. Phys.**, 1983, **21**, 1357.

(147) Meier, D.J. **J. Polym. Sci.**, 1969, **C26**, 81.

(148) Krause, S. **Macromol.**, 1970, **3**, 84.

(149) Grassie, N. "Chemistry of High Polymer Degredation Processes", Butterworth Scientific Publications, London, 1956, p.315-319.

(150) Bruscato, S.; Tidewall, A.; Thomas, J. **Chem. Communications**, 1972, **17**, 958.

(151) Coleman, M.N.; Tabb, D.L.; Brame, E.G. **Rubber Chem. Technol.**, 1977, **50(1)**, 49.

(152) Zemel, I.; Woodward, A.E., unpublished results.

(153) Davies, C.K.L.; Long, D.E. **J. Mater. Sci.**, 1979, **14**, 2529.